Charles University
Third Faculty of Medicine

Doctoral Dissertation

M.Sc. Bohdan Kysilov

The study of functional and pharmacological properties of glutamate receptors

Studium funkčních a farmakologických vlastností glutamátových receptorů

Supervisor: Prof. Ladislav Vyklický

Prague, 2022

Declaration:

I declare that I worked out this doctoral thesis independently with my original results and used only the cited sources and literature. I also did not use any sources figures than those stated in the bibliography. This work has never been submitted by me or by anyone else at Charles or any other university and has not been used to obtain a Ph.D. or any other academic degree.

I agree that an electronic version of this work will be permanently saved in the database system of the inter-university project Theses.cz for the systematic control of the similarity of theses.

In Prague, 28. 11. 2022 Bohdan Kysilov

Identification record:

Kysilov, Bohdan. *The study of functional and pharmacological properties of glutamate receptors. [Studium funkčních a farmakologických vlastností glutamátových receptorů]*. Prague, 2022. 130 pages, 3 attachments. Doctoral dissertation. Charles University, Third Faculty of Medicine, Institute of Physiology CAS . Supervisor: Prof. Ladislav Vyklický.

Keywords: NMDA receptors, neuroactive steroids, disease-associated mutations, positive allosteric modulators

Klíčová slova: NMDA receptory, neuroaktivní steroidy, mutace spojené s onemocněním, pozitivní alosterické modulátory

Acknowledgements

I am deeply indebted to my supervisor Professor Ladislav Vyklický for his guidance, professional help, and excellent advice that he offered to me. Many thanks to all the members of the Laboratory of Cellular Neurophysiology of the Institute of Physiology of the Czech Academy of Sciences for their contribution to the implementation of the research mentioned in this dissertation and for the very friendly, welcoming, and pleasant environment that they created. Special thanks to the security guards of the campus of the Institutes of the Czech Academy of Sciences for letting me enter the Institute of Physiology of the Czech Academy of Sciences over the weekends for all these years.

Abstract

N-methyl-D-Aspartate receptors (NMDAR) are ionotropic glutamate receptors that are involved in the regulation of nearly every process in the brain. Therefore, even a subtle disturbance in NMDAR function may result in severe pathological consequences. Loss-of-function mutations in the NMDAR-encoding genes have been implicated in numerous neuropsychiatric disorders, including intellectual disability, developmental delay, schizophrenia, autism spectrum disorders, epilepsy, and movement disorders. Insufficient NMDAR function can be rectified by positive allosteric modulators, including neurosteroids; however, the mechanism underlying the potentiating effect of steroids is not well understood.

By employing patch-clamp electrophysiology we assessed the effect of newly synthesized neurosteroid-like pregnane analogues on recombinant GluN1/GluN2B receptors. We demonstrated that compounds with short C3 residues, such as pregnanolone acetate (PA-Ace) and pregnanolone carboxylate (PA-Car), are negative modulators of NMDAR, whereas compounds with longer C3 residues, such as pregnanolone butyrate (PA-But) and epipregnanolone butyrate (EPA-But), are positive modulators of NMDARs. Furthermore, we revealed that EPA-But has a disuse-dependent positive allosteric effect, being similar in that regard to endogenous neurosteroid pregnenolone sulfate (PE-S).

Combining electrophysiology, molecular biology, and computational modelling, we identified the PE-S and EPA-But binding sites at the transmembrane domain of the GluN1/GluN2B receptor. Our results indicate that EPA-But binds the NMDAR at the GluN1(M4)/GluN2B(M1), GluN2B(M4)/GluN1(M1), and GluN2B(M1/M4) interfaces. In contrast, PE-S binds the receptor only at the GluN2B(M1/M4) interface. Moreover, we proposed the mechanisms by which the steroids potentiate NMDAR function.

Next, we characterized the effect of ten *de novo* disease-associated mutations in the hGluN2B subunit on the receptor functional properties and surface expression. In addition, we evaluated the effect of EPA-But and PE-S at NMDARs harbouring disease-associated mutations in hGluN1 and hGluN2B subunits. Our results uncovered the potential of EPA-But and PE-S in compensation for the effect of loss-of-function mutations.

In this study, we revealed structural principles underlying the potentiating effect of steroids. Our results open up new possibilities for developing new steroid-based drugs for treating disorders associated with the hypofunction of NMDAR.

Abstrakt

N-methyl-D-aspartátové receptory (NMDAR) jsou ionotropní glutamátové receptory, které se podílejí na regulaci téměř všech procesů v mozku. Proto i nepatrná porucha funkce NMDAR může vést k závažným patologickým důsledkům. Mutace v genech kódujících NMDAR, které vedou ke snížení jejich funkce, se podílejí na mnoha neuropsychiatrických poruchách, jako jsou například mentální retardace, schizofrenie, poruchy autistického spektra, epilepsie a poruchy pohybu. Nedostatečnou funkci NMDAR lze korigovat pozitivními alosterickými modulátory, včetně neurosteroidů. Mechanismus který je základem potenciačního účinku steroidů však není dosud dostatečně objasněn.

Pomocí elektrofyziologické metody terčíkového zámku jsme změřili účinek nově syntetizovaných analogů pregnanů, které jsou podobné neurosteroidům, na rekombinantní NMDAR s podjednotkovým složením GluN1/GluN2B. Prokázali jsme, že sloučeniny s krátkými residui na uhlíku C3, jako je pregnanolon acetát (PA-Ace) a pregnanolon karboxylát (PA-Car), jsou negativními modulátory NMDAR, zatímco sloučeniny s delšími residui na C3, jako je pregnanolon butyrát (PA-But) a epipregnanolon butyrát (EPA-But), jsou pozitivními modulátory NMDAR. Dále jsme odhalili, že EPA-But má "disuse-dependentní" pozitivní alosterický účinek, přičemž je v tomto ohledu podobný endogennímu neurosteroidu pregnenolon sulfátu (PE-S).

Kombinací elektrofyziologie, molekulární biologie a počítačového modelování jsme identifikovali vazebná místa PE-S a EPA-But v transmembránové doméně receptoru GluN1/GluN2B. Naše výsledky ukazují, že EPA-But se váže na NMDAR na rozhraní transmembránových domén M4 a M1 sousedících podjednotek GluN1(M4)/GluN2B(M1), GluN2B(M4)/GluN1(M1) a dále na toto rozhraní v jedné podjednotce GluN2B(M1/M4). Naproti tomu PE-S se váže na receptor pouze na rozhraní GluN2B(M1/M4). Zde jsme navrhli mechanismy, kterými steroidy potencují funkci NMDAR.

Dále jsme provedli charakterizaci vlivu více než deseti *de novo* mutací asociovaných s neuropsychiatrickými onemocněními v lidské variantě podjednotek hGluN2B a hGluN1 na funkční vlastnosti a povrchovou expresi NMDAR. Zkoumali jsme účinek EPA-But a PE-S u těchto mutovaných NMDAR a naše výsledky ukázaly potenciál EPA-But a PE-S kompenzovat hypofunkci NMDAR, které nesou tyto mutace.

V této studii jsme odhalili strukturální principy, které jsou základem potenciačního účinku steroidů. Naše výsledky otevírají nové možnosti vývoje léčiv na bázi steroidů, které budou určeny pro léčbu poruch spojených s hypofunkcí NMDAR.

Abbreviations

2R,6R-HNK	2R,6R-hydroxynorketamine
4-Cl-KYN	L-4-chlorokynurenine
7-CKA	7-chlorokynurenic acid
AA	amino acids
AMPAR	α-amino-3-hydroxy-5-methyl-4isoazolepropionic receptor
AND-hSuc	androst-5-en-3β-yl hemisuccinate
ANDS	5α-Androstan-3β-yl-sulfate
AP7	2-amino-7-phosphonoheptanoic acid
ASD	autism spectrum disorder
ATD	amino-terminal domain
BAPTA	1,2-bis(o-aminophenoxy)ethane-N,N,N′,N′-tetraacetic acid
BPD	bipolar disorder
CIQ	(3-chlorophenyl)(6,7-dimethoxy-1-((4-methoxyphenoxy)methyl)-3,4-dihydroisoquinolin-2(1H)-yl)methanone
C_m	membrane input capacitance
CMC	critical micelle concentration
CNS	central nervous system
CTD	carboxyl-terminal domain
D-AP5	D-2-amino-5-phosphonovaleric acid
DD	developmental delay
DMD	dyskinetic movement disorder
DMSO	dimethyl sulfoxide
EC_{50}	half-maximal effective concentration
ECS	extracellular solution
EDTA	ethylenediaminetetraacetic acid
EEG	electroencephalogram
EMEM	Eagle's Minimum Essential
EPA-But	4-(20-oxo-5β-pregnan-3β-yl) butanoic acid (epipregnanolone butyrate)
Epi	epilepsy
EPSC	excitatory postsynaptic currents
ES	epileptic spasms
FBS	fetal bovine serum
FDA	Food and Drug Administration

Glu	glutamate
GluDR	glutamate delta receptor
Gly	glycine
GNE-9278	4-cyclohexyl-N-(5-methyl-7-oxo-2-propyl-4,7-dihydro-[1,2,4]triazolo [1,5-a]pyrimidin-6-yl) benzenesulfonamide
GRIN	glutamate receptor ionotropic N-methyl-D-aspartate
GVL	generalized cerebral volume loss
HEK293	human embryonic kidney 293 cells
HEPES	4-(2-hydroxyethyl)-1-piperazineethanesulfonic acid
IC_{50}	half-maximal inhibitory concentration
ICS	intracellular solution
ID	intellectual disability
iGluRs	ionotropic glutamate receptors
KAR	kainate receptors
KYNA	kynurenic acid
LB	lysogeny broth
LBD	ligand-binding domain
MATra	Magnet Assisted Transfection
MD	molecular dynamics
MDD	major depressive disorder
MK-801	(5S,10R)-(+)-5-methyl-10,11-dihydro-5H-dibenzo[a,d]cyclohepten-5,10-imine hydrogen maleate (dizocilpine)
MM/PBSA	Molecular Mechanics Poisson-Boltzmann Surface Area
NAM	negative allosteric modulator
NMDAR	N-methyl-D-aspartate receptor
NR	not responding
PA	3α-hydroxy-5β-pregnan-20-one
PA-Ace	20-oxo-5β-pregnan-3α-yl acetate
PA-But	20-oxo-5β-pregnan-3α-yl butyrate
PA-Car	20-oxo-5β-pregnan-3α-yl carboxylate
PAM	positive allosteric modulator
PA-Pro	20-oxo-5β-pregnan-3α-yl propionate
PA-S	5β-pregnan-20-on 3α-yl sulfate
PBS	phosphate-buffered saline

PCP	phencyclidine
PCR	polymerase chain reaction
PE-S	20-oxo-pregn-5-en-3β-yl sulfate
P_o	opening probability
SCAM	substituted cysteine accessibility method
SE	surface expression
SEM	standard error of the mean
TCN-201	3-chloro-4-fluoro-N-[4-[[2-(phenylcarbonyl)hydrazino]carbonyl]benzyl] benzenesulfonamide
TMD	transmembrane domain
WS	West syndrome
WT	wild type
βCDX	β-cyclodextrin
γCDX	methyl-γ-cyclodextrin
τ_w	weighted time constant

Contents

1 Introduction

1.1 Ionotropic glutamate receptors

Ionotropic glutamate receptors (iGluRs) are a family of ligand-gated ion channels that play a pivotal role in excitatory synaptic transmission. The iGluRs are ubiquitously expressed in neurons and glial cells throughout the mammalian central nervous system (CNS) and are the most prevalent excitatory neurotransmitter receptors in the CNS (Hollmann and Heinemann, 1994). Moreover, glutamatergic synapses comprise the majority of synapses in the mammalian CNS, especially in the cortex, where they comprise about 80-90% of synapses (Somogyi et al., 1998). The iGluRs control nearly all CNS circuits and their malfunction is implicated in the pathogenesis of numerous neuropsychiatric disorders (Hansen et al., 2021).

Based on ligand specificity and sequence homology, iGluRs have been divided into four subtypes: N-methyl-D-aspartate receptors (NMDARs), α-amino-3-hydroxy-5-methyl-4isoazolepropionic receptors (AMPARs), kainate receptors (KARs), and delta receptors (GluDRs) (Traynelis et al., 2010). All iGluRs share common structural features such as tetrameric assembly and subunit topology (Twomey & Sobolevsky, 2018). Furthermore, iGluRs of different subtypes are commonly colocalized within postsynaptic membranes and are activated by the same pulse of glutamate therefore conjointly contributing to the generation of excitatory postsynaptic currents (EPSCs) (Bekkers & Stevens, 1989; Clements, 1996). However, iGluR subtypes differ considerably in their kinetics, pharmacological properties, and physiological functions.

In contrast to other iGluRs, GluDRs are incapable to form functional ion channels or mediate ion currents. Nonetheless, GluDRs have been shown to regulate synapse formation and stabilization, pre- and post- synaptic organization, and synaptic plasticity by non-ionotropic mechanisms (Yuzaki & Aricescu, 2017). AMPARs are characterized by rapid gating and desensitization kinetics and play a key role in the initial rapid component of EPSCs (Hansen et al., 2021; Traynelis 2010; Twomey et al., 2019). Overall, AMPARs mediate the bulk of fast excitatory synaptic transmission in the CNS (Jonas, 2000). In contrast, the KAR contribution to the excitatory postsynaptic transmission is modest due to a limited subset of neurons expressing KARs postsynaptically and the small amplitude of KAR-mediated EPSCs. In most cases, KAR-mediated EPSCs are much slower than AMPAR-mediated EPSCs (Castillo et al., 1997; Kidd & Isaac, 1999, 2001; Traynelis et al., 2010). However, in particular types of synapses, KAR-mediated EPSCs are as fast as AMPAR-mediated EPSCs (Cossart et al., 2002; DeVries & Schwartz, 1999). KARs are considered to

be particularly important for the generation of tonic depolarization (Frerking & Ohliger-Frerking, 2002). The NMDARs account for the slow component of EPSCs due to their slow gating and desensitization kinetics and relatively weak desensitization. NMDARs stand out from the other iGluRs by high calcium (Ca^{2+}) permeability. NMDAR-mediated Ca^{2+} signalling is of considerable importance for the control of synaptic development and plasticity. At the same time, excessive NMDAR-mediated Ca^{2+} influx may lead to neuronal damage or death and is implicated in the pathogenesis of numerous neurodegenerative disorders (Hansen et al., 2021; Traynelis et al., 2010).

1.2 Structure of the NMDA receptor

Mammalian NMDARs are encoded by seven genes: GRIN1, GRIN2A-D, and GRIN3A-B. The GRIN1 gene encodes the GluN1 subunit, the GRIN2A-D genes encode the GluN2A-D subunits, and the GRIN3A-B genes encode the GluN3A-B subunits. Functional NMDAR is a heteromeric complex composed of two obligatory GluN1 subunits and two GluN2 and/or GluN3 subunits. NMDARs can be either diheteromeric assemblies that contain the same type of GluN2 or GluN3 subunits or triheteromeric assemblies that contain different types of GluN2 or/and GluN3 subunits (Traynelis et al., 2010; Vyklicky et al., 2014).

The structure of all NMDAR subunits is highly similar and includes the intracellularly located carboxyl-terminal domain (CTD), transmembrane domain (TMD), and extracellularly located ligand-binding domain (LBD) and amino-terminal domain (ATD) (Figure 1.1*A,B*). The CTD is intrinsically disordered and varies in length between the subunits in range from about 50 amino acids (AA) in GluN1 to about 650 AA in GluN2B. Multiple sites for posttranslational modulation and interaction with regulatory proteins are located at the CTD. The CTD thus plays a key role in the regulation of NMDAR trafficking and function (Ishchenko et al., 2021). The TMD is comprised of the re-entrant loop M2, and the transmembrane helices M1, M3, and M4. The channel pore is formed by the M3 helices and the M2 loop (Figure 1.1*B*). The M3 helices line the transmembrane part of the pore and form the channel gate that governs the channel opening. The M2 loops line the internal part of the pore, including the Q/N/S site, the narrowest part of the pore that delineates the ion selectivity and incorporates the Mg^{2+}-block site. The LBD forms a bilobed clamshell-like structure that is subdivided into the upper S1 segment and lower S2 segment (Figure 1.1*B*). The S2 segment is connected to the TMD via M3-S2 and S2-M4 linkers while the S1 segment is connected to

the TMD via the S1-M1 linker. The interface between the S1 and S2 contains the binding site for the agonists: the glycine binding site at the GluN1 and GluN3 subunits and the glutamate binding site at the GluN2 subunits. The binding of both agonists leads to conformational rearrangement of the LBD, which is a fundamental step for channel gating. The ATD also forms a bilobed structure that is subdivided into R1 and R2 subdomains (Figure 1.1*B*). The interface between the R1 and R2 hosts sites of action for numerous allosteric modulators. In addition, the ATD is crucial for NMDAR assembly and trafficking (Hansen et al., 2018; Karakas & Furukawa, 2014; Twomey & Sobolevsky, 2018).

The transcript of GRIN genes is a subject of alternative splicing. As a result, GluN1 has eight splice isoforms: GluN1-1a, GluN1-1b, GluN1-2a, GluN1-2b, GluN1-3a, GluN1-3b, GluN1-4a, and GluN1-4b. GluN1-1a isoforms differ from GluN1-1b isoforms by the lack of the polypeptide cassette N1 in the ATD. The GluN1-(1-4) isoforms are distinguished by the presence or absence of the polypeptide cassettes C1, C2, and C2' in the CTD: the GluN1-1 isoform contains the cassettes C1 and C2, the GluN1-2 isoform contains the cassette C2, the GluN1-3 isoforms contain the cassettes C1 and C2', and GluN1-4 isoform contains the cassette C2' (Stephenson, 2006). The human GluN2A subunit also has different splice isoforms: the GluN2A-S isoform with a shorter CTD and the GluN2A-F isoform with a longer CTD (Dingledine et al., 1999; Ishchenko et al., 2021; Warming et al., 2019). Several splice variants of GluN3A and GluN3B subunits were found in rodents but not humans. The alternative splicing of NMDARs substantially impacts receptor trafficking, pharmacology, expression, and NMDAR-mediated metabotropic signalling (Hansen et al., 2021; Horak & Wenthold, 2009; Li et al., 2021; Sengar et al., 2019).

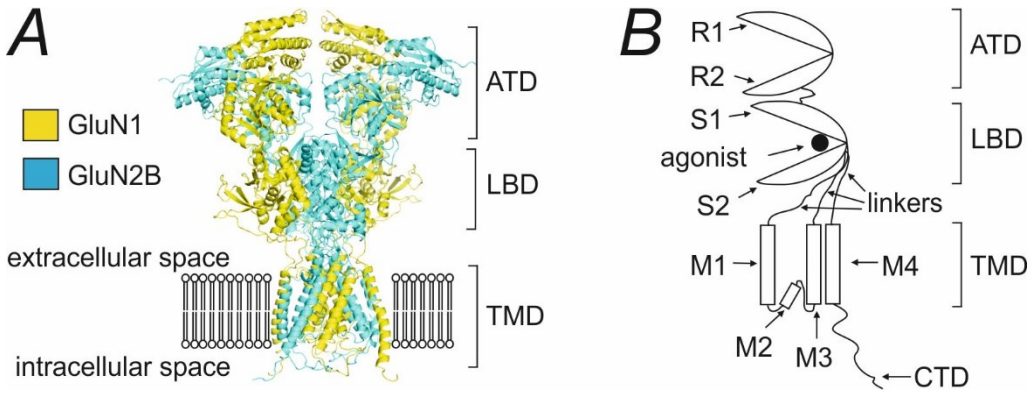

Figure 1.1. Domain structure of the NMDAR. ***(A)*** Crystal structure of GluN1/GluN2B receptor. The GluN1 subunit is marked in orange and GluN2B subunit is marked in blue. The CTD is not presented. Adapted from (Karakas & Furukawa, 2014). ***(B)*** Schematic representation of the NMDAR subunit structure. The agonist is schematically represented as a black circle.

1.2.1 Subunit composition of NMDA receptor

The combination of different subunits produces various NMDAR subtypes that differ in functional and pharmacological characteristics. So-called conventional NMDARs that are composed of GluN1 and GluN2 subunits constitute the majority of native NMDARs (Kehoe et al., 2013; Traynelis et al., 2010). Such receptors require simultaneous binding of glutamate and glycine for activation, exhibit high Ca^{2+} permeability, and are sensitive to Mg^{2+}-block. In contrast, unconventional GluN1/GluN3 receptors are activated by glycine alone, Ca^{2+}-impermeable, and almost insensitive to Mg^{2+}. Interestingly, the triheteromeric GluN1/GluN2/GluN3 receptors exhibit mixed properties: they have low Ca^{2+}-permeability and low sensitivity to Mg^{2+}- block (Amin et al., 2021; McClymont et al., 2012; Pachernegg et al., 2012; Pérez-Otaño et al., 2016).

NMDAR subunit expression distributes differentially in different CNS regions and remarkably changes during development. Since GluN1 is an obligatory subunit, it is the most abundant NMDAR subunit that is widely expressed through the CNS. GluN2B and GluN2D subunits are ubiquitously expressed in the embryonic CNS, whereas GluN2A and GluN2C subunits are absent. During embryogenesis, the GluN2B subunit is expressed in the cortex, thalamus, and spinal cord. In addition, GluN2B is expressed in the hippocampus, colliculi, and hypothalamus at a moderate level but is poorly present in the cerebellum. In contrast, the GluN2D subunit is absent in embryonic telencephalon but abundant in the spinal cord, mesencephalon, and diencephalon. The expression of GluN2B and GluN2D remains high in the neonatal brain but then decreases considerably. In adults, GluN2D expression is minor and occurs predominately in the diencephalon and mesencephalon. The expression GluN2B is primarily confined to the telencephalon (Akazawa et al., 1994; Doss et al., 2014; Monyer et al., 1994; Sheng et al., 1994; Vergnano et al., 2014; Williams et al., 1993). Moreover, ageing-related GluN2B expression declines in the cortex (Pegasiou et al., 2020). GluN2A expression starts early after birth and is abundant throughout the brain, while GluN2C expression occurs later in development and is greatly restricted to the cerebellum. GluN3A expression is low during embryogenesis, peaks early after birth, and progressively decreases later in development. In the neonatal period, GluN3A is abundant and widespread in the CNS. In contrast, GluN3B is absent during embryogenesis, gradually increases expression with development and peaks in adulthood. The overall expression of GluN3B is mostly limited to the prosencephalon (Akazawa et al., 1994; Henson et al., 2010; Monyer et al., 1994; Pachernegg et al., 2012; Pérez-Otaño et al., 2016; Vergnano et al., 2014). Overall, GluN2A

and GluN2B subunit-containing NMDARs predominate in the adult brain (Traynelis et al., 2010).

1.3 NMDA receptor activation

Activation of conventional NMDARs requires the binding of two co-agonists, glutamate and glycine. Agonist affinity varies among the NMDARs of different subunit compositions. Thus, the glutamate EC_{50} for diheteromeric GluN1/2A-D receptors corresponds to 1.8-7.7 μM; 0.9-4.0 μM; 1.0 μM; and 0.4 μM, respectively. In turn, the glycine EC_{50} for GluN1/2A-D receptors is 0.86 μM; 0.34 μM; 0.14 μM; and 0.12 μM, respectively. Interestingly, the saturation of glycine binding sites decreases the glutamate affinity of NMDARs (Benveniste et al., 1990; Lester et al., 1993; Mayer et al., 1989). In addition, the affinity to agonists can also be affected by allosteric modulators (Hansen et al., 2021).

Glycine is persistently present in the cerebrospinal fluid at the concentration of 2-6 μM, which provides high but not complete saturation of glycine-binding sites (Hansen et al., 2021). However, it was shown that glycine serves as a co-agonist mainly at the extrasynaptic NMDARs, whereas D-serine is the main co-agonist at the synaptic NMDARs (Papouin et al., 2012). The concentration of D-serine is highly influenced by astroglial and neuronal D-serine release in a synaptic activity-dependent manner. Therefore, the control of ambient D-serine concentration serves as a tool to regulate NMDAR activity (Kalbaugh et al., 2009; Martineau et al., 2014; Yang et al., 2003).

Estimates of ambient glutamate levels in the extracellular space performed by electrophysiology studies indicate a concentration of 25-90 nM. Conversely, microdialysis and biosensor studies show a glutamate concentration of 1-20 μM, which is likely to be an artefact resulting from local tissue damage by the probe (Herman & Jahr, 2007; Moldavski et al., 2020; Moussawi et al., 2011; Sun et al., 2014). However, the concentration of ambient glutamate is sufficient for tonic activation in certain neural populations, such as granule and pyramidal cells in the hippocampus. Tonic activation engages mostly extrasynaptic NMDARs, whereas synaptic NMDARs show no or only little tonic activation (Le Meur et al., 2007; Yang Yang & Xu-Fried, 2015). The difference in activation of synaptic and extrasynaptic NMDARs may be associated with distinct subunit composition. GluN2B subunit-containing receptors that prevail at extrasynaptic sites are more sensitive to glutamate than GluN2A subunit-containing receptors that prevail at synaptic sites (Paoletti et al., 2013).

In addition, the ambient glutamate concentration in the synaptic cleft is lower than in the extrasynaptic space because of glutamate uptake (Lozovaya et al., 2004).

Upon presynaptic release, the glutamate concentration in the synaptic cleft exceeds millimolar concentration but then drops rapidly due to uptake by specific transporters (Clements et al., 1992). Such glutamate transients result in phasic activation of synaptic NMDARs, which is crucial for synaptic transmission and believed to have a neuroprotective effect. In contrast, excessive tonic NMDAR activation is implicated in excitotoxicity and neurodegeneration (Gladding & Raymond, 2011; Hardingham & Bading, 2010; Olney, 1969).

The LBD clamshell structure is open in an unbounded apo state. Upon the binding of co-agonists, the S2 rotates toward the S1 segment to close the LBD clamshell. Upon the conformational change, the S2 segment generates tension at the M3-linker to displace the M3 helix. The displacement of the M3 initiates a set of conformational rearrangements that results in the channel pore opening. The non-pore forming M1 and M4 helices are also displaced during gating and play important roles in the pore opening (Banke & Traynelis, 2003; Černý et al., 2019; Hansen et al., 2021; Twomey & Sobolevsky, 2018).

1.3.1 Kinetic scheme for NMDA receptor activation

At a simplified level, the activation of the conventional NMDAR can be described by the kinetic scheme (Figure 1.2) (Lester & Jahr, 1992). The NMDAR is considered saturated at the glycine-binding site in the scheme. Therefore the glycine-binding steps are not shown and only glutamate is designated as an agonist (A) in the scheme. The kinetic scheme shows the glutamate binding as two identical but independent steps that transit the receptor (R) into the one agonist molecule bound (AR) and the two agonist molecules bound (A_2R) state. In this scheme, the glutamate binding is characterized by the on-rate constant k_{on} and the glutamate unbinding is characterized by the off-rate constant k_{off}. In the A_2R state, the NMDAR can transit either into the desensitized (D) or the open (O) state. Since the opening and closing rate constants (β and α, respectively) are substantially faster than the desensitization and resensitization rate constants (k_d and k_r, respectively), the onset of receptor desensitization is protracted. The transition into the D state is preceded by swift transitions between the A_2R and O states. Resensitization along with agonist unbinding contribute to the NMDAR current decay (Lester & Jahr, 1992).

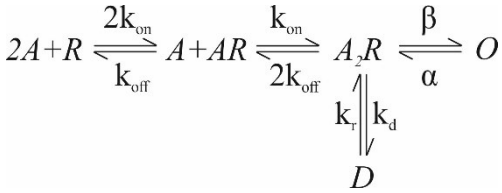

Figure 1.2. Kinetic scheme describing the activation of the NMDAR**.** *A* indicates the agonist (glutamate). *R*, *AR*, A_2R, *O*, and *D* indicate the receptor in the glutamate-unbound, single-molecule bound, two-molecule bound, open, and desensitized states, characterized by the on-rate constants $2k_{on}$ and k_{on}, off-rate constants $2k_{off}$ and k_{off}, desensitization rate constant k_d, resensitization rate constant k_r, opening rate constant β, and closing rate constant α. Adapted from (Lester & Jahr, 1992).

Although the indicated kinetic scheme is sufficient for the overall characterization of macroscopic NMDAR currents, it is vastly simplified and, therefore, not fully accurate. For instance, the scheme skips the glycine binding step, an allosteric interaction between glycine and glutamate binding sites, and Ca^{2+}-dependent inactivation. Kinetic schemes that consider these factors have also been proposed (Benveniste et al., 1990; Cais et al., 2008). Furthermore, the scheme in Figure 2 is oversimplified and cannot be used for single-channel data analysis since the channel opening is not a direct transition from A_2R to *O* state, but rather a sequence of multiple intermediate transitions between pre-open and closed states (Amin et al., 2021; Gibb & Colquhoun, 1991; Howe et al., 1991). To analyze such intermediate transitions, several more complex kinetic schemes have been proposed (Auerbach & Zhou, 2005; Banke & Traynelis, 2003; Borschel et al., 2015; Erreger et al., 2005; Maki & Popescu, 2014).

1.4 Pharmacology of NMDA receptor

The NMDAR activity can be modulated by numerous ligands of endogenous and exogenous origin, including competitive antagonists, open channel blockers, and allosteric modulators.

1.4.1 Competitive antagonists

Competitive antagonists bind to the NMDAR at the agonist binding site but do not activate the receptor. Hence, a competitive antagonist competes with an agonist for the same binding site, which results in the reduction of receptor activation.

Kynurenic acid (KYNA; Figure 1.3*A*), a naturally-occurring metabolite of L-tryptophan, is a competitive NMDAR antagonist at the glycine- and, with substantially lower affinity, the glutamate-binding site (Birch et al., 1988; Kessler et al., 1989). 7-chlorokynurenic acid (7-CKA; Figure 1.3*B*), a derivative of KYNA, is a potent glycine-site selective competitive antagonist of NMDAR. 7-CKA has shown a neuroprotective effect in an animal model of ischemia. Interestingly, L-4-chlorokynurenine (4-Cl-KYN; Figure 1.3*C*), which acts in the organism as a prodrug of 7-CKA, displayed an antihyperalgesic and rapid-acting antidepressant effect in animal studies (Yaksh et al., 2017; Zanos et al., 2015). Selective glutamate-binding site NMDAR antagonist D-2-amino-5-phosphonovaleric acid (D-AP5; Figure 1.3*D*) and 2-amino-7-phosphonoheptanoic acid (AP7; Figure 1.3*E*) are well-known tool compounds which are used for selective inhibition of NMDAR currents. In animal studies, D-AP5 and AP7 showed an anticonvulsant effect (Meldrum et al., 1988; Zivanovic et al., 1999). A potent glutamate-site antagonist CGP-37849 (Figure 1.3*F*) has neuroprotective, anticonvulsant, antidepressant and anxiolytic effects (Fagg et al., 1990; Fujikawa et al., 1994; Gutnikov & Gaffan, 1996; Jessa et al., 1996; Papp & Moryl, 1994; Rundfeldt et al., 1994).

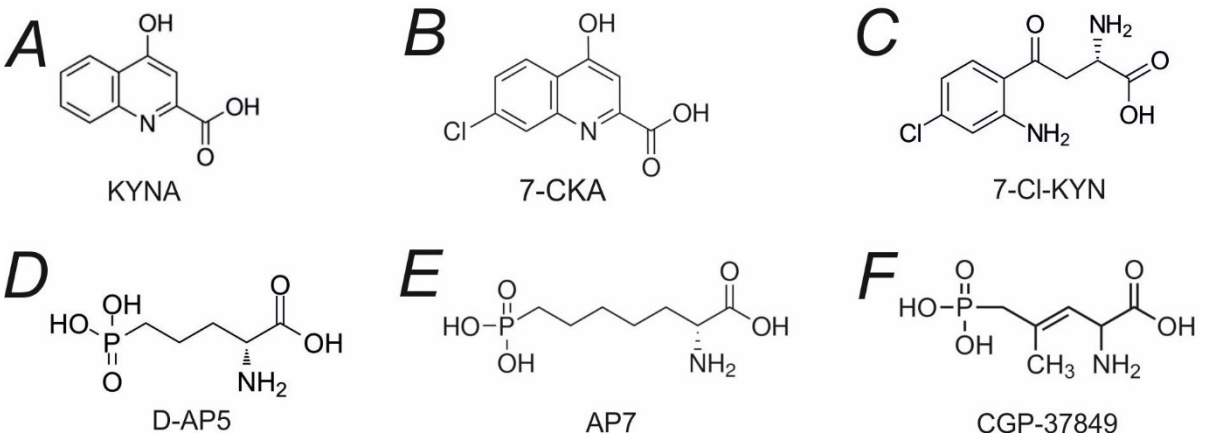

Figure 1.3. Competitive NMDAR antagonists. Projection structures of glycine-site antagonists ***(A)*** kynurenic acid (KYNA), ***(B)*** 7-chlorokynurenic acid (7-CKA), ***(C)*** L-4-chlorokynurenine (4-Cl-KYN), and glutamate-site antagonists ***(D)*** D-2-amino-5-phosphonovaleric acid (D-AP5), ***(E)*** 2-amino-7-phosphonoheptanoic acid (AP7), and ***(E)*** CGP-37849.

1.4.2 Open channel blockers

Open channel blockers bind the NMDAR within the open channel pore, therefore preventing the ion flux. Since most blockers are positively charged compounds, they bind to the receptor in a voltage-dependent manner. The inhibitory effect of blockers is use-dependent, i.e., prior receptor activation is required for the block (Hansen et al., 2021).

Based on the mechanism of action, the channel blockers can be divided into 1) ”trapping” blockers, 2) ”foot in the door” blockers, and 3) ”partial trapping” blockers. The “trapping” blockers are small molecules that physically enter the channel pore for binding and then remain bound inside the pore after agonist dissociation and channel closure. Therefore, channel reopening is needed for trapping blockers to unbind. In contrast, the “foot in the door” blockers prevent channel closure upon binding. As a result, the agonists are unable to unbind from the receptor while blocked by “foot in the door” blockers. The “partial trapping” blockers hinder but do not completely prevent the channel closure and can escape the channel pore upon agonist unbinding (Hansen et al., 2021). At NMDARs, ketamine and MK-801 act as trapping blockers, 9-aminoacridine acts as a “foot in the door” blocker, and memantine acts as a partial trapping blocker (Bolshakov et al., 2003; Mealing et al., 2001).

Magnesium (Mg^{2+}) is an endogenous NMDAR blocker that is abundant in the extracellular fluid. Mg^{2+} produces stronger inhibition in GluN1/GluN2A and GluN1/GluN2B than in GluN1/GluN2C and GluN1/GluN2D receptors (Monyer et al., 1994; Kuner and Schoepfer, 1996). Furthermore, GluN1/GluN2A and GluN1/GluN2B receptors have a higher affinity to Mg^{2+} in comparison to GluN1/GluN2C and GluN1/GluN2D receptors (Kuner and Schoepfer, 1996). Despite the low sensitivity of GluN1/GluN2C and GluN1/GluN2D receptors to Mg^{2+}, the physiological Mg^{2+} concentration of 1 mM is sufficient to inhibit the majority of NMDARs at the resting potential (Kotermanski & Johnson, 2009). Therefore, for the NMDAR activation, the agonist binding alone is not enough and membrane depolarization is needed to relieve the voltage-dependent Mg^{2+} block (Nowak et al., 1984; Tabone & Ramaswami, 2012). Because of this, NMDARs act as coincidence detectors of neuronal activity. The NMDAR role as a coincidence detector is the basis of synaptic plasticity (Tabone & Ramaswami, 2012).

Memantine (Figure 1.4*A*) is a low-affinity NMDAR blocker that is widely used to treat Alzheimer’s disease (Lipton, 2005). At the NMDAR, the binding sites for memantine and Mg^{2+} are partially overlapping. As a result, the physiological concentration of Mg^{2+} strongly reduces the memantine-induced block at GluN1/GluN2A and GluN1/GluN2B receptors, making it almost negligible at the concentration achieved in the brain. In contrast, Mg^{2+} only moderately reduces the memantine inhibition of GluN1/GluN2C and GluN1/GluN2D receptors. Therefore, the GluN1/GluN2C and GluN1/GluN2D receptors are considered a particular target for memantine (Kotermanski & Johnson, 2009).

Memantine preferentially inhibits extrasynaptic over synaptic NMDAR (Xia et al., 2010). Since the excessive activation of extrasynaptic NMDAR is one of the major causes of

excitotoxicity, preferential inhibition of extrasynaptic NMDAR by memantine is considered to underlie its neuroprotective effect (Bading, 2017). Memantine does not impair normal synaptic transmission and, as a partial trapping blocker, is characterized by fast unbinding kinetics (Kotermanski et al., 2009; Lipton, 2005). Due to these characteristics, memantine is clinically well-tolerated and, in contrast to other channel blockers, such as MK-801 and ketamine, produces almost no psychotomimetic side effects (Krystal et al., 2003; Parsons et al., 1999). Memantine has shown its effectiveness to slow the cognitive decline associated with Alzheimer's disease and vascular dementia (Lipton, 2005). In addition, memantine improves cognitive impairments in patients suffering from alcohol-related dementia (Cheon et al., 2008).

Ketamine (Figure 1.4*B*) which acts as an inhibitor of the NMDAR, has been used as an anaesthetic since the 1960s. The inhibitory effect of ketamine at the NMDAR is mediated by two mechanisms: by channel block at lower concentrations and by negative allosteric modulation at higher concentrations (Orser et al., 1997). Similarly to memantine, ketamine shows higher selectivity for the GluN1/GluN2C and GluN1/GluN2D over GluN1/GluN2A and GluN1/GluN2B receptors in the presence of a physiological concentration of Mg^{2+} (Kotermanski & Johnson, 2009). In subanesthetic doses, ketamine demonstrates its effectiveness as a potent analgesic. However, ketamine has a dissociative effect at similar subanesthetic doses therefore, its use as an analgesic is limited due to psychotomimetic side effects (Krystal et al., 2003; Vadivelu et al., 2016). Ketamine is also renowned for rapid-acting and sustained antidepressant effects (Matveychuk et al., 2020; Musazzi et al., 2018).

A low-affinity voltage-dependent NMDAR blocker amantadine (Figure 1.4*C*) accelerates the channel closure and stabilizes the closed state of the channel (Blanpied, 2005; Blanpied et al., 1997). In clinical use, amantadine is commonly prescribed as a medication to reduce levodopa-induced dyskinesia in Parkinson's disease patients (Hansen et al., 2021).

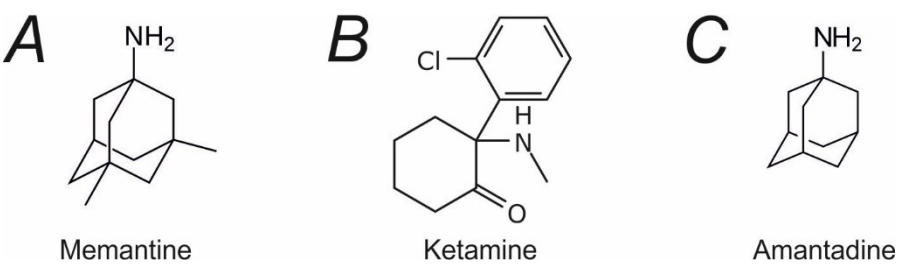

Figure 1.4. Open channel NMDAR blockers. Projection structure of ***(A)*** memantine, ***(B)*** ketamine, and ***(C)*** amantadine.

1.4.3 Allosteric modulators

Allosteric modulators bind the receptor at specific sites other than the agonist sites. Positive allosteric modulators (PAMs) potentiate the receptor function, whereas negative allosteric modulators (NAMs) inhibit the receptor function. Numerous ligands of different natures can modulate the NMDAR activity, including protons, divalent cations, steroid compounds, ethanol, and polyamines.

Zinc ions (Zn^{2+}) are the NMDAR NAM that is stored in high amounts inside the glutamate vesicles in presynaptic terminals. Upon vesicle release, synaptic Zn^{2+} concentration increases from a low nanomolar concentration to a millimolar concentration (Frederickson et al., 2006; Kay & Tóth, 2008). Interestingly, Zn^{2+} and glutamate, which are co-released together, mutually increase each other's affinity upon binding. Zn^{2+}-induced enhancement of glutamate affinity is the underlying mechanism of Zn^{2+}-dependent desensitization of NMDAR. The site of action for Zn^{2+} is located at the ATD of the NMDAR. Zn^{2+} inhibits the NMDAR function by a mechanism involving the reduction of probability of channel opening (P_o). NMDARs with various subunit compositions have different affinity to Zn^{2+}. GluN2A subunit-containing receptors, including the triheteromeric GluN1/GluN2A/GluN2B and GluN1/GluN2A/GluN2C receptors, demonstrate high sensitivity to Zn^{2+} with the IC_{50} in the range of 40-100 nM. In contrast, GluN1/GluN2C receptors are characterized by the Zn^{2+} IC_{50} of 23 μM, therefore, the physiological Zn^{2+}concentration produces only slight inhibition of the receptors of this subtype. In addition to voltage-independent inhibition by allosteric modulation, Zn^{2+} acts as a voltage-dependent channel blocker at GluN1/GluN2A and GluN1/GluN2B receptors in the concentration of several tens of millimoles (Hansen et al., 2021).

Protons negatively modulate the NMDAR function with the IC_{50} value of 50-100 nM, corresponding to the pH range of 7.0-7.4 (Giffard et al., 1990; Tang et al., 1990; Vyklický et al., 1990). Hence, NMDARs are tonically inhibited by extracellular protons at the physiological pH. Furthermore, extracellular proton concentration is not constant and can be changed under various physiological and pathological conditions. For example, neurotransmitter release leads to the liberation of proton-rich vesicle content decreasing the pH inside the synaptic cleft to about 6.9 (Blaustein et al., 2020). Ischemic conditions can reduce the extracellular pH values to as low as 6.5 (Larkin et al., 2022). Such pH decrement can result in substantial inhibition of NMDARs. Protons seem to have no specific site of action at the NMDAR but rather interact with multiple sites at the ATD, LTD, linkers, and

transmembrane helices and decrease the P_o and glycine affinity of the NMDAR (Banke, 2005). In addition, protons affect the NMDAR sensitivity to other modulators and blockers, such as Zn^{2+}, Mg^{2+}, and polyamines.

Ethyl alcohol also acts as a non-selective NAM at the NMDAR. The GluN1/GluN2A and GluN1/GluN2B receptors show a higher affinity for ethanol than GluN1/GluN2C and GluN1/GluN2D receptors. The site of action for ethanol is located at the transmembrane helices of the NMDAR (Chandrasekar, 2013).

Several subunit-specific NMDAR NAMs were developed as tool compounds to distinguish the responses of different NMDAR subtypes. One of the first developed subunit-specific NAMs, ifenprodil (Figure 1.5*A*) was discovered in the 1980s (Carter et al., 1989). Ifenprodil inhibits the GluN2B-containing receptors with 100-400 times higher affinity over the receptors containing other types of GluN2 subunit (Hansen et al., 2021). The NAM effect of ifenprodil is voltage-independent. Upon binding to its site of action at the cleft between GluN1 and GluN2B ATDs, ifenprodil increases the receptor proton sensitivity and thus enhances tonic inhibition of the receptor at physiological pH (Mott et al., 1998; Pahk & Williams, 1997). As a result, the P_o of the receptor decreases (Amico-Ruvio et al., 2012). Ifenprodil can inhibit the GluN1/GluN2B receptor by 90% of its maximal response. In addition, ifenprodil can inhibit triheterometic GluN1/GluN2A/GluN2B receptors by 30% and GluN1/GluN2B/GluN2D receptors by 70% (Hansen et al., 2021). At non-GluN2B-containing receptors, ifenprodil does not exert allosteric modulation but inhibits them by voltage-dependent channel block (Hansen et al., 2021). TCN-201 (Figure 1.5*B*) is a potent NAM that is highly selective to GluN2A-containing NMDARs (Edman et al., 2012). TCN-201 inhibition is mediated by a reduction of glycine affinity (Hansen et al., 2012).

Extracellular polyamines, like endogenous compounds spermine and spermidine (Figure 1.5*C*,*D*) are NMDAR PAMs that act in a voltage-independent and use-dependent manner. NMDARs are potentiated by polyamines by two independent mechanisms: 1) enhancing maximal amplitudes of NMDAR-mediated currents and 2) increasing glycine affinity (McGurk et al., 1990; Ransom & Deschenes, 1990). Polyamine-induced potentiation of GluN1/GluN2B receptor responses is based on the relief of tonic inhibition by protons (Traynelis et al., 1995). However, this mechanism is not involved in the potentiation of GluN1/GluN2A, GluN1/GluN2C, and GluN1/GluN2D receptor responses. Polyamine-induced enhancement of glycine affinity is observed in both GluN1/GluN2A and GluN1/GluN2B receptors. However, triheteromeric GluN1/GluN2A/GluN2B receptors demonstrate no potentiation by polyamines (Yi et al., 2018). In addition to positive

modulation, polyamines can block GluN1/GluN2A and GluN1/GluN2B receptor pores at higher concentrations (Williams, 1997).

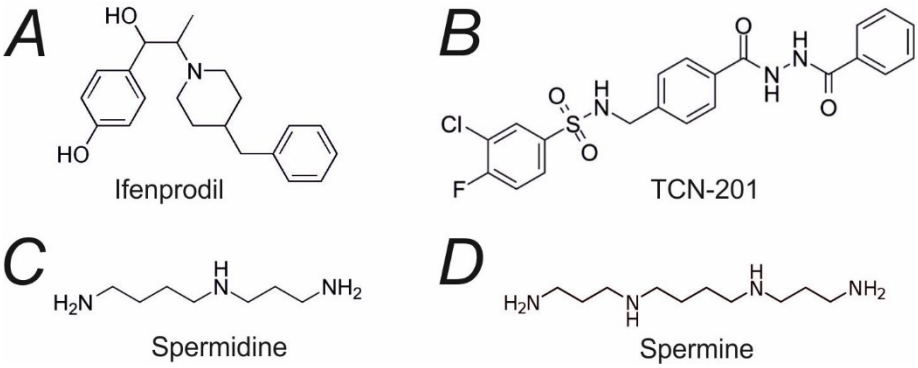

Figure 1.5. Allosteric modulators of NMDAR. Projection structure of ***(A)*** ifenprodil, ***(B)*** TCN-201, ***(C)*** spermidine, and ***(D)*** spermine.

1.4.4 Neuroactive steroids

Neuroactive steroids are steroids of endogenous or exogenous origin that modify the excitability of neurons by binding to membrane receptors (Paul & Purdy, 1992). The class of neuroactive steroids includes neurosteroids, which are neuroactive steroids that are synthesized *de novo* in the CNS from cholesterol (Corpechot et al., 1981). As steroid compounds, neurosteroids have a specific core structure of four fused carbon rings. Neurosteroids that are capable of modulating the NMDAR share the same structural feature – the presence of a negatively-charged group at the carbon C3 of the core structure (Park-Chung et al., 1997).

Naturally-occurring neurosteroid pregnanolone sulfate (5β-pregnan-20-on 3α-yl sulfate; PA-S) (Figure 1.6*A*) negatively modulates the NMDAR function in a voltage-independent and use-dependent manner (Park-Chung et al., 1994; Petrovic, 2005). The effect of PA-S depends on the receptor subunit composition. PA-S shows about two times stronger inhibition of GluN1/GluN2C and GluN1/GluN2D receptors than GluN1/GluN2A and GluN1/GluN2B receptors (Petrovic, 2005). The molecular mechanism of negative modulation by PA-S is ascribed to the increase of NMDAR desensitization and the reduction of channel P_o (Kussius et al., 2009; Park-Chung et al., 1994; Petrovic, 2005). It was shown that PA-S inhibits the NMDAR when approaching the receptor from the outside but not the inside of the cell (Park-Chung et al., 1994; Petrovic, 2005). A study from our laboratory indicated that mutations in the SYTANLAAF motif – a part of the M3 helix that forms the outer channel

vestibule – dramatically diminish the inhibitory effect of PA-S. These data, together with the results of computational modelling, suggest that the outer channel vestibule is the PA-S site of action (Vyklicky et al., 2015). PA-S has been shown to exhibit a neuroprotective effect in an animal model of ischemia (Lapchak, 2006).

Naturally-occurring neurosteroid pregnenolone sulfate (20-oxo-pregn-5-en-3β-yl sulfate; PE-S) (Figure 1.6*B*) demonstrates both positive and negative modulatory effects on the NMDAR. However, at the predominating GluN2A and GluN2B subunit-containing NMDARs, the disuse-dependent positive modulatory effect of PE-S is stronger than the use-dependent negative modulatory effect; therefore PE-S is considered an NMDAR PAM. As already mentioned, the PE-S effect depends on the receptor subunit composition. PE-S potentiation is about twice more potent at GluN1/GluN2A and GluN1/GluN2B receptors than at GluN1/GluN2C and GluN1/GluN2D receptors (Bowlby, 1993; Gibbs et al., 2006; Horak et al., 2004, 2006; Malayev et al., 2002; Wu et al., 1991). On the contrary, the inhibitory effect of PE-S is more potent at GluN1/GluN2C and GluN1/GluN2D receptors than at GluN1/GluN2A and GluN1/GluN2B receptors (Horak et al., 2006). At GluN1/GluN2B receptors, PE-S enhances glycine and glutamate affinity, slows deactivation and desensitization, and increases the P_o (Ceccon et al., 2001). PE-S induces more significant potentiation while binding the resting receptor, i.e. PE-S potentiation is disuse-dependent (Horak et al., 2004). PE-S has a cognitive-enhancing effect. Animal studies have indicated that PE-S has the potential to treat positive and negative symptoms of schizophrenia (Ratner et al., 2019).

A recent study by our laboratory demonstrated that synthetic hemiester analogues of PE-S, such as androst-5-en-3β-yl hemisuccinate (AND-hSuc) (Figure 1.6*C*), are also potent NMDAR PAMs. For example, AND-hSuc is a 4-times more potent PAM of GluN1/GluN2B receptors than PE-S. Similarly to PE-S, the potentiating effect of its hemiester analogues is disuse-dependent (Krausova et al., 2018).

Cholesterol (Figure 1.6*D*) is one of the major lipids in the cell membrane that works as a PAM of the NMDAR. Acute cholesterol depletion has been shown to diminish NMDAR current amplitudes by decreasing the P_o. In addition, cholesterol depletion enhances NMDAR desensitization by increasing the desensitization rate constant. In contrast, cholesterol enrichment potentiates the NMDAR responses by increasing the P_o of the receptors (Korinek et al., 2015). A cholesterol metabolite 24(S)-hydroxycholesterol (24(S)-HC) (Figure 1.6*E*) also acts as a PAM at the NMDAR. 24(S)-HC has been shown to improve the induction of

long-term potentiation (LTP) and decrease the ketamine-induced LTP deficits in hippocampal slices (Paul et al., 2013).

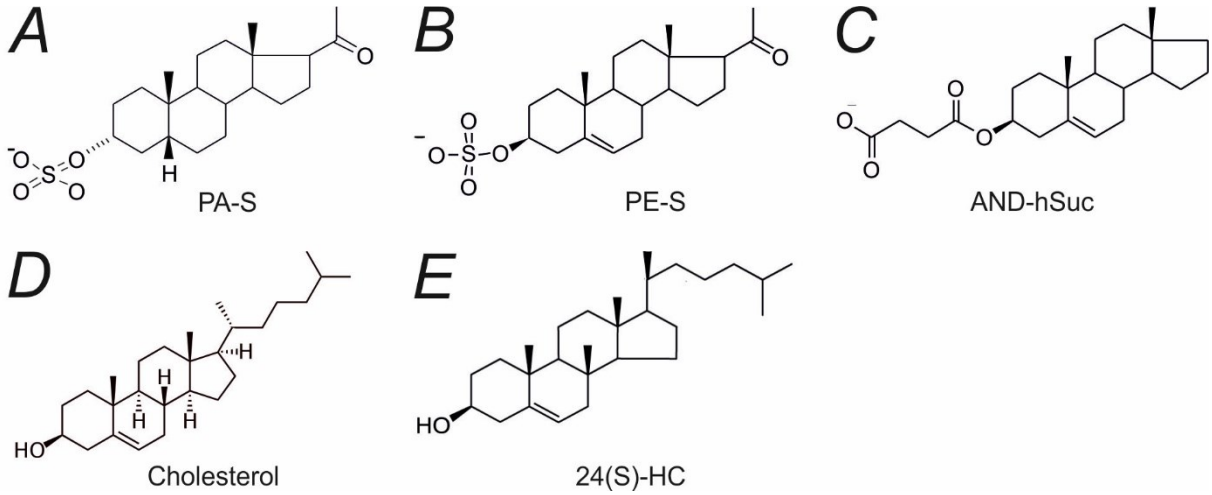

Figure 1.6. Neuroactive steroids modulating NMDAR function. Projection structure of ***(A)*** pregnanolone sulfate (PA-S), ***(B)*** pregnanolone sulfate (PE-S), ***(C)*** androst-5-en-3β-yl hemisuccinate (AND-hSuc), ***(D)*** cholesterol, and ***(E)*** 24(S)-hydroxycholesterol (24(S)-HC).

1.5 Role of NMDA receptors in the pathophysiology of neuropsychiatric disorders

NMDAR-mediated signalling plays a critical role in brain development and synaptic plasticity, and even a slight disturbance in NMDAR function may have serious pathophysiological consequences. NMDAR malfunction was implicated in a wide range of neuropsychiatric disorders. More than 700 *de novo* mutations in the GRIN genes were found in patients suffering from various neuropsychiatric disorders but were absent in healthy individuals. The majority of neuropsychiatric disorder-related mutations were found in the GRIN2A (44%) and GRIN2B (38%) genes. In contrast, only 18% of disorder-related mutations were found in the GRIN1 gene. Overall, GRIN1 mutations were observed in patients with a variety of neuropsychiatric disorders, including intellectual disability, developmental delay, schizophrenia, autism spectrum disorders (ASD), epilepsy, movement disorders, and attention deficit hyperactivity disorder. Among patients with GRIN2A mutations, epilepsy was the predominant phenotype but movement disorders and intellectual disability also occurred in some patients. The great majority of patients with GRIN2B mutations exhibited intellectual disability and developmental delay (Hansen et al., 2021).

1.5.1 NMDA receptor and excitotoxicity

Excessive glutamate levels may trigger neuronal death (Olney, 1969). This effect, known as excitotoxicity, is induced by NMDAR overstimulation-mediated intracellular Ca^{2+} surges. Traumatic brain injury and ischemic brain damage may lead to profound ambient glutamate level increases that result in massive excitotoxic neuronal death (Choi, 2020). Excitotoxic neuronal death was also implicated in neurodegenerative diseases, such as Alzheimer's disease, Huntington's disease, and Parkinson's disease (Dong et al., 2009). Therefore, NMDAR inhibition by antagonists, such as competitive glycine site antagonist 7-CKA, open-channel blocker memantine, or the NAM PA-S, has a neuroprotective effect (Bading, 2017; Lapchak, 2006; Nozaki & Beal, 1992). In addition, memantine has proven its effectiveness in slowing Alzheimer's disease progression (Lipton, 2005).

1.5.2 Affective disorders

Several findings indicate an important role of the glutamatergic system in the pathology of affective disorders, such as major depressive disorder (MDD) and bipolar disorder (BPD). Thus, MDD and BPD are associated with altered glycine and glutamate concentrations in the brain. Numerous studies have indicated elevated glutamate and glycine levels in the serum of both MDD and BPD patients (Ghasemi et al., 2014). Intracerebral microdialysis demonstrated increased glutamate levels in the prefrontal cortex of stressed rats (Moghaddam, 1993). Post-mortem brain tissue analysis also reported increased glutamate concentration in the frontal cortex samples from MDD and BPD patients (Hashimoto et al., 2007). In addition, magnetic resonance spectroscopy studies have indicated elevated glutamate concentration in the prefrontal and frontal cortex, basal ganglia, and thalamic grey matter of both BPD and MDD patients (Ghasemi et al., 2014).

Changes in NMDAR gene expression were reported in MDD. Thus, post-mortem studies showed that the expression of GluN2B and GluN2A subunits was reduced in the perirhinal and prefrontal cortex but elevated in the lateral amygdala of MDD subjects (Adell, 2020). No difference was found between total GluN1 expression in tissue samples of the prefrontal cortex from MDD subjects and controls. Nevertheless, a comparative assessment of splice isoform expression demonstrated an increased portion of the GluN1-1 and GluN1-3 isoforms but a decreased portion of the GluN1-2 and GluN1-4 isoforms in the prefrontal cortex of MDD subjects (Rodríguez-Muñoz et al., 2017). Further studies revealed increased

expression of GluN2B and GluN2C subunits in patients with MDD. In addition, several genetic variants of GluN2B were associated with MDD (Adell, 2020).

Increased NMDAR expression was also found in animal models of MDD. A study on rats that underwent early maternal separation, a widely-used rodent model of depression, indicated increased hippocampal expression of the GluN2B subunit (Masrour et al., 2018). Furthermore, elevated expression of GluN1, GluN2A, and GluN2B subunits was observed in the hippocampus of chronically stressed rats (Calabrese et al., 2012).

Stressor-induced increase in glutamate concentration and NMDAR hyperactivation was suggested as the key factor in the pathogenesis of MDD (Mathews et al., 2012). Therefore, attenuation of NMDAR activity by genetic inactivation or pharmacological inhibition may result in antidepressant-like effects. In line with this assumption, a robust reduction of depression- and anxiety-related behaviour was attained by the GluN2A subunit knock-out in mice (Boyce-Rustay & Holmes, 2006). Furthermore, it was demonstrated that the NMDAR is a target for conventional antidepressants. Thus, tricyclic antidepressants, such as clomipramine, amitryptiline, protriptyline, desmethylpiramine, nortriptyline, and imipramine prevent MK-801 from binding to NMDAR (Reynolds & Miller, 1988). Selective serotonin-reuptake inhibitor fluoxetine inhibits GluN2B- but not GluN2A-containing NMDARs. In contrast, tricyclic antidepressant desipramine inhibits both GluN2A- and GluN2B- containing NMDARs (Kiss et al., 2012).

(S)-ketamine, the S(+) enantiomer of ketamine, has been recently approved by the FDA as a medication for treatment-resistant depression. The antidepressant effect of (S)-ketamine develops within hours after administration and is sustained for several days up to weeks. Single administration was shown to be sufficient to produce a profound antidepressant effect. Because of this, ketamine may be beneficial over conventional antidepressants, which may require administration for several weeks or even several months before the antidepressant effect onset (Matveychuk et al., 2020; Musazzi et al., 2018). Nevertheless, it is not clear if ketamine antidepressant action is produced by (S)-ketamine itself or its metabolite 2R,6R-hydroxynorketamine (2R,6R-HNK). 2R,6R-HNK has displayed a ketamine-like antidepressant effect in mice at much lower pharmacological doses than ketamine. Similarly to (S)-ketamine, 2R,6R-HNK acts as a voltage-dependent channel blocker at the NMDAR. 2R,6R-HNK-induced NMDAR-block was shown to be crucial for its antidepressant effect (Kavalali & Monteggia, 2018). However, several studies suggested the antidepressant effect of 2R,6R-HNK may result from positive modulation of AMPAR activity (van Velzen & Dahan, 2014; Zanos et al., 2016).

In addition, several other NMDAR inhibitors have been also shown to be promising drugs to treat depression. NMDAR channel blocker dextromethadone exerts a rapid-acting and sustained antidepressant effect (Peng et al., 2020). Similarly, rapid antidepressant properties have been demonstrated for 4-Cl-KYN and GluN1/GluN2B receptor NAM CP-101,606 (Preskorn et al., 2008; Zanos et al., 2015).

1.5.3 Epilepsy

NMDAR-mediated signalling plays a key role in epileptogenesis. In 1954, a pioneering study by T. Hayashi demonstrated that high levels of glutamate in the brain could induce seizures (Hayashi, 1954). The NMDAR agonist quinolinic acid is also able to elicit seizures in rats upon intracranial injection (Vezzani et al., 1988). In addition, NMDA injection may result in infantile spasms in rat pups (Velíšek et al., 2007). In turn, glycine-site NMDAR antagonist 7-CKA is characterized by an anticonvulsant effect (Rundfeldt et al., 1994). A low-affinity NMDAR receptor inhibitor remacemide is an anticonvulsant that is capable to prevent seizure recurrence in patients with newly diagnosed epilepsy (Brodie et al., 2002). Altogether, these findings indicate a significant role of NMDAR overstimulation as a seizure-provoking factor.

Epilepsy is associated with altered NMDAR gene expression. Seizure activity led to a rapid increase of GluN1 subunit expression in the rat cortex (Jensen et al., 1997). Moreover, a northern blot study on kindled rats also indicated persistently increased expression of cortical GluN1 subunit (Kikuchi et al., 2000). In turn, acquired epilepsy models have demonstrated a reduction of GluN1 subunit expression in the hippocampus. Altered expression of GluN2A, GluN2B, GluN2C, and GluN2D subunits was also reported in epilepsy (Ghasemi & Schachter, 2011).

Numerous *de novo* mutations in GRIN genes have been implicated in epilepsy. Both gain-of-function and loss-of-function mutations are associated with epilepsy. Generally, mutations in genes encoding prenatally expressed subunits, i.e. GRIN1, GRIN2B, and GRIN2D, lead to more severe clinical phenotypes than mutations in GRIN2A. Thus, epilepsy-related mutations in GRIN1, GRIN2B, and GRIN2D tend to be accompanied by developmental delay (DD) and intellectual disability (ID), whereas GRIN2A mutations tend to be accompanied by language disorders (Xu & Luo, 2018). Moreover, the GluN1 subunit is essential for all functional NMDARs; therefore GluN1 mutations may affect all brain

structures and have a strong impact on neural activity in general. As a result, GRIN1 mutations are characterized by consistently severe phenotypes (Lemke et al., 2016). Overall, GRIN2A mutations comprise the bulk of epilepsy-associated NMDAR mutations (Xu & Luo, 2018). Mouse models demonstrated that the introduction of epilepsy-related NMDAR mutations is sufficient to produce epileptic phenotypes. Thus, *de novo* missense GRIN2A mutation 1930A>G was found in a child with epileptic encephalopathy. This mutation results in amino acid substitution S644G and is characterized by a gain-of-function phenotype. Homozygous mice harbouring the GluN2A(S644G) mutation displayed lethal tonic-clonic seizures in the third postnatal week. Treatment of such mice with NMDAR antagonists, such as dextromethorphan or radiprodil, significantly postponed lethal seizure onset (Amador et al., 2020; Krizay et al., 2019). In contrast, the heterozygous mutant mice exhibit reduced seizure threshold, hyperactivity, and repetitive behaviour. Both homozygous and heterozygous mutant mice demonstrated altered hippocampal morphology (Krizay et al., 2019). *De novo* missense GRIN2A mutation c.1845C>A leads to amino acid substitution N615S. This mutation was identified in a patient with early-onset epileptic encephalopathy (Endele et al., 2010). Similarly, mice with the GluN2A(N615S) mutation demonstrated decreased seizure threshold (Bertocchi et al., 2021).

1.5.4 Schizophrenia

Schizophrenia is a severe mental disorder that affects about 1% of the human population. The symptoms of schizophrenia can be divided into negative, positive, and cognitive. Negative symptoms reflect deficits in emotional responses and include blunted affect (emotional blunting), alogia (poverty of speech), anhedonia (inability to gain pleasure from enjoyable activities), asociality (lack of motivation for social interaction), avolition (lack of motivation), and apathy (Correll & Schooler, 2020). Positive symptoms refer to psychotic manifestations and may include hallucinations, delusions (false fixed beliefs), disorganised speech, and movement disorders. Cognitive symptoms include executive dysfunction deficit, attention deficit, memory impairment, and disorganised thinking. Typically, the onset of schizophrenia occurs in early adulthood (Patel et al., 2014).

The mechanisms of schizophrenia are not well understood yet, although many hypotheses have been proposed. For several decades, dopamine hypothesis has been considered predominant. This hypothesis suggests dopamine dysregulation as the main factor

underlying schizophrenia pathophysiology. The dopamine hypothesis was based on pharmacological studies that reveal the potent antipsychotic effect of dopamine antagonists. Thus, the majority of antipsychotic drugs act as antagonists at the D2-like dopamine receptors. In addition, stimulants, such as amphetamine and cocaine, increase dopamine levels in the CNS and can produce psychotic symptoms similar to the positive symptoms of schizophrenia. However, the dopamine hypothesis does not readily explain the cognitive and negative symptoms of schizophrenia (Erhardt et al., 2007; Plitman et al., 2017).

Glutamate hypothesis of schizophrenia indicates NMDAR hypofunction as a key factor in the pathogenesis of schizophrenia. The glutamate hypothesis is supported by numerous pharmacological studies that demonstrate the capability of NMDAR antagonists to resemble positive, negative, and cognitive symptoms of schizophrenia. Thus, acute administration of NMDAR blockers, such as ketamine and phencyclidine (PCP), may provoke psychosis and cognitive impairments in healthy individuals (Coyle, 2006; Krystal et al., 2003). Moreover, ketamine-treated schizophrenic patients reported similarities between their positive and ketamine-induced psychotic symptoms (Lahti et al., 2001). In addition, ketamine can induce several schizophrenia-related physiological abnormalities, such as increased striatal dopamine release, eye-tracking abnormalities, and event-related potential abnormalities in healthy individuals (Balu, 2016). Subchronic administration of ketamine or PCP has been shown to provoke social withdrawal, mimicking the negative symptoms of schizophrenia. Furthermore, chronic PCP treatment may lead to anhedonic symptoms in rodents (Neill et al., 2014).

Kynurenic acid hypothesis of schizophrenia associates the pathogenesis of the disorder with altered KYNA concentration in the brain. Numerous studies reported elevated KYNA levels in the CNS of schizophrenia patients (Plitman et al., 2017). Similarly to ketamine and PCP, KYNA inhibits the NMDAR function. In addition, KYNA increases dopamine release in the striatum (Erhardt et al., 2007). Elevated KYNA levels may result in cognitive deficits and psychotic symptoms (Balu, 2016). Pharmacological inhibition of KYNA biosynthesis prevented ketamine-induced cognitive impairment (Kozak et al., 2014). Since endogenous KYNA is synthesized as a product of tryptophan metabolism, the kynurenic acid hypothesis of schizophrenia serves as a link between the dopamine and glutamate hypotheses.

In addition to pharmacological studies, several morphological, molecular biology, and genetic findings implicate NMDAR hypofunction in schizophrenia. Nuclear magnetic resonance spectroscopy studies revealed decreased glutamate levels in the prefrontal cortex of schizophrenia patients (Marsman et al., 2013). Post-mortem studies demonstrated reduced

expression of GluN1 and GluN2C subunits in the prefrontal cortex of patients with schizophrenia (Adell, 2020; Balu, 2016). In animal studies, GluN1 knockdown resulted in symptoms resembling negative and cognitive symptoms of schizophrenia, including cognitive impairments, social withdrawal, and anhedonia (Belforte et al., 2010). Moreover, the GluN1 knockdown mice exhibited abnormal schizophrenia-like gamma-oscillations (Jadi et al., 2016). In addition, several *de novo* GRIN mutations have been associated with schizophrenia (Balu, 2016).

1.5.5 Intellectual disability and developmental delay

Intellectual disability (ID) is a neurodevelopmental disorder characterized by considerably impaired intellectual and adaptive functioning. Developmental delay (DD) is defined as an inability to reach developmental milestones at the expected age range (Vasudevan & Suri, 2017). ID and DD affect 1-2% of children (Bowling et al., 2017). Numerous *de novo* mutations in GRIN genes have been identified in ID and DD patients. Overall, GRIN2B mutations are the most frequent among ID/DD-related GRIN mutations. GRIN1 mutations are most often associated with severe intellectual disability with absent speech and profound developmental delay (Hansen et al., 2021; Poot, 2019).

1.5.6 Autism-spectrum disorders

Autism-spectrum disorders (ASD) are a group of neurodevelopmental disorders which are characterized by two main core symptoms: 1) impaired social interaction and 2) restricted and repetitive behaviours. Numerous *de novo* GRIN mutations are associated with ASD. Among GRIN genes, GRIN2B has been identified as the most frequently mutated in ASD patients (Lee et al., 2015; Vieira et al., 2021). Pharmacological modulation of NMDAR may help to relieve ASD symptoms. It was shown that treatment with D-cycloserine – a partial glycine-site agonist of NMDAR – significantly improves social withdrawal and repetitive behaviour in ASD patients (Lee et al., 2015).

2 Objectives of the study

2.1 Functional and pharmacological properties of disease-associated *de novo* mutations in hGluN2B subunit

Hypothesis:

Recent advances in high-throughput DNA sequencing technology enabled broad genetic screening of patients with various neuropsychiatric disorders. As a result, numerous mutations in the hGluN2B subunit have been identified in patients with intellectual disability, developmental delay, autism spectrum disorder, schizophrenia, epileptic encephalopathy, attention deficit hyperactivity disorder, Alzheimer's disease, and cerebral visual impairment (Awadalla et al., 2010; Freunscht et al., 2013; Hamdan et al., 2011, 2014; Lelieveld et al., 2016; Lemke et al., 2014; Platzer et al., 2017; Yavarna et al., 2015). However, the effect of many of these mutations on NMDAR function is unknown.

Objectives:

1) To perform complex characterization of the effect of selected human disease-associated mutations in the hGluN2B subunit on the surface expression and functional characteristics of NMDARs by the combination of electrophysiological and immunofluorescence techniques.
2) To evaluate the potential of a pharmacological compensation for mutation-induced impairments in receptor function by neuroactive steroids.

2.2 Identification of the site of action for pregnenolone sulfate at the NMDAR

Hypothesis:

Endogenous neurosteroid pregnenolone sulfate (PE-S) is widely-known as a PAM of GluN2A and GluN2B subunit-containing NMDARs (Bowlby, 1993; Gibbs et al., 2006; Horak et al., 2004, 2006; Malayev et al., 2002; Wu et al., 1991). However, the location of the PE-S site of action at the NMDAR and the mechanism of PE-S-induced positive allosteric modulation are still unknown.

Objectives

1) To identify the site of action for PE-S at the GluN1/GluN2B receptor using a

combination of the patch-clamp technique, alanine-scanning mutagenesis, and *in silico* modelling.

2) To uncover the mechanism by which PE-S positively modulates NMDAR activity.

2.3 Structure requirements for potentiating neuroactive steroids

Hypothesis:

Neurosteroids are well-known allosteric modulators of NMDARs, capable of modulating NMDAR activity, either positively or negatively. Depending on the spatial organization of chiral carbons C3 and C5, the shape of the neurosteroid molecule can be delineated as either "planar" or "bent". Several studies indicated that "planar" neurosteroids, such as PE-S, potentiate the NMDAR activity, whereas "bent" neurosteroids, such as PA-S, inhibit the NMDAR activity (Borovska et al., 2012; Korinek et al., 2011; Kudova et al., 2015; Park-Chung et al., 1994; Stastna et al., 2009; Weaver et al., 2000; Wu et al., 1991). However, the structural determinants for positive and negative modulatory neurosteroid effects are not well understood and require further investigation.

Objectives

1) To perform structure/activity relationship screening for newly synthesized pregnane analogues in which the ester bond was replaced with the C-C bond (ω5β-pregnan-3β-yl derivatives of carboxylic acids) at recombinant NMDARs using the patch-clamp electrophysiology technique. By performing the structure/activity relationship screening for these novel pregnane-based steroids, we expect to uncover the structural requirements for positive and negative modulatory effects of neurosteroids.
2) To characterize the mechanism of action and identify the site of action for epipregnanolone butyrate (EPA-But), a representative compound selected from the pregnane derivatives mentioned above.

3 Materials and methods

3.1 Materials and chemicals

Unless otherwise noted, ultrapure water with a resistivity of 18.2 MΩ·cm was used for the preparation of all solutions. Ultrapure water was obtained by the Simplicity 185 Water Purification System (Millipore, Billerica, USA). Unless otherwise stated, all chemicals and reagents were purchased from MilliporeSigma (Burlington, USA). The steroids used in experiments were synthesized at the Institute of Organic Chemistry and Biochemistry of the Czech Academy of Sciences (Prague, Czech Republic). The purity of steroids was verified by the Fourier transform nuclear magnetic resonance spectroscopy and thin-layer chromatography.

3.1.1 Lysogeny Broth medium (LB medium)

LB medium contained 1% casein peptone (Serva Electrophoresis, Heidelberg, Germany), 1% NaCl, and 0.5% yeast extract (Serva Electrophoresis). Bottled LB media were sterilized by autoclaving at 121ºC for 15 min.

3.1.2 Agar plates

Freshly prepared 4% solution of Nutrient agar No 2 (Biolife, Milan, Italy) in ultrapure water was sterilized by autoclaving at 121ºC for 15 min. After cooling the agar solution to approximately 50ºC, ampicillin in the concentration of 100 mg/l was added to the solution. The solution was poured into 100 mm Petri dishes and cooled to room temperature to allow the agar to solidify. Agar plates were stored at 4ºC.

3.1.3 Phosphate-buffered saline (PBS)

The composition of phosphate-buffered saline **(**PBS) was as follows: 137 mM NaCl, 2.7 mM KCl, 4.3 mM Na_2HPO_4, and 1.5 mM KH_2PO_4. The pH of the solution was adjusted to 7.3 with NaOH. PBS was sterilized by sterile filtration with a 0.2 μm Porafil membrane filter (Macherey-Nagel, Duren, Germany). Bottled PBS was stored at 4ºC

3.1.4 Trypsin-EDTA solution

Trypsin-ethylenediaminetetraacetic acid (EDTA) solution contained 0.2% trypsin and 0.02% EDTA in PBS. The pH of the solution was adjusted to 7.3 with NaOH. The solution was sterilized by sterile filtration, bottled, and stored at 4ºC.

3.1.5 Culture medium

The culture medium that was used for transfection was composed of Opti-MEM medium (Thermo Fischer Scientific, Waltham, USA) supplemented with 1% fetal bovine serum (FBS, Thermo Fischer Scientific), 20 mM $MgCl_2$, 3 mM KYNA, and 1 mM D,L-AP5.

3.1.6 Intracellular solution (ICS)

Intracellular solution (ICS) had the following composition: 120 mM D-gluconic acid cesium salt, 15 mM CsCl, 10 mM 1,2-bis(o-aminophenoxy)ethane-N,N,N′,N′-tetraacetic acid (BAPTA), 10 mM 4-(2-hydroxyethyl)-1-piperazineethanesulfonic acid (HEPES), 3 mM $MgCl_2$, 1 mM $CaCl_2$, and 2 mM adenosine triphosphate magnesium salt ($ATP{\cdot}Mg^{2+}$). The pH of the ICS was adjusted to 7.2 with CsOH. The ICS was sterilized by sterile filtration with a 0.22 μm syringe filter unit (MilliporeSigma), aliquoted, and stored at -20ºC. The final osmotic concentration of the ICS was 290 mOsm/l.

3.1.7 Mg^{2+}- free extracellular solution (ECS)

The extracellular solution (ECS) contained 160 mM NaCl, 2.5 mM KCl, 10 mM HEPES, 10 mM glucose, 0.2 mM EDTA, and 0.7 mM $CaCl_2$. To avoid glycine contamination, ultrapure grade chemicals and HPLC water were used for the preparation of the ECS for the experiments assaying glycine dose-response effect. Acid cleaning of glassware was introduced as an additional precaution to manage glycine contamination. The pH of the ECS was adjusted to 7.3 with NaOH. The ECS was sterilized by sterile filtration with a 0.2 μm Porafil membrane filter (Macherey-Nagel) and stored at 4ºC. The final osmotic concentration of the ECS was 320 mOsm/l.

3.1.8 Mg^{2+}- containing extracellular solution (Mg^{2+}-ECS)

Mg^{2+}-ECS contained 160 mM NaCl, 2.5 mM KCl, 10 mM HEPES, 10 mM glucose, 1 mM $MgCl_2$, and 2 mM $CaCl_2$. The pH of Mg^{2+}-ECS was adjusted to 7.3 with NaOH. The ECS was sterilized by sterile filtration with a 0.2 μm Porafil membrane filter and stored at 4ºC. The final osmotic concentration of the Mg^{2+}-ECS was 320 mOsm/L.

3.1.9 cDNA constructs

For transfection, the following cDNA constructs were used:
GluN1-1a (GenBank accession no. U08261) in the pcDNA I/Amp expression vector;
GluN1-4a (GenBank accession no. NP_001257539) in the pcDNA3 expression vector;
GluN2A (GenBank accession no. D13211) in the RK7 expression vector;
GluN2B (GenBank accession no. M91562) in the RK7 expression vector;
GluN2C (GenBank accession no. M91563) in the RK7 expression vector;
GluN2D (GenBank accession no. L31611) in the RK7 expression vector;
GluN3A (GenBank accession no. Q9R1M7) in the iGFP-N3 expression vector;
hGluN1 (GenBank accession no. NP_015566) in the pCl-Neo expression vector;
hGluN2B (GenBank accession no. NP_000825) in the pCl-Neo expression vector;
Enhanced green fluorescent protein (eGFP) in the pQBI 25 expression vector (Tacara Bio Inc., Tokyo, Japan).

3.2 Site-directed mutagenesis

Site-directed mutagenesis technique was used to generate receptors with disease-associated mutations and alanine scanning. Mutations were introduced in the wild-type NMDAR by polymerase chain reaction (PCR) using custom-designed overlapping oligonucleotide primers, QuikChange II XL Site-Directed Mutagenesis Kit (Agilent Technologies, Santa Clara, USA), and Eppendorf 5333 MasterCycler Thermal Cycler (Eppendorf AG, Hamburg, Germany). PCR primers were designed in a way to incorporate the desired nucleotide change in the central part of the primer and synthesized by Eurofins Genomics (Ebersberg, Germany). PCR amplifications were performed in the total volume of 20 μl according to the QuikChange II XL Site-Directed Mutagenesis Kit. The obtained PCR product was incubated with DpnI restriction enzyme (New Englan Biolabs, Ipswich, MA, USA) to eliminate the template cDNA. 2 μl of the PCR product was added into tubes

containing 50 µl of XL10-Gold ultracompetent *Escherichia coli* cells and incubated on ice for 15 min. Transformation of XL10-Gold cells was performed by heat shock via incubation at 42ºC for 45 s. After transformation, the tubes were incubated on ice for 2 min to reduce cell damage. The cells were transferred into culture tubes with 200 µl of LB medium and incubated on a shaker with 200 rpm rotation at 37ºC for 1 hour. The resulting culture was spread on agar plates and incubated overnight at 37ºC to grow bacterial colonies. Selected colonies were picked, transferred into culture tubes LB medium with ampicillin (100 mg/l), and incubated overnight on a shaker at 37ºC and 200 rpm. The obtained culture was centrifuged at 16000 g to pellet bacteria. Plasmid cDNA was isolated using a High-Speed Plasmid Mini Kit (Geneaid Biotech, New Taipei City, Taiwan) according to the manufacturer's instructions. The concentration of obtained plasmid cDNA was evaluated by spectrophotometer ND-1000 (NanoDrop Technologies, Wilmington, USA). All mutations were verified by DNA sequencing (Eurofins Genomics).

3.3 Cell culture and transfection

HEK293T cells (Human Embryonic kidney cells, ATCC, Manassas, USA) were used as an expression system for recombinant NMDARs used in electrophysiology experiments. The cells were cultured in 24-well plates (TPP, Trasadingen, Switzerland) coated with collagen (Serva, Heidelberg, Germany) in Opti-MEM medium supplemented with 5% FBS. COS-7 cells were cultured in poly-L-lysine (Serva, Heidelberg, Germany) coated glass-bottom 12-well plates (TPP) in Eagle's Minimum Essential Medium (EMEM) supplemented with 10% FBS, 22 mM KCl, gentamicin (20 mg/l, Life Technologies, Carlsbad, USA), 2 mM L-glutamine (Life Technologies), and 2% neural supplement B27 (Life Technologies). Cell cultures were maintained in a CO_2 incubator at 37ºC and 5% CO_2 concentration. The medium was changed every 48-72 hours and repetitive passaging was performed when the cells reached 80% confluence.

The transfection of HEK293T cells was performed with the Magnet Assisted Transfection (MATra) technique. In brief, 0.8 µl of MATra transfection reagent (IBA Lifesciences, Gottingen, Germany) and 0.9 µg of cDNA (0.3 µg of GluN1, 0.3 µg of GluN2, and 0.3 µg of eGFP) were added into 50 µl of Opti-MEM media and mixed gently by pipetting. The mixture was incubated at room temperature for 20 min. Before transfection, the cells were washed with PBS to remove serum, Opti-MEM/MATra/cDNA mixture was added

to the cells, and incubated at the Universal Magnet Plate (IBA Lifesciences) for 30 min in a CO_2 incubator at 37ºC and 5% CO_2. After this, the cells were washed with PBS, dissociated from the well surface with trypsin-EDTA solution, aspirated by pipetting in pre-warmed culture medium, and plated to 24 mm round coverslips (Glaswarenfabrik Karl Hecht, Sondheim vor der Rhön, Germany) coated with poly-L-lysine (1 mg/ml, Serva, Heidelberg, Germany). The cells were grown in a CO_2 incubator at 37ºC and 5% CO_2.

The transfection of COS-7 cells was performed with Lipofectamine 2000 reagent (Life Technologies). At 18-24 hours following transfection, the cells were seeded on 24 mm round coverslips coated with poly-L-lysine (1 mg/ml, Serva). The cells were transfected with 4 µl of Lipofectamine 2000 and 1.8 µg of cDNA, as described (Kaniakova et al., 2012).

3.4 Cholesterol depletion

For cholesterol depletion, HEK293T cells underwent 60 min incubation in culture medium supplemented with 10 mM methyl-β-cyclodextrin (βCDX) at 37ºC and 5% CO_2. Estimation of cholesterol content by liquid chromatography-mass spectrometry indicated 50-60% cholesterol depletion.

3.5 Immunofluorescence microscopy

At 24-36 hours after transfection, COS-7 cells were washed with PBS and incubated in blocking solution (PBS containing 10% normal goat serum) on ice for 10 min. In the next step, the cells were stained with primary rabbit anti-GFP (1:1000; Merck Millipore) and secondary goat anti-rabbit Alexa Fluor 555 (1:1000; Thermo Fischer Scientific) antibodies for 30 min, washed with PBS, fixed by incubation in 4% paraformaldehyde in PBS for 20 min, and mounted with ProLong Antifade reagent (Thermo Fischer Scientific). Fluorescent images were taken with the Olympus Cell-R system (Olympus, Tokyo, Japan). The analysis of the total and surface fluorescent intensities was performed using ImageJ software (NIH, Bethesda, MD, USA) as described (Lichnerova et al., 2014).

3.6 Electrophysiology

Electrophysiological experiments were conducted on HEK293T cells 24-48 hours after transfection. Successfully transfected cells were identified by eGFP expression using a fluorescence inverted microscope Olympus CKX41 (Olympus). All electrophysiological measurements were performed using the patch-clamp technique in the voltage-clamp mode. If not mentioned otherwise, the holding potential was kept at -60 mV. Correction of liquid junction potential (-14 mV) was not performed. All patch-clamp experiments were conducted in whole-cell or outside-out configurations. NMDAR currents were recorded using an Axon Axopatch 200B Microelectrode Amplifier (Molecular Devices, San Jose, USA) after compensation of series resistance (<10MΩ) and capacitance by 80-90%. The analogue signal from the amplifier was filtered at 2 kHz by a low-pass Bessel filter and digitized with Axon Digidata 1550B Low-Noise Data Acquisition System (Molecular Devices) at a sampling rate of 10 kHz. Recording of digitized data was implemented by software pClamp 10.6 (Molecular Devices). To avoid the influence of electromagnetic fields and vibrations, the experimental setup was placed on an anti-vibration table (TMC, Peabody, USA) inside a Faraday cage. A pipette puller P-1000 (Sutter Instrument, Novato, USA) was used to produce glass microelectrodes (4-6 MΩ) from borosilicate glass capillaries with an external diameter of 1.5 mm and an internal diameter of 0.86 mm (BioMedical Instruments, Zöllnitz, Germany). Glass microelectrodes were filled with the ICS. Accurate microelectrode placement was achieved by a motorized micromanipulator MP-225 (Sutter Instrument). All electrophysiological experiments were performed at room temperature. The application of the ECS was performed by a custom microprocessor-controlled multibarrel perfusion system. The perfusion system provides a high solution exchange rate (∼12 ms) around the cell. Mg^{2+}-free ECS was used in all electrophysiological experiments, while Mg^{2+}-ECS was used to wash the cells in between experiments. Unless otherwise stated, NMDAR responses were evoked by the co-application of 30 μM glycine and the specified concentration of glutamate dissolved in the Mg^{2+}-free ECS. Steroids were dissolved in DMSO and added to Mg^{2+}-free ECS at the specified concentration. The final dilution of steroids was made by 1 min sonication in an ultrasonic water bath Sonorex Digitec DT 100/H (Badelin Electronic, Berlin, Germany). All control and test ECS contained the final DMSO concentration of 1%. (+)-MK-801 maleate (Hello Bio, Bristol, UK) was dissolved in ultrapure water to obtain a stock solution of 2 mM and added to Mg^{2+}-free ECS with the final MK-801 concentration of 1 μM.

3.7 Data analysis

3.7.1 Electrophysiological recordings analysis

Analysis of electrophysiological recordings was performed using Clampfit 10.6 (Molecular Devices).

3.7.2 Steroid effect assessment

The degree of steroid modulation (E; either potentiation or inhibition) was calculated using the following equation:

$$E = (I_S - I_A)/I_A \times 100, \quad \text{Equation 1}$$

where I_A is the current amplitude of the response to glutamate application and I_S is the current amplitude of the response to the co-application of glutamate and the steroid (Figure 3.1*A-B*). Glutamate concentration was equal to 1 μM in the experiments performed at GluN2B-containing recombinant NMDARs or 3 μM in the experiments performed at GluN2A-containing recombinant NMDARs.

The relative degree of potentiation (E) induced by different steroid doses in individual HEK293T cells was fit to the following equation:

$$E = E_{max}/(1 + (EC_{50}/[steroid])^h \quad \text{Equation 2}$$

where E_{max} is the maximal degree of steroid-induced potentiation, EC_{50} is the steroid concentration that produces half-maximal modulation, $[steroid]$ is the concentration of the steroid, and h is the Hill coefficient.

3.7.3 Agonist dose-response analysis

To fit the normalized currents (I) measured in individual HEK293T cells, the following logistic equation was used:

$$I = 1/(1 + (EC_{50}/[agonist])^h), \quad \text{Equation 3}$$

were EC_{50} is the agonist concentration that produces a half-maximal NMDAR response, $[agonist]$ is the concentration of agonist (glycine or glutamate), and h is the Hill coefficient.

Glutamate dose-response assessment was made in the presence of 30 µM glycine and glycine dose-response assessment was made in the presence of 1 mM glutamate.

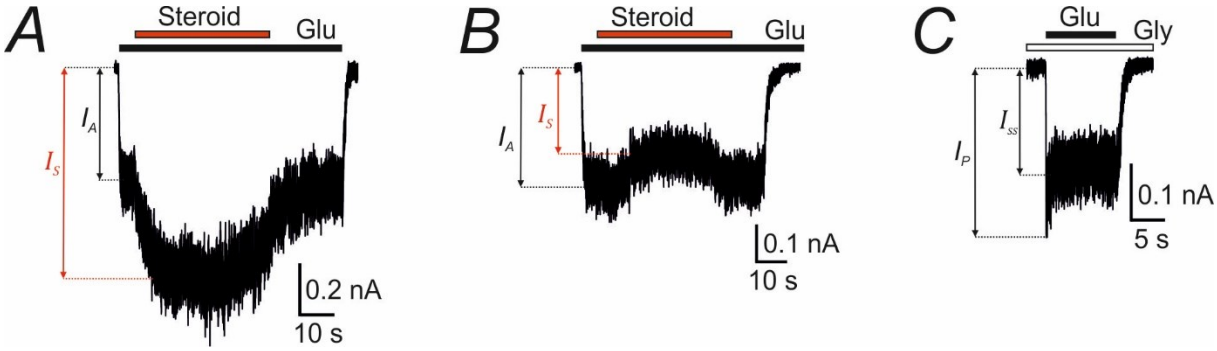

Figure 3.1. ***(A-B)*** Representative recordings demonstrate the effect of potentiating ***(A)*** and inhibitory ***(B)*** steroids on GluN1/GluN2B receptor responses to 1 µM glutamate in the presence of 30 µM glycine. I_A indicates the amplitude of the current response to glutamate alone and I_S is the current amplitude of response to the co-application of glutamate and steroid. ***(C)*** Representative recording demonstrates the response of GluN1/GluN2B receptors induced by 1 mM glutamate in the presence of 30 µM glycine. I_P indicates the peak response and I_{SS} indicates the steady-state response.

3.7.4 Current density analysis

The current density (j) was determined using the following formula:

$$j = I_{max} / C_{m,} \qquad \text{Equation 4}$$

where I_{max} is the maximal peak amplitude of NMDAR response to 1 mM glutamate and 30 µM glycine and C_m is the membrane input capacitance.

3.7.5 Open probability analysis

The NMDAR open probability (P_o) was estimated from the kinetics of MK-801 block onset. 1 µM MK-801 was used to inhibit the NMDAR responses to 1 mM glutamate and 30 µM glycine. Gepasi 3.21 (Mendes, 1993; Mendes, 1997; Mendes & Kell, 1998) was used to fit the data to the following kinetic model:

$$D \underset{k_d}{\overset{k_r}{\rightleftharpoons}} R \underset{k_c}{\overset{k_o}{\rightleftharpoons}} O \underset{k_u}{\overset{k_b}{\rightleftharpoons}} B \quad ,$$

where *D, R, O*, and *B* indicate desensitized, closed, open, and MK-801 blocked state of the receptor, respectively. Calculations based on the rate constants determined earlier (Cais et al., 2008) predict a high probability of the existence of the NMDAR in the doubly liganded state in the presence of 1 mM glutamate; therefore, glutamate binding steps are neglected and not considered in the scheme. The fitting was implemented by a two-step procedure (Turecek et al., 2004). In the first step, the NMDAR desensitization and desensitization kinetics were characterized. Desensitization (*D*) was calculated as:

$$D = 1 - (I_{SS}/\, I_P), \qquad \text{Equation 5}$$

where I_{SS} is the steady-state response and I_P is the peak response to 1 mM glutamate (Figure 3*C*). The kinetic constants characterizing the onset of desensitization (k_d) and resensitization (k_r) were calculated by the following equations:

$$k_d = \mathrm{D}/\, \tau_d\ , \qquad \text{Equation 6}$$

$$k_r = (1 - \mathrm{D})/\, \tau_d\ . \qquad \text{Equation 7}$$

The rate of desensitization onset (τ_d) was calculated in Clampfit 10.6 by a single exponential function using the Levenberg–Marquardt algorithm.

In the second step, the kinetic constants k_r and k_d were fixed at values determined in the first step. The close rate constant (k_c) was set at an arbitrary value of 200 s^{-1}. The opening rate constant (k_o) was set as a free parameter. The time course of MK-801 inhibition was fitted to the kinetic model mentioned above. The MK-801 blocking rate constant (k_b) was set at the value of 25 $\mu M^{-1}\ s^{-1}$ (Huettner & Bean, 1988; Jahr, 1992; Rosenmund et al., 1995).

3.7.6 Comparative analysis of MK-801 blocking rate

The NMDAR responses to 1 mM glutamate were inhibited by the application of MK-801 (1 μM) in the continuous presence of glutamate. The time course of the MK-801 blockade was fitted to a double-exponential function to determine time constants, τ_{slow} and τ_{fast}. The weighted time constant τ_w was calculated using the following equation:

$$\tau_w = (\tau_{fast} \times I_{fast} + \tau_{slow} \times I_{slow})/\, (I_{fast} + I_{slow})\ , \qquad \text{Equation 8}$$

where I_{fast} is the current amplitude of the fast component and I_{slow} is the current amplitude of the slow component.

3.7.7 Statistical analysis

Data was compared as an effect in control conditions versus an effect in experimental conditions. Statistical analysis was performed with Sigma Plot 14.0 software package (Systat Software Inc., Palo Alto, USA). All data are presented as the mean ± standard error of the mean (SEM), *n* indicates the number of cells that have been tested. Data distribution was evaluated by the Shapiro-Wilk normality test and the equality of group variances was assessed by the Brown–Forsythe test. Parametric statistics (Student's *t*-test, paired *t*-test, or ANOVA) was used for data sets with normal distribution whereas nonparametric statistics (Wilcoxon-signed rank test, Mann–Whitney rank-sum test, or Kruskal–Wallis one-way ANOVA on ranks) was used for data sets without normal distribution. At multiple group comparisons, post hoc tests were performed when a significant difference had been found. Correlation between data sets was assessed with the Pearson product-moment correlation coefficient. The p-value ≤ 0.05 was considered significant in the study.

4 Results

4.1 Functional and pharmacological properties of disease-associated *de novo* mutations in hGluN2B subunit

Mutations in the TMD region of NMDAR often result in profound changes in receptor function (Dai & Zhou, 2013; Kazi et al., 2014; Vyklicky et al., 2015; Wang et al., 2017). Therefore, in this study, we evaluated the functional characteristics and surface expression of selected human disease-associated mutations in the TMD of the hGluN2B subunit. For this purpose, we screened publicly accessible databases (https://www.ncbi.nlm.nih.gov/clinvar) and selected 10 *de novo* missense mutations (P553L; V558I; W607C; V618G; S628F; E657G; G820E; G820A; M824R; L825V) within the TMD of GluN2B subunit (Figure 4.1*A-C*) that were found in patients with various neuropsychiatric disorders (Table 4.1). In the following experiments, we assessed the current density, agonist affinity, degree of receptor desensitization, P_o, and sensitivity to selected neurosteroids of receptors with the hGluN2B(P553L; V558I; W607C; V618G; S628F; E657G; G820E; G820A; M824R; L825V) mutations. The results of this study were published in *Frontiers in Molecular Neuroscience* (Vyklicky et al., 2018).

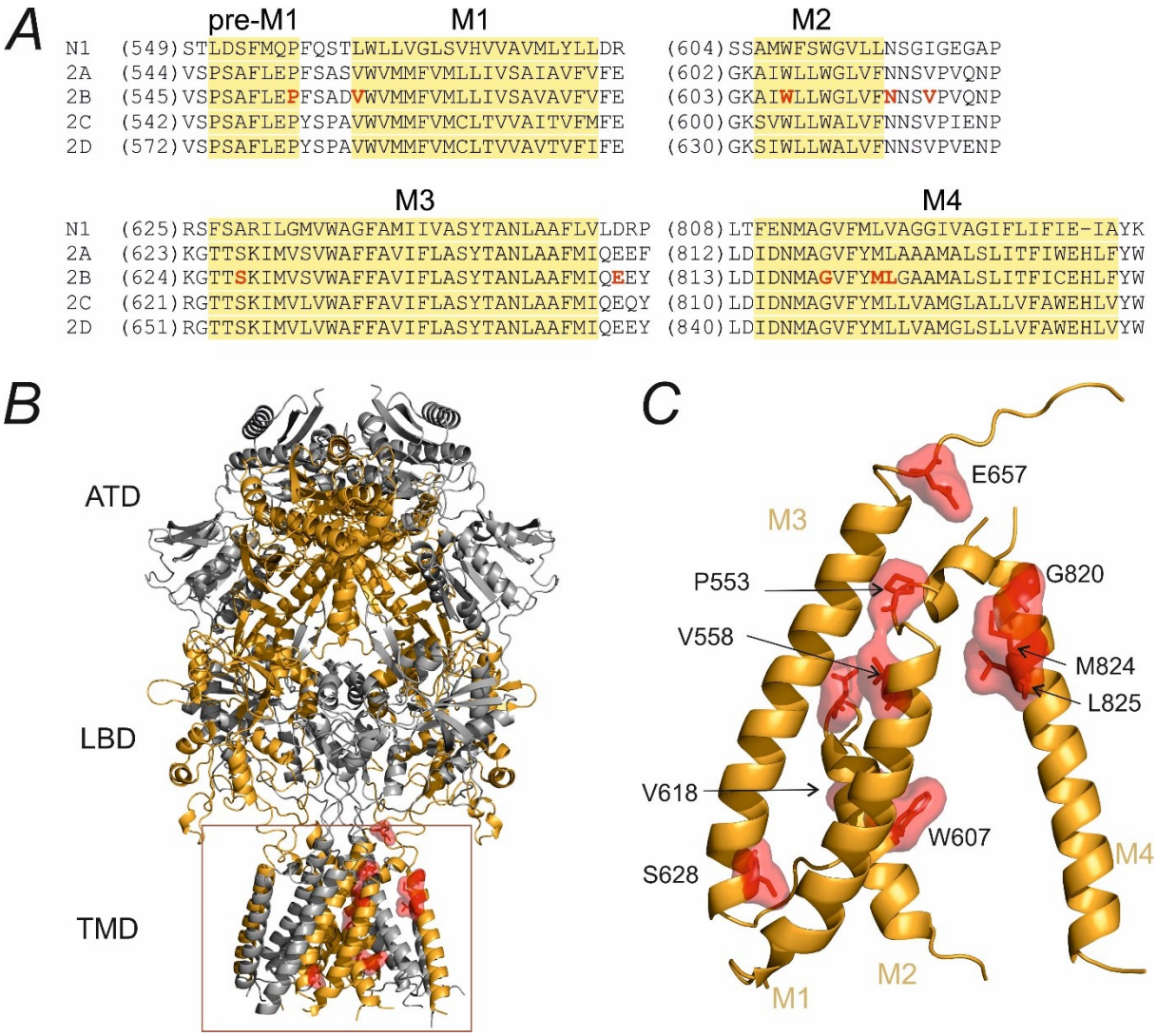

Figure 4.1. Location of the mutated residues in the NMDAR TMDs. ***(A)*** Multiple amino acid sequence alignment of hGluN1, hGluN2A, hGluN2B, hGluN2C, and hGluN2D subunits. The pre-M1, M1, M2, M3, and M4 helices of the TMD are marked in orange. **(*B-C*)** Ribbon structure of hGluN1/hGluN2B receptor (Karakas & Furukava, 2014; Lee et al., 2014). The hGluN1 subunit is labelled in grey and the hGluN2B subunit is labelled in orange. The TMDs are indicated by an orange rectangle. The mutated amino acid residues that have been found in individuals with neuropsychiatric disorders are highlighted in red.

Table 4.1. Selected *de novo* mutations in the h*GRIN2B* subunit and their phenotypic profiles.

Amino acid substitution	Genotype	Phenotype	Age of onset	References
P553L	c.1658C>T	ID, hypotonia	Early postnatal	(de Ligt et al., 2012)
V558I	c.1672G>A	ID	-	(Hamdan et al., 2014; Lelieveld et al., 2016)
W607C	c.1821G>T	DD, ID, dysmorphic features	-	(Yavarna et al., 2015)

V618G	c.1853T>G	ID, WS, epi,	4 months	(Lemke et al., 2014)
S628F	c.1883C>T	ID, DD, epi	-	(Platzer et al., 2017)
E657G	c.1970A>G	ID, DD	-	(Platzer et al., 2017)
G820E	c.2459G>A	ID, microcephaly	Early postnatal	(Hamdan et al., 2014)
G820A	c.2459G>C	ID, DD, ES, GVL, DMD, ASD	-	(Platzer et al., 2017)
M824R	c.2471T>G	ID, DD, Rett-like phenotype, microcephaly, epi activity on the EEG	2 months	(Zhu & Paoletti, 2015)
L825V	c.2473T>G	ASD	-	(Awadalla et al., 2010; Swanger et al., 2016)

Abbreviations: ID - intellectual disability; DD - developmental delay; WS - West Syndrome; epi – epilepsy and/or seizures, infantile spasms; ASD - Autism Spectrum Disorder; ES - epileptic spasms; GVL - generalized cerebral volume loss; DMD - Dyskinetic Movement Disorder.

4.1.1 Disease-associated mutations affect the current density and surface expression of NMDAR

HEK293T cells were transfected with eGFP, hGluN1 subunit, and either WT or mutated hGluN2B subunit. The amplitude of a response to the application of 1 mM glutamate in the continuous presence of 10 μM glycine was evaluated by the patch-clamp technique. The normalized peak current density of HEK293T cells expressing the WT receptors was 66 pA/pF (Figure 4.2*A-B*). A subset of mutated receptors (hGluN1/hGluN2B(P553L; S628F; G820E; M824R)) demonstrated no response (peak current <5 pA) to glutamate (Figure 4.2*A-B*). Receptors with hGluN2B(W607C; V618G; E657G; G820A) mutations exhibited significantly diminished current densities (Figure 4.2*A-B*). The values of current densities mediated by hGluN1/hGluN2B(V558I) and hGluN1/hGluN2B(L825V) receptors were similar to those mediated by WT receptors Figure 4.2*B*).

Next, we evaluated the surface expression of mutated receptors using immunofluorescence microscopy. COS-7 cells were transfected with DNA vectors encoding YFP-tagged hGluN1 subunit and either WT or mutated hGluN2B subunit. The analysis of obtained immunofluorescence microscopy images indicated that the surface expression of mutated hGluN1/hGluN2B(W607C; S628F) receptors was significantly lower than that of WT receptors (Figure 4.2*C-D*). In contrast, hGluN1/hGluN2B(G820E) receptors exhibited

increased surface expression. The surface expression of hGluN1/hGluN2B(P553L; V558I; V618G; E657G; G820A; M824R; L825V) was similar to that in WT receptors.

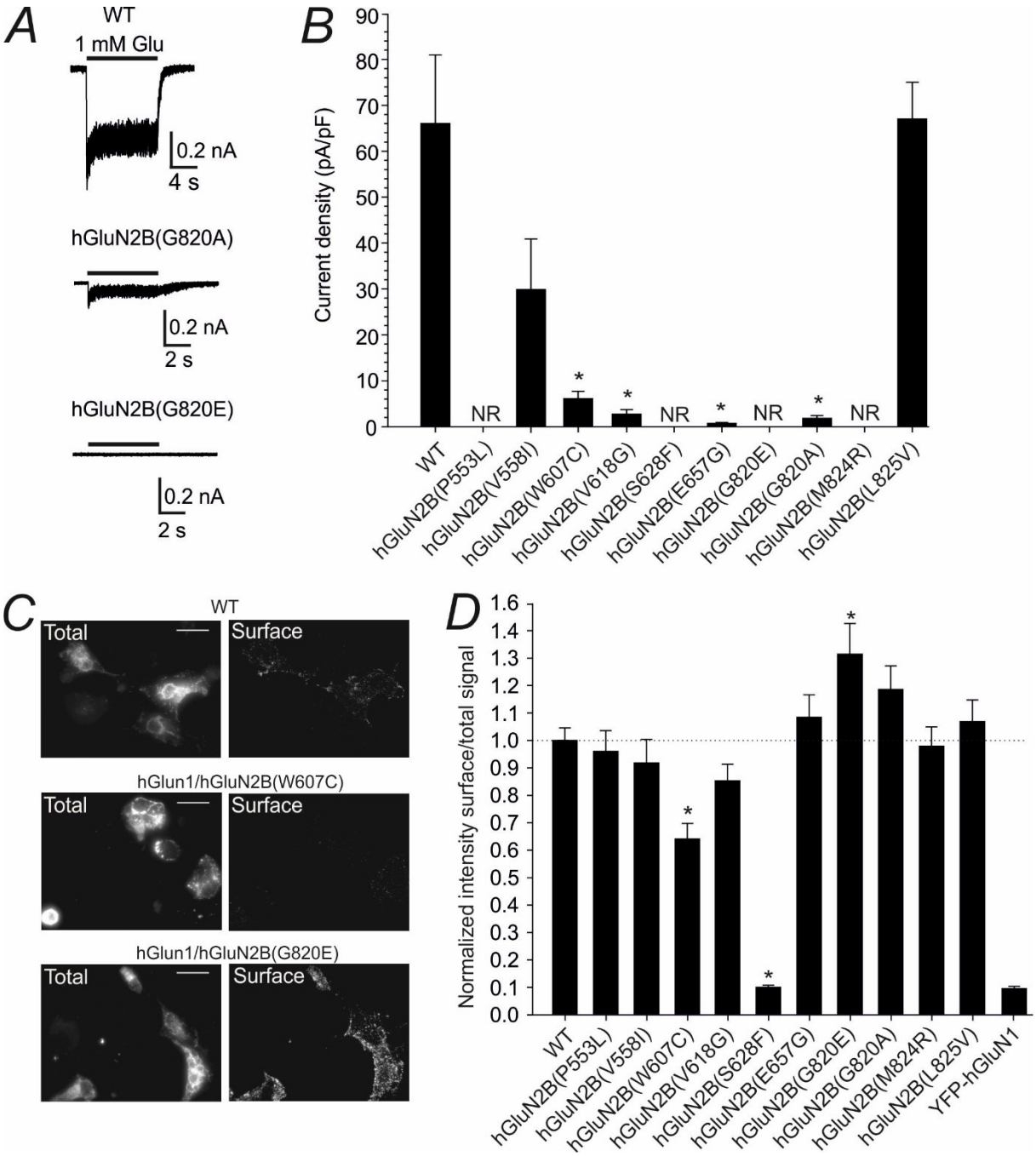

Figure 4.2. Effect of disease-associated mutations on the current density and surface expression of NMDARs. ***(A)*** Representative current responses elicited in WT, hGluN1/hGluN2B(G820A), and hGluN1/hGluN2B(G820E) receptors by 1 mM glutamate. The recordings were performed in the presence of 10 μM glycine; the duration of glutamate application is indicated by black bars. ***(B)*** The bar graph shows average current densities ± SEM recorded in HEK293T cells expressing NMDARs with WT and mutated hGluN2B subunits (n = 5-23). Mutations that demonstrated no glutamate-induced currents were indicated as NR (non-responding). Statistical differences between the groups were tested by Kruskal-Wallis one-way ANOVA on Ranks. Mann-Whitney Rank Sum Test was used to

check the statistical difference between WT and mutated receptors; * $p < 0.05$. ***(C)*** Representative images show the total (left panel) and surface expression (right panel) of WT, YFP-hGluN1/hGluN2B(W607C), and YFP-hGluN1/hGluN2B(G820E) receptors in COS-7 cells. Scale bars denote 20 μm. ***(D)*** Bar graph shows the relative surface-to-total expression levels of WT and mutated hGluN1/hGluN2B receptors and YFP-hGluN1 subunit alone in COS-7 cells ($n = 35$); * $p < 0.05$. Error bars indicate the SEM.

4.1.2 Mutations in the TMD alter NMDAR agonist affinity

To perform dose-response analysis of agonist-evoked responses, the activity of WT and mutated receptors was evaluated at various concentrations of glutamate (0.1; 0.3; 1; 3; 10; 30; 100; and 1000 μM) and glycine (0.1; 0.3; 1; 3; 10; and 30 μM). These experiments demonstrated that hGluN1/hGluN2B(W607C) receptors have a 3.2-fold lower glutamate affinity in comparison to that of WT receptors (Figure 4.3*A*; Table 4.2). In contrast, hGluN1/hGluN2B (E657G) receptors showed 2.3 times higher glutamate affinity than the WT receptors (Figure 4.3*A*-*B*; Table 4.2). In addition, hGluN1/hGluN2B(W607C) and hGluN1/hGluN2B(E657G) receptors exhibited significantly lower (2.0- and 1.8- fold, respectively) glycine affinity than WT receptors (Figure 4.3*B*; Table 4.2). Interestingly, the changes in glutamate affinity in hGluN1/hGluN2B(E657G) receptors and glycine affinity in GluN1/hGluN2B(W607C) and hGluN1/hGluN2B(E657G) receptors were accompanied by a reduction in the Hill coefficient values (Table 4.2**)**. A decrease in the Hill coefficient may indicate the altered degree of cooperativity among agonists binding to the receptor (Weiss, 1997).

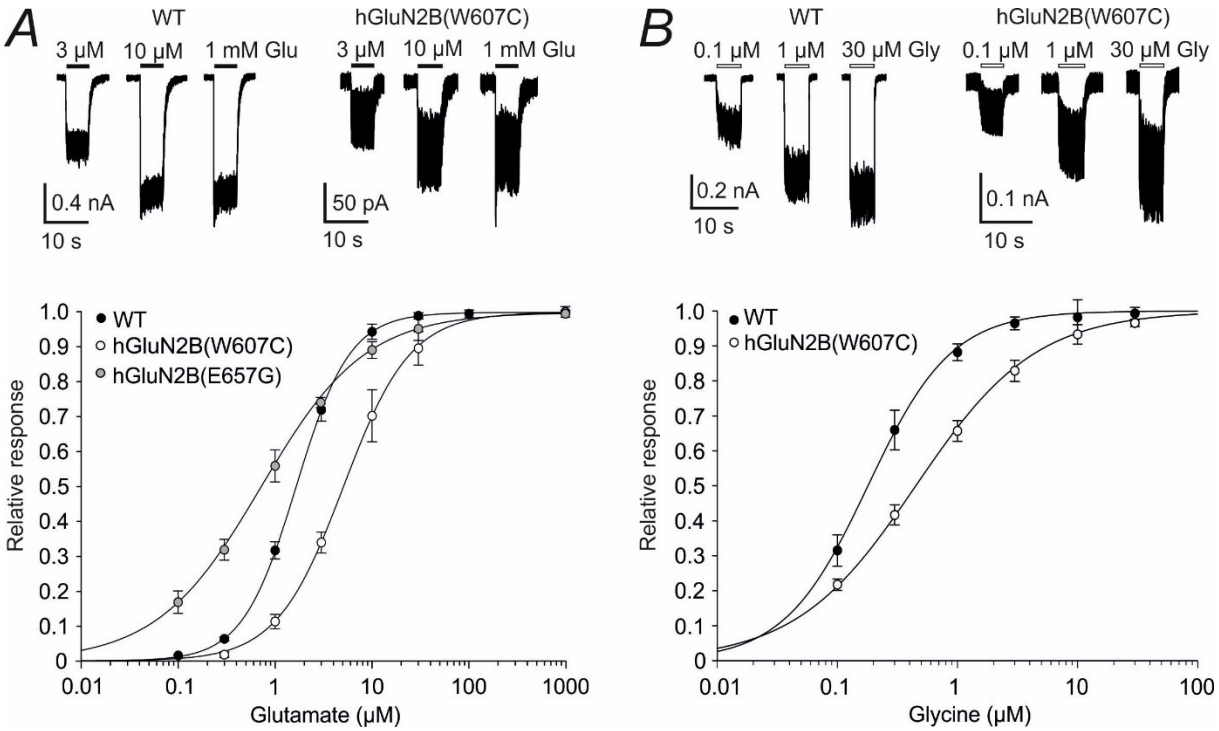

Figure 4.3. Disease-associated mutations in hGluN2B alter the receptor sensitivity to the agonists. ***(A)*** At the top, representative current responses to 3, 10, and 1000 μM glutamate recorded from HEK293T cells expressing WT and hGluN1/hGluN2B(W607C) receptors. At the bottom, glutamate dose-response curves recorded from the HEK293T cells expressing WT, hGluN1/hGluN2B(W607C), and hGluN1/hGluN2B(E657G) receptors. The experiments were performed in the continuous presence of 30 μM glycine; the duration of glutamate application is indicated by filled bars. ***(B)*** At the top, representative current responses to 0.1, 1, and 30 μM glycine were recorded from the HEK 293T cells expressing the WT and hGluN1/hGluN2B(W607C) receptors. At the bottom, glycine dose-response curves for WT and hGluN1/hGluN2B(W607C) receptors. The experiments were performed in the continuous presence of 1 mM glutamate; the duration of glycine application is indicated by open bars. Data points in ***(A-B)*** are the averaged values of relative current responses. Error bars indicate the SEM.

Table 4.2. Summary of the agonist affinity data for the WT and mutated receptors.

Mutation	Glutamate			Glycine		
	EC_{50} ± SEM (μM)	h ± SEM	n	EC_{50} ± SEM (μM)	h ± SEM	n
hGluN2B(WT)	1.6 ± 0.1	1.4 ± 0.1	15	0.22 ± 0.03	1.45 ± 0.11	9
hGluN2B(V558I)	1.6 ± 0.3	1.5 ± 0.2	5	0.22 ± 0.05	1.14 ± 0.05	5
hGluN2B (W607C)	5.1 ± 0.4*	1.3 ± 0.2	5	0.45 ± 0.08*	0.87 ± 0.05*	7
hGluN2B (V618G)	1.7 ± 0.2	1.2 ± 0.1	5	0.28 ± 0.03	1.43 ± 0.09	5
hGluN2B (E657G)	0.7 ± 0.1*	0.8 ± 0.1*	9	0.39 ± 0.08*	0.97 ± 0.10*	5
hGluN2B (G820A)	1.5 ± 0.3	1.0 ± 0.2	4	0.20 ± 0.09	1.15 ± 0.05	3
hGluN2B (L825V)	1.5 ± 0.1	1.1 ± 0.1	9	0.16 ± 0.01	1.26 ± 0.12	5

Statistical analysis was performed on logEC_{50} and logHill using one-way ANOVA and Tukey posthoc Dunnett's method; *h* is the Hill coefficient; *n* indicates the number of cells in the group; * < 0.05.

4.1.3 Disease-related mutations affect receptor desensitization and open probability

For desensitization analysis, WT and mutated NMDARs were activated by saturating concentrations of glutamate and glycine (1 mM and 30 μM, respectively) to reach maximum desensitization. The degree of desensitization was determined by the analysis of the ratio between the peak and steady-state current responses (see Equation 5). Whereas the WT receptors were desensitized by 16% (Figure 4.4*A,D*), hGluN1/hGluN2B(V618G) receptors were desensitized by only 4% (Figure 4.4*D*). In contrast, the degree of desensitization of the GluN1/hGluN2B(V558I) receptors was increased to 73% (Figure 4.4*B*,*D*).

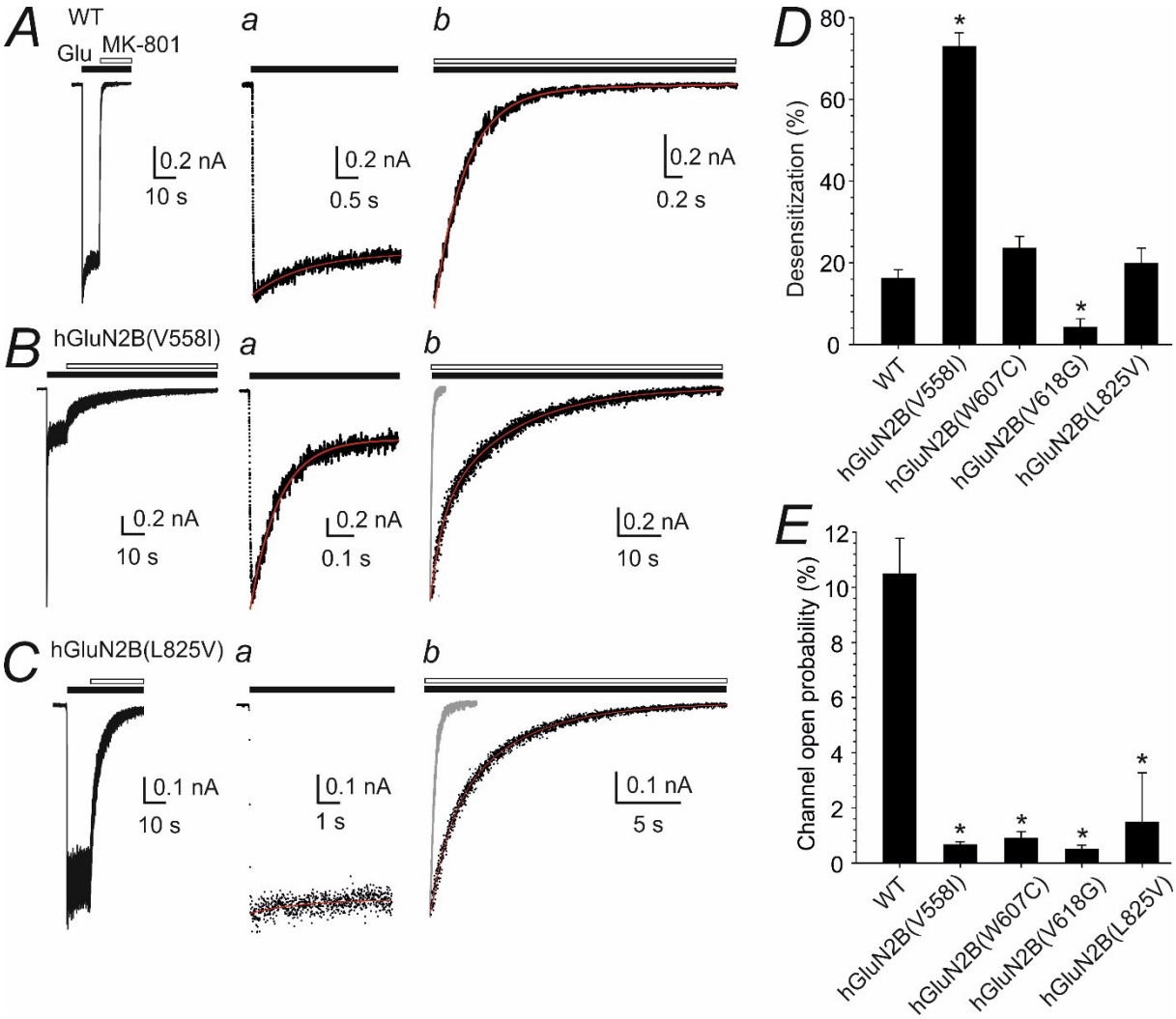

Figure 4.4. Disease-associated mutations affect the desensitization and the P_o of the receptor. ***(A-C)*** Representative current responses to 1 mM glutamate and their inhibition by 1 μM MK-

801 in the WT ***(A)***, hGluN1/hGluN2B(V558I) ***(B)***, and hGluN1/hGluN2B(L825V) ***(C)*** receptors. ***(Aa-Ca)*** Demonstrate the glutamate-induced responses on an extended time scale. ***(Ab-Cb)*** Demonstrate the onset of MK-801 block on an extended time scale at the WT (grey traces) and mutated (black traces) receptor responses. Duration of glutamate and MK-801 application is indicated by filled and open bars, respectively. ***(D-E)*** Bar graphs represent the desensitization ***(D)*** and open probability ***(E)*** of WT and mutated receptors. Statistical differences between the groups were tested by Kruskal-Wallis one-way ANOVA on Ranks. Mann-Whitney Rank Sum Test was used to check the statistical difference between the WT and mutated receptors. Error bars indicate SEM; n = 4-19; * $p < 0.05$.

To calculate the kinetic constants of desensitization (k_d) and resensitization (k_r) in WT and mutated receptors, we determined the rate of the desensitization onset (see Equations 6-7). The desensitization of the WT receptor responses was characterized by the k_d = 0.24 s^{-1} (Table 4.3). In contrast, the values of the k_d in hGluN1/hGluN2B(V558I) and hGluN2B(W607C) receptors were 14.8- and 6.6- fold higher than in the WT receptors (Table 4.3**)**. The values of the k_d in hGluN1/hGluN2B(L825V) receptors were similar to those in the WT receptors (Table 4.3). The responses of the WT receptors were characterized by the k_r = 1.06 (Table 4.3). The value of the k_r determined in hGluN1/hGluN2B(W607C) receptors was 4.5- fold higher in comparison to those determined in the WT receptors. No statistically significant difference was found between the k_d values determined in WT receptors and mutated hGluN1/hGluN2B(V558I) and hGluN1/hGluN2B(L825V) receptors (Table 4.3). Analysis of the kinetic constants for the hGluN1/hGluN2B(V618G) receptors was precluded due to the low amplitude of the current responses.

Table 4.3. Summary of the kinetic constants of desensitization (k_d) and resensitization (k_r) determined in WT and mutated receptors

Mutation	k_d ± SEM (s^{-1})	k_r ± SEM (s^{-1})	n
hGluN2B(WT)	0.24 ± 0.08	1.06 ± 0.17	10
hGluN2B(V558I)	3.55 ± 0.46*	1.29 ± 0.28	7
hGluN2B(W607C)	1.59 ± 0.54*	4.79 ± 1.22*	4
hGluN2B(L825V)	0.43 ± 0.16	1.47 ± 0.20	6

Statistical differences between the groups were tested by Kruskal-Wallis one-way ANOVA on Ranks. Mann-Whitney Rank Sum Test was used to check the statistical difference between WT and mutated receptors; n indicates the number of cells in the group; * $p <$ 0.05.

The P_o of the WT and mutated receptors was evaluated by analysing the kinetics of the MK-801 blockade. The receptors were activated by 1 mM glutamate and then the glutamate-induced currents were inhibited by the application of 1 μM MK-801. The rate of MK-801

blockade was fitted to the kinetic model (see Equation 8). The results indicated that the P_o of the hGluN1/hGluN2B(V558I), hGluN1/hGluN2B(W607C), hGluN1/hGluN2B(V618G), and hGluN1/hGluN2B(L825V) receptors was substantially lower than that in WT receptors (Figure 4*D*).

4.1.4 hGluN1/hGluN2B (L825V) receptors exhibit increased sensitivity to potentiating neurosteroids

Next, we evaluated the effect of hGluN2B(V558I; W607C; V618G; L825V) mutations on the receptor sensitivity to naturally-occurring potentiating neurosteroid PE-S and its synthetic analogue AND-hSuc. Due to the disuse-dependent effect of potentiating steroids (Horak et al., 2004), a low concentration of glutamate (1 μM) was used in these experiments. At hGluN1/hGluN2B(L825V) receptors, both PE-S (100 μM) and AND-hSuc (30 μM) induced significantly greater potentiation of glutamate-induced responses than that at WT receptors ($p < 0.05$, unpaired t-test) (Figure 4.5*A*-*C*). In contrast, the responses of hGluN1/hGluN2B(V558I; W607C; V618G) receptors were potentiated to the same extent as the responses of WT receptors (Figure 4.5*A*-*C*). Next, performed the dose-response analyses of PE-S (10-100 μM) and AND-hSuc (1-30 μM) potentiation at the WT and hGluN1/hGluN2B(L825V) receptors (Figure 4.5*D*-*E*). The dose-response curves for PE-S and AND-hSuc effects indicate that the augmented steroid potentiation in hGluN1/hGluN2B(L825V) receptors is associated with elevated steroid efficacy rather than with increased affinity.

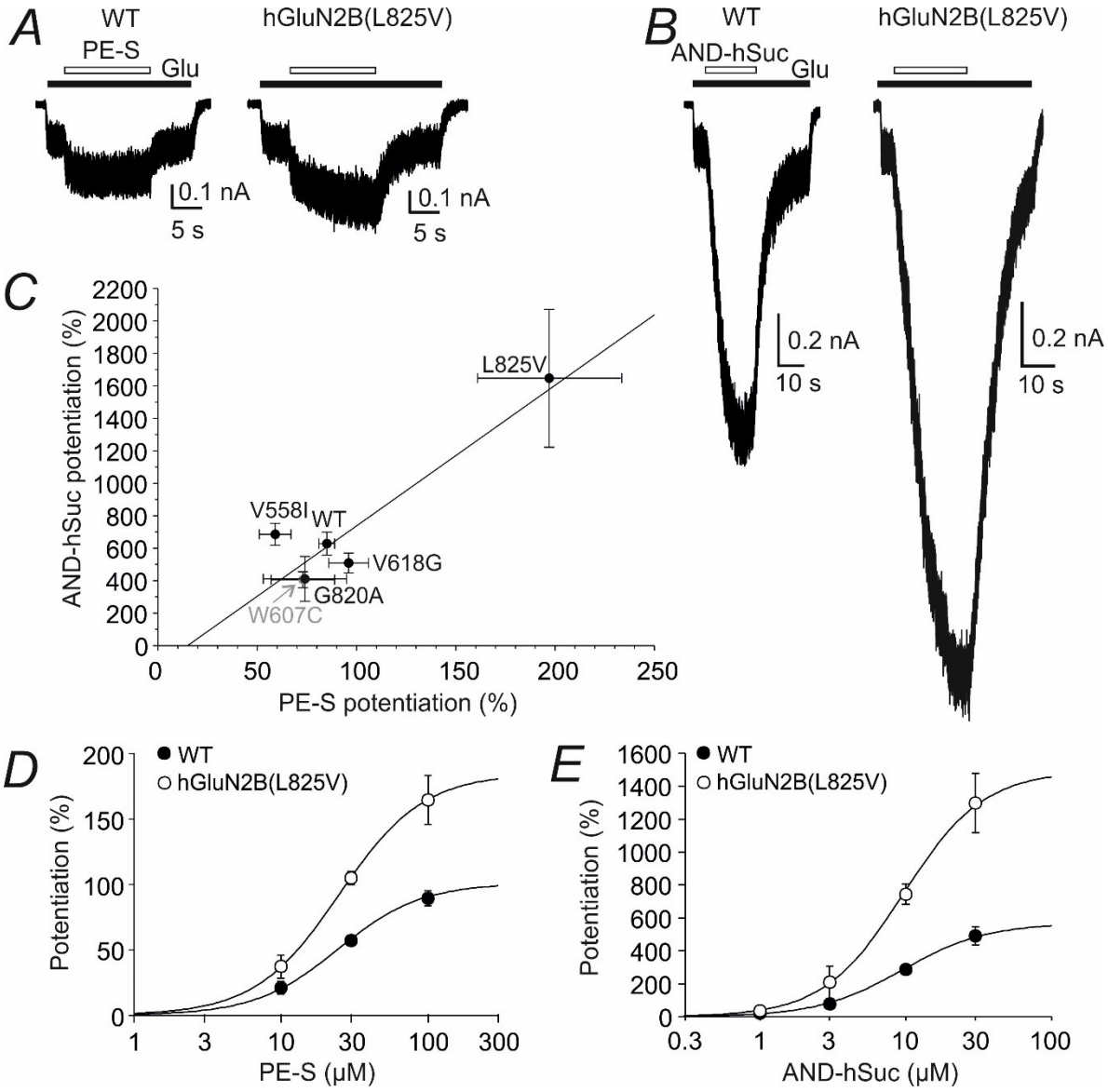

Figure 4.5. hGluN1/hGluN2B(L825V) receptors exhibit increased sensitivity to PE-S and AND-hSuc. ***(A-B)*** Representative current responses of WT and hGluN1/hGluN2B(L825V) receptors to 1 mM glutamate alone and in the presence of 100 μM PE-S ***(A)*** or 30 μM AND-hSuc ***(B)***. Duration of glutamate and steroid application is indicated by filled and open bars, respectively. ***(C)*** Graph shows the degree of PE-S (100 μM) and AND-hSuc (30 μM) potentiation of glutamate (1 μM) responses in WT and mutated hGluN1/hGluN2B receptors. The black line shows a linear regression for data points from all mutated receptors (correlation coefficient $r^2 = 0.928$; $p = 0.001$). ***(D-E)*** Dose-response curves for the potentiation of WT (filled) and hGluN1/hGluN2B(L825V) receptor responses by 10-100 μM PE-S ***(D)*** and 1-30 μM AND-hSuc ***(E)***. In WT receptors, PE-S induced potentiation was characterized by the following parameters: $E_{max} = 101 \pm 9$ %; $EC_{50} = 24.3 \pm 1.8$ μM; $h = 1.54 \pm 0.08$ ($n = 7$); AND-hSuc induced potentiation was characterized by the following parameters: $E_{max} = 570 \pm 57$ %; $EC_{50} = 9.5 \pm 1.0$ μM; $h = 1.50 \pm 0.16$ ($n = 6$). In hGluN1/hGluN2B(L825V) receptors, the PE-S potentiation was characterized by the following parameters: $E_{max} = 185 \pm 50$ % ($p = 0.030$ versus WT); $EC_{50} = 24.5 \pm 1.2$ μM ($p = 0.842$ versus WT); $h = 1.52 \pm 0.12$ ($n = 5$); the AND-hSuc potentiation was characterized by the following parameters: $E_{max} = 1492 \pm 514$% ($p = 0.030$ versus WT); $EC_{50} = 9.6 \pm 2.03$ μM ($p = 0.961$ versus WT); $h = 1.58 \pm 0.36$ ($n = 6$).

4.2 Identification of the site of action for pregnenolone sulfate at the NMDAR

Endogenous neurosteroid pregnenolone sulfate (PE-S) is well known for its disuse-dependent potentiating effect on the NMDAR (Bowlby, 1993; Gibbs et al., 2006; Horak et al., 2004, 2006; Malayev et al., 2002; Wu et al., 1991). However, the molecular mechanism of PE-S modulation and the binding site for PE-S at the NMDAR are not known. Therefore, in this study, we used a combination of site-directed mutagenesis, electrophysiological assessments, and *in silico* modelling to characterize the interaction of PE-S with the NMDAR and identify the binding sites for PE-S. The results of this study were published in *The Journal of Neuroscience* (Hrcka Krausova et al., 2020).

4.2.1 The transmembrane domain of NMDAR is crucial for PE-S potentiation

To assess the dose-response of the PE-S effect, the responses of rat GluN1/GluN2B receptors to 1 μM glutamate were examined during the co-application of different PE-S concentrations (3-100 μM) (Figure 4.6*A*). The results indicated that PE-S potentiation was characterized by the following parameters: E_{max} = 120 ± 16%; EC_{50} = 21 ± 3 μM; h = 1.5 ± 0.2.

As a lipid, PE-S is an amphipathic compound. Therefore, upon reaching the critical micelle concentration (CMC), PE-S self-assembles into micelles in an aqueous medium. The light scattering analysis of the ECS containing 0.1-100 μM PE-S showed the presence of micelle-like particles at all tested concentrations indicating that the CMC for PE-S < 100 nM. After exceeding the CMC, all additional steroid molecules added into the solution form micelles (McNaught & Wilkinson, 1997). Therefore, the steroid exists in monomer form only at a concentration below the CMC. Since the free monomer concentration for PE-S (< 100 nM) is not sufficient to modulate the GluN1/GluN2B receptor responses (Figure 4.6*A*), it is plausible that the action of PE-S is mediated by the interaction between the receptor and PE-S that is present in the ECS in the micelle form. Therefore, we considered potential routes for PE-S to access the receptor: 1) PE-S in the micelle form fuses with the plasma membrane and directly binds at the TMD of the receptor (steps 1 and 4 in the scheme Figure 4.6*B*), and 2) PE-S in the micelle form fuses with the membrane, leaves the membrane in the monomer form, and binds at the intracellular or extracellular domains of the receptor (steps 1, 2, 3 and 1, 5, 6 in the scheme Figure 4.6*B*).

For further investigation of the route of PE-S to access the NMDAR, we used methyl-γ-cyclodextrin (γCDX), a cyclic oligosaccharide that can accommodate steroids, therefore decreasing their free membrane concentration (Ohtani et al., 1989; Szejtli, 1998). Extracellular application of γCDX (10 mM) abolished PE-S potentiation of GluN1/GluN2B receptor responses to 1 μM glutamate. Thus, PE-S (100 μM) potentiated the receptor responses by 103 ± 11% (Figure 4.6*C*), whereas the subsequent co-application of PE-S and γCDX diminished the receptor responses to a value smaller than the control glutamate response (-8 ± 2%) (Figure 4.6*C*). In control experiments (without PE-S application), γCDX decreased the receptor responses to glutamate to the same extent (-13 ± 2%) as the co-application of glutamate, PE-S, and γCDX (Figure 4.6*C*). In all experiments, the effect of γCDX was fully reversible (Figure 4.6*C*).

Next, we examined whether PE-S action is associated with interaction with the intracellular domain of the receptor. To remove intracellularly available PE-S, GluN1/GluN2B receptor-expressing HEK293T cells were subjected to intracellular dialysis with ICS containing 10 mM γCDX via a patch pipette. No significant differences were observed between the degree of potentiation of 1 μM glutamate-elicited responses by extracellularly applied PE-S in HEK293T cells dialysed with control and γCDX-containing ICS (Figure 4.6*D*). Further, we evaluated the effect of intracellularly dialysed PE-S on the capability of extracellularly applied PE-S to potentiate GluN1/GluN2B receptor responses. Since PE-S is a highly lipophilic compound and a cell contains numerous intracellular membranes, considerable time may be required to achieve equilibrium between the intrapipette and intracellular steroid concentration. To accelerate the process of intracellular dialysis, an outside-out patch-clamp approach was used instead of the whole-cell configuration. Outside-out patches were pulled from HEK293T cells expressing GluN1/GluN2B receptors and dialyzed with control or PE-S-containing (100 μM) ICS. In patches dialyzed with PE-S-containing ICS, a 10 s pre-application of PE-S (100 μM) potentiated the responses to 1 mM glutamate to the same extent as in patches dialyzed with control ICS (Figure 4.6*E*). Similarly, intracellular dialysis with γCDX (10 mM) showed no effect on PE-S-induced potentiation of GluN1/GluN2B receptors (Figure 4.6*F*). Pre-application of PE-S (100 μM) for 10 s resulted in a similar degree of potentiation of receptor responses in outside-out patches dialyzed with control and patches dialyzed with γCDX-containing ICS (Figure 4.6*E*). These findings oppose the location of the PE-S binding site within the intracellular domain of NMDAR.

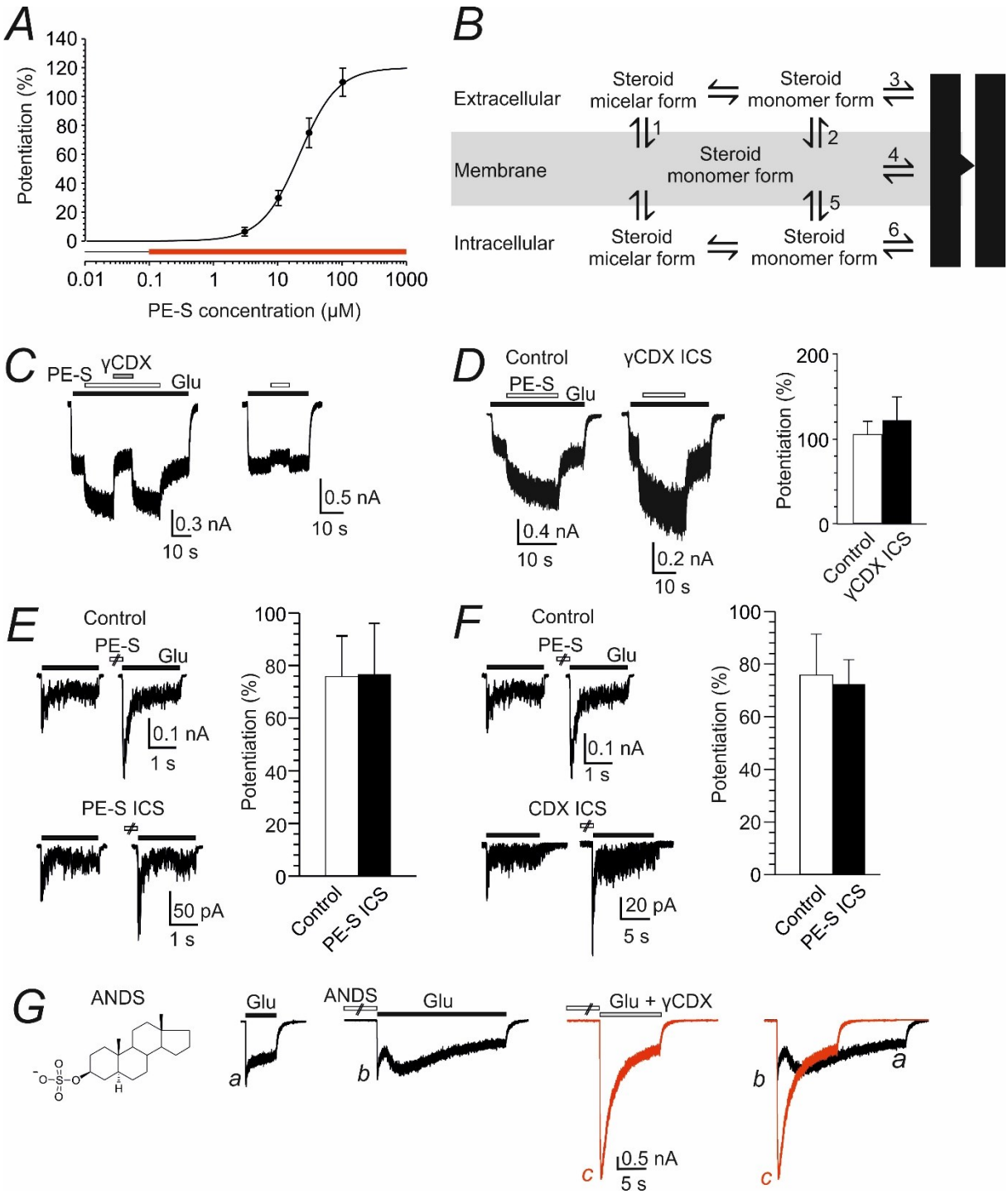

Figure 4.6. ***(A)*** Dose-response curve for the PE-S effect (3; 10; 30; and 100 μM). Data points are averaged values of the degree of potentiation measured from 7 cells. The concentration range in which PE-S forms micelles is indicated by the red bar. ***(B)*** Scheme portraying potential routes for the steroid to access its binding sites at the receptor. ***(C)*** Extracellular application of γCDX reversibly abolished PE-S-induced potentiation. Representative recordings of the current responses obtained from HEK293T cells transfected with GluN1/GluN2B receptors. Left trace, the effect of γCDX (10 mM) on the receptor response to glutamate (1 μM) co-applied with PE-S (100 μM). Right trace, the effect of γCDX on the glutamate-induced response. Duration of glutamate, PE-S, and γCDX application is indicated by black-filled bars, open bars, and grey-filled bars, respectively. ***(D)*** Representative responses of GluN1/GluN2B receptors to the co-application of 100 μM PE-S and 1 μM

glutamate obtained from HEK293T cells dialyzed with control ICS (left) or ICS containing 10 mM γCDX (right). Duration of glutamate and PE-S application is indicated by filled and open bars, respectively. Bar graph shows the degree of PE-S-induced potentiation measured in cells dialyzed with control ($n = 4$) and γCDX-dialyzed ICS ($n = 5$). No significant difference was found between the groups ($p = 0.666$, unpaired *t*-test). ***(E)*** Representative responses of GluN1/GluN2B receptors to glutamate (1 mM) obtained from outside-out patches isolated from HEK293T cells before (left) and following (right) PE-S (100 μM) pre-application for 10 s. Patches were dialyzed with control ICS (upper traces) or ICS containing 100 μM PE-S (lower traces). Duration of glutamate application and PE-S pre-application is indicated by filled and open bars, respectively. Bar graph shows the degree of PE-S-induced potentiation in patches dialyzed with control ($n = 11$) and PE-S-containing ICS ($n = 8$). No significant differences were found ($p = 0.997$, unpaired t-test). ***(F)*** Representative responses of GluN1/GluN2B receptors to glutamate (1 mM) obtained from outside-out patches isolated from HEK293T cells before (left) and following (right) 100 μM PE-S pre-application for 10 s. Patches were dialyzed with control ICS (upper traces) or ICS containing 10 mM γCDX (lower traces). Duration of glutamate application and PE-S pre-application is indicated by filled and open bars, respectively. Bar graph shows the degree of PE-S-induced potentiation in patches dialyzed with control ($n = 11$) and γCDX-dialyzed ICS ($n = 8$). No significant differences were found between the groups ($p = 0.997$, unpaired t-test). ***(G)*** Representative responses of GluN1/GluN2B receptors to glutamate (1 mM) recorded before (*a*) and following (*b*) ANDS pre-application for 15 s. (*c*) The response to co-application of glutamate (1 mM) and γCDX (10 mM) made following ANDS pre-application. Right, superimposition of responses to glutamate application (black trace) and glutamate co-applied with γCDX following ANDS pre-application. Duration of glutamate application, ANDS pre-application, and co-application of glutamate with γCDX is indicated by black-filled bars, open bars, and grey-filled bars, respectively. Inset, projection structure of ANDS. Error bars indicate the SEM.

Afterwards, we tested whether the potentiating steroids act at the extracellular domain of the NMDAR similarly to the steroids with inhibitory action (Vyklicky et al., 2015). We hypothesized that if the potentiating and inhibitory effects of steroids are mediated by binding to the extracellular domain, then both effects will be affected to a similar extent by the extracellular application of γCDX. For the next experiments, we have selected 5α-androstan-3β-yl-sulfate (ANDS), a steroid that demonstrated a dual (positive and negative) effect at the NMDAR. After a 15 s pre-application, ANDS (100 μM) potentiated GluN1/GluN2B receptor responses to 1 mM glutamate by 17 ± 6% ($n = 5$) and displayed complex kinetics due to the mixed effect of the steroid **(**Figure 4.6*G*). In contrast, NMDAR responses to the co-application of glutamate and 10 mM γCDX were potentiated by ANDS pre-application significantly more (by 172 ± 18%; $n = 5$ (Figure 4.6*G*). We reasoned that γCDX precluded the inhibitory effect of ANDS by preventing access to the inhibitory site of action at the extracellular domain of the receptor, therefore unmasking the potentiating effect of ANDS. In turn, the fact that the ANDS potentiation was not abolished by extracellular γCDX indicates that the potentiating site of action for ANDS is not located at the extracellular receptor

domains. Altogether, these results suggest distinct sites of action to mediate positive and negative modulatory effects of steroids at the NMDAR.

4.2.2 PE-S and sterols act at distinct sites at the NMDAR

Similarly to PE-S, sterols, such as cholesterol and 24(S)-HC, are potent positive modulators of NMDAR function (Korinek et al., 2015; Paul et al., 2013). Cholesterol and 24(S)-HC share structure similarities with PE-S and all three have molecules of the planar shape. Hence, we examined whether the site of action for PE-S is similar to that for sterols. We hypothesized that if PE-S shares the sites of action at the NMDAR with cholesterol, then PE-S will be able to rectify the cholesterol-depletion-induced reduction of NMDAR currents. For cholesterol depletion, we used methyl-β-cyclodextrin (βCDX), a cyclic oligosaccharide that is able to bind plasma membrane sterols, especially cholesterol, therefore decreasing the membrane cholesterol level (Christian et al., 1997). In control HEK293T cells ($n = 5$), the mean amplitude of GluN1/GluN2B receptor responses to 1 μM glutamate was −547 ± 193 pA and the degree of potentiation by PE-S (100 μM) was 119 ± 32% (Figure 4.7*A,C*). The effect of cholesterol depletion on PE-S potentiation was evaluated in a sister culture where HEK293T cells were incubated with 10 mM βCDX for 60 min. Cholesterol depletion led to an 11-fold decrease in the mean amplitude of glutamate responses (Figure 4.7*C*). In cholesterol-depleted cells, PE-S potentiated the glutamate-induced responses by 122 ± 66% ($n = 6$), to the same degree as in control cells ($p = 0.973$) (Figure 4.7*B,C*). The PE-S potentiation was insufficient to rectify the reduction of NMDAR currents in cholesterol-depleted cells (Figure 4.7*C*).

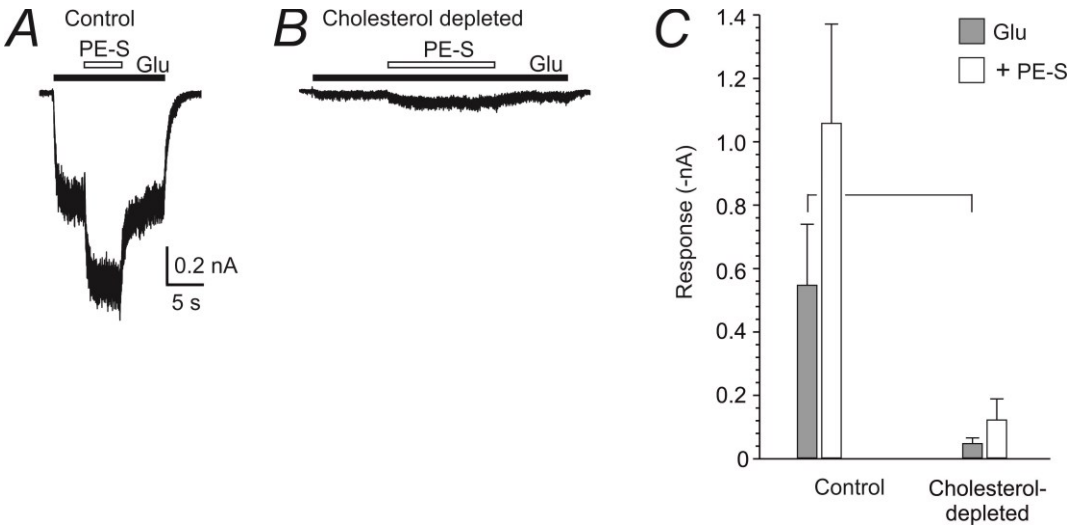

Figure 4.7. PE-S is unable to compensate for the reduction of the NMDAR currents in cholesterol-depleted cells. ***(A)*** Representative response of GluN1/GluN2B receptors to glutamate (1 μM) before and upon co-application with PE-S (100 μM). Duration of glutamate and PE-S application is indicated by filled and open bars, respectively. ***(B)*** Representative responses to glutamate (1 μM) before and upon co-application with PE-S (100 μM) obtained from cholesterol-depleted HEK293T cells. Duration of the glutamate and PE-S application is indicated by filled and open bars, respectively. To achieve cholesterol depletion, the cells were incubated with βCDX (10 mM) for 60 min at 37ºC prior to recording. ***(C)*** Bar graph representing the amplitude of GluN1/GluN2B receptor currents in control and cholesterol-depleted cells. Grey bars indicate responses to glutamate (1 μM) alone; white bars indicate responses to the co-application of glutamate (1 μM) and PE-S (100 μM). Each bar represents data from at least 5 cells; error bars indicate SEM. The amplitude of glutamate-induced currents was significantly reduced in cholesterol-depleted cells (*, unpaired t-test).

4.2.3 Amino-acid residues at the TMD are essential for PE-S potentiation

To determine the PE-S binding site, we analysed the effect of mutations in the TMD of the GluN1 and GluN2B subunits on PE-S potentiation. For this purpose, we performed alanine-scanning mutagenesis of the following amino-acid residues in the M1 and M4 helices: GluN1(Q559-V572; T809-V825) and GluN2B(S555-I568; D814-A830). All non-alanine residues within the mentioned regions were substituted with alanine and alanine residues were substituted with threonine. The assessment of PE-S (100 μM) modulatory effect on WT and mutated GluN1/GluN2B receptors expressed in HEK293T cells was performed upon its co-application with glutamate (1 μM). Since GluN1/GluN2B(W559A) receptors produced only negligible responses to glutamate (< 5 pA), they were considered non-functional and excluded from further analysis. GluN1(W563A)/GluN2B and GluN1/GluN2B(D816A) receptors exhibited spontaneous activity in the absence of externally applied glutamate. Whereas PE-S potentiated the responses of the WT receptors by 104 ± 4% (n = 158), the PE-S effect on mutated receptor responses varied in the range from inhibition by -33 ± 2% (n = 7) in GluN1/GluN2B(M824A) receptors to potentiation by 292 ± 57% (n = 7) in GluN1(G815A)/GluN2B receptors (Figure 4.8*A-D*). The degree of PE-S-induced potentiation observed in the GluN1(S569A; G815A; M818A; L819A; G822A)/GluN2B receptors was significantly greater than that in the WT receptors ($p < 0.05$, one-way ANOVA) (Figure 4.8*A-B*). In contrast, the degree of PE-S-induced potentiation at the GluN1(Q559A; W563A; L564A; N812A; F817A)/GluN2B and GluN1/GluN2B(M562A; V564A; L567A; M818A; G820A; F822A; L825A; M829A; A830T) receptors was significantly lower than in the WT receptors ($p < 0.05$, one-way ANOVA) (Figure 4.8*B,C*). At the GluN1/GluN2B(D816A; Y823A; M824A) receptors, PE-S application led to the inhibition of glutamate-induced

responses (Figure 4.8*C*). As it was mentioned earlier, PE-S has both a potentiating and an inhibitory effect at the NMDAR; therefore, the elimination of the potentiating effect of PE-S at mutated receptors results in the unmasking of its inhibitory effect.

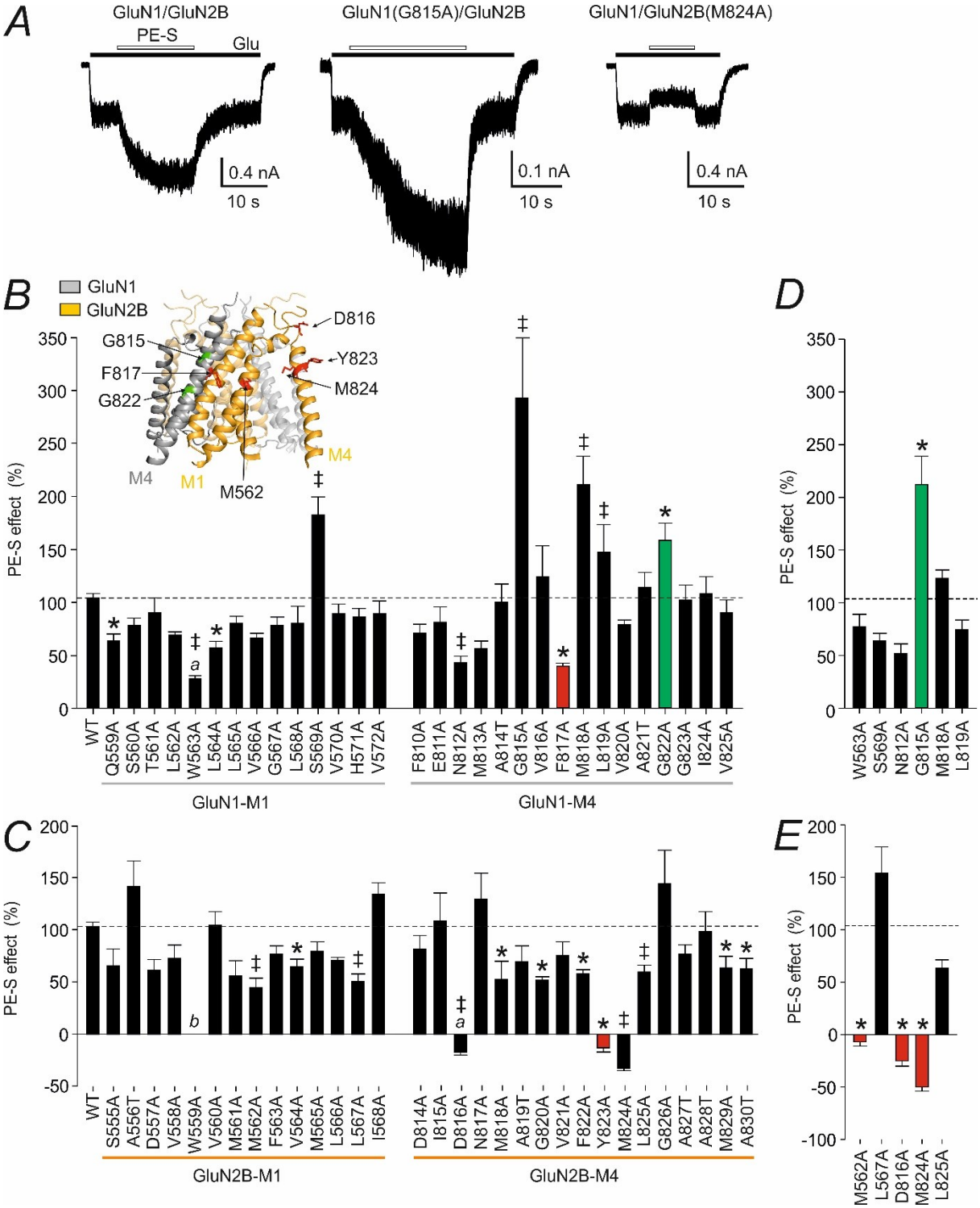

Figure 4.8. Positive modulatory effect of PE-S is affected by mutations in the M1 and M4 helices of the GluN1 and GluN2B subunits. ***(A)*** Representative responses of the WT, GluN1(G815A)/GluN2B, and GluN1/GluN2B(M824A) receptors to glutamate (1 μM) before and upon co-application with PE-S (100 μM). The duration of glutamate and PE-S application

is indicated by filled and open bars, respectively. ***(B-C)*** Bar graphs representing the PE-S (100 μM) effect on responses to glutamate (1 μM) of GluN1/GluN2B receptors mutated at the GluN1 ***(B)*** or GluN2B ***(C)*** subunits (n = 4-158 cells). Data are indicated as mean ± SEM. ‡ signifies receptors that showed significantly altered PE-S sensitivity and whose glutamate EC_{50} was significantly different (Table 4.4) from that in WT receptors; * indicates receptors whose PE-S sensitivity was different but the glutamate EC_{50} was similar to those in the WT receptors (Table 4.4) in comparison to the WT receptors (one-way ANOVA ($p < 0.001$) followed by an unpaired t-test for single comparisons versus WT ($p < 0.050$)). *a* signifies spontaneously active receptors; *b* signifies nonresponding receptors. ***(D-E)*** Bar graph representing the mean effect of PE-S (100 μM) on receptors with altered glutamate EC_{50} (n = 4-10 cells). Error bars indicate SEM. The PE-S effect was evaluated at glutamate concentrations (0.08-3.20 μM) inducing ~38% of the maximal receptor response.* signifies the receptors that had altered PE-S sensitivity in comparison to the WT receptors. Statistical analysis was performed by one-way ANOVA ($p < 0.001$) followed by an unpaired t-test for single comparisons versus WT ($p < 0.050$). ***(B-E)*** Red bars indicate mutations that decreased the potentiation effect of PE-S by >50%; green bars indicate mutations that increased the potentiation effect of PE-S by >50%. The dashed line shows the mean degree of PE-S potentiation in the WT receptors. ***(B)*** Insert, the GluN1/GluN2B receptor TMD homology model (Černý et al., 2019). The GluN1 and GluN2 subunits are labelled in grey and orange, respectively. Amino-acid residues whose mutations reduced the PE-S potentiation by >50% are labelled in red; amino-acid residues whose mutations increased the PE-S potentiation by >50% are labelled in green.

Since PE-S potentiates NMDAR responses in a disuse-dependent manner (Horak et al., 2004), the degree of PE-S potentiation depends on the glutamate dose. To avoid the indirect impact of altered glutamate affinity in mutated receptors on PE-S potentiation, we performed a set of additional experiments. For the mutations that led to significant reduction or enhancement of the PE-S effect, the EC_{50} values for glutamate were determined (Table 4.4). The calculation of EC_{50} was performed using Equation 3, the Hill coefficient was fixed at the value of 1.6 (Laube et al., 1997). Subsequent analysis demonstrated that the values of glutamate EC_{50} in the GluN1(W563A; S569A; N812A; G815A; M818A; L819A)/GluN2B and GluN1/GluN2B (M562A; L567A; D816A; M824A; L825A) receptors were significantly different from those in the WT receptors (Table 4.4). Thus, the modulatory action of PE-S (100 μM) on these receptors was reassessed at glutamate concentrations corresponding to the effect of 1 μM glutamate at the WT receptors (38% of the maximal response). In these circumstances, the extent of PE-S-induced potentiation/inhibition in the GluN1(G815A)/GluN2B and GluN1/GluN2B (M562A; D816A; M824A) receptors was significantly higher than in the WT receptors (Figure 4.8*D-E*); however, the degree of potentiation of the GluN1(W563A; S569A; N812A; M818A; L819A)/GluN2B and

GluN1/GluN2B (L567A; L825A) receptor responses was similar to that in the WT receptors (Figure 4.8*D-E*).

Table 4.4 | Summary of the glutamate EC_{50} for the WT and mutated GluN1/GluN2B receptors that have altered PE-S effect.

Receptor	EC_{50} (μM)	*n*
WT	1.41 ± 0.04	50
GluN1(Q559A)/GluN2B	1.65 ± 0.06	6
GluN1(W563A)/GluN2B	0.10 ± 0.01 *	6
GluN1(L564A)/GluN2B	1.43 ± 0.16	3
GluN1(S569A)/GluN2B	3.69 ± 0.27 *	4
GluN1(G638A)/GluN2B	1.41 ± 0.11	4
GluN1(I642A)/GluN2B	1.24 ± 0.03	5
GluN1(N812A)/GluN2B	0.36 ± 0.02 *	7
GluN1(G815A)/GluN2B	2.65 ± 0.33 *	5
GluN1(F817A)/GluN2B	1.48 ± 0.14	4
GluN1(M818A)/GluN2B	2.97 ± 0.21 *	4
GluN1(L819A)/GluN2B	2.89 ± 0.24 *	4
GluN1(G822A)/GluN2B	1.58 ± 0.16	4
GluN1/GluN2B(W559L)	1.24 ± 0.06	3
GluN1/GluN2B(M562A)	3.74 ± 0.30 *	4
GluN1/GluN2B(V564A)	1.41 ± 0.13	5
GluN1/GluN2B(L567A)	1.08 ± 0.20 *	4
GluN1/GluN2B(D816A)	0.17 ± 0.01 *	6
GluN1/GluN2B(M818A)	1.74 ± 0.27	3
GluN1/GluN2B(G820A)	1.56 ± 0.15	6
GluN1/GluN2B(F822A)	1.35 ± 0.07	5
GluN1/GluN2B(Y823A)	1.63 ± 0.16	4
GluN1/GluN2B(M824A)	4.05 ± 0.67 *	4
GluN1/GluN2B(L825A)	4.17 ± 0.31 *	5
GluN1/GluN2B(M829A)	1.67 ± 0.10	4
GluN1/GluN2B(A830T)	1.69 ± 0.08	5
One-way ANOVA[a]	$p < 0.001$	

All values are mean ± SEM; *n* represents the number of individual cells from which data were obtained. One-way ANOVA followed by unpaired t-test, for single comparisons versus WT; *$p < 0.050$; statistical analysis was conducted for the $logEC_{50}$ values.

Positive modulation of the NMDAR function by PE-S is mediated by a mechanism that involves an increase of the channel P_o (Horak et al., 2004). Therefore, we tested whether mutation-induced changes in P_o affect the PE-S potentiation. The responses of WT and mutated receptors to glutamate (1 mM) were inhibited by the co-application of MK-801 (1 μM) (Figure 4.9*A*) and the time course of MK-801-induced inhibition was fitted with a double exponential function to determine the weighted time constant (τ_w) (Equation 9). The relative MK-801 blocking rate (Figure 4.9*B*) was obtained as the ratio between the τ_w for mutated receptors and the τ_w for the WT receptors. Since the rate of the MK-801 channel block linearly correlates with P_o (Hansen et al., 2013), a significantly changed blocking rate in mutated receptors was considered an indicator of altered P_o. Figure 4.9*B* illustrates the absence of a correlation between the rate of MK-801 block and the steroid effect at mutated receptors. Similarly, the correlation analysis specifically of data from mutated receptors with decreased PE-S sensitivity showed no correlation between the rate of MK-801 block and the PE-S effect (Figure 4.9*B*). These results suggest that the effects of mutations in the TMD on the P_o and PE-S sensitivity of GluN1/GluN2B receptors are independent of each other.

Although the GluN2B(D816) mutation results in the complete abolition of the PE-S potentiation, this residue is unlikely to be a part of the steroid site of action. First, GluN2B(D816) is located within the M4-S2 linker, whereas our previous experiments indicated that PE-S interacts with the TMD of the receptor (Figure 4.6). In addition, molecular dynamics simulation suggests high conformational flexibility of linker domains (Ladislav et al., 2018) that makes this region improbable to act as a binding site for a rigid steroid molecule. Moreover, mutations in the linker domain strongly affect the receptor's functional properties (Ladislav et al., 2018). In line with this, the GluN1/GluN2B(D816A) receptors displayed increased P_o and glutamate affinity in comparison to the WT, as well as spontaneous activity (Figure 4.8*C,* 4.9*B*; Table 4.4).

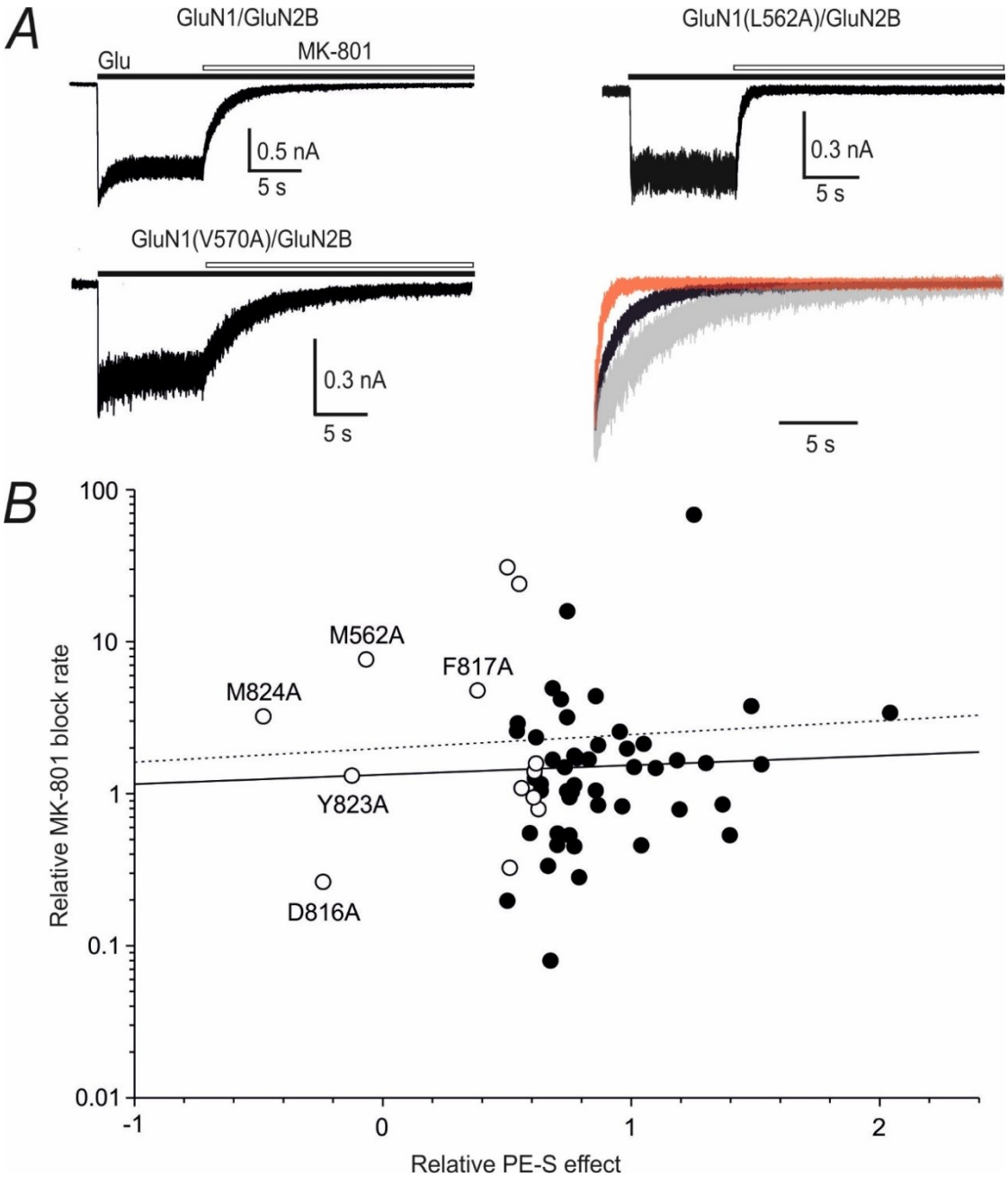

Figure 4.9. Mutations in the TMD of GluN1 and GluN2B subunits affect the receptor P_o and the PE-S sensitivity by independent mechanisms. ***(A)*** Representative recordings demonstrate the responses of WT, GluN1(L562A)/GluN2B, and GluN1(V570A)/GluN2B receptors to glutamate (1 mM) and their inhibition by MK-801 (1 μM). Duration of glutamate and MK-801 application is indicated by filled and open bars, respectively. Bottom right, overlay comparing the time course of the MK-801 block in the WT (black trace), GluN1(L562A)/GluN2B (red trace), and GluN1(V570A)/GluN2B (grey trace) receptors. ***(B)*** Graph representing the relationship between the relative effect of 100 μM PE-S (ratio between the mean values of the PE-S effect at the WT and mutated receptors) and the relative block rate for 1 μM MK-801(ratio between the mean values of the τ_w for the WT and mutated receptors) of mutated GluN1/GluN2B receptors. Black line shows a linear regression for data points from all mutated receptors (Pearson's correlation coefficient $r^2 = 0.005$; $p = 0.608$). Dotted line shows a linear regression for data points from the receptors with decreased PE-S effect (open symbols; Pearson's correlation coefficient $r^2 = 0.027$; $p = 0.596$).

4.2.4 Identification of PE-S binding interface at the NMDAR

Amino-acid sequence alignment demonstrated that the GluN2B residues M562, V564, M818, Y823, M824, and M829, that have decreased the PE-S potentiation in the alanine-scanning experiments (Figure 4.8), are conserved across all GluN2 subunits (Figure 4.10*A*). In agreement with this, PE-S has been shown to potentiate the responses of GluN1/GluN2A-D receptors (Horak et al., 2006). This is also supported by experiments on receptors with the GluN2A(M823A) mutation, which is homologous to the GluN2B(M824A) mutation. PE-S inhibited the responses of GluN1/GluN2A(M823A) receptors to 3 μM glutamate (the concentration that corresponds to 46 ± 3% (n = 6) of maximal response) by 58 ± 4% (n = 7) (Figure 4.10*B*), that is similar to the PE-S effect on GluN1/GluN2B(M824A) receptors (Figure 4.8). In contrast, sequence alignment displays little homology over the GluN2B residues that are essential for the steroid potentiation and corresponding residues within the GluN3A subunit (Figure 4.10*A*). To decrease receptor desensitization of GluN3A-containing receptors, the GluN3A subunit was co-expressed with the mutated GluN1-4a(F484A) subunit in HEK293T cells (Smothers & Woodward, 2009). At GluN1-4a(F484A)/GluN3A receptors, PE-S (50 μM) diminished the responses to glycine (100 μM) by 68 ± 3% (n = 7) (Figure 4.10*C*). Similarly, the responses of GluN1-4a/GluN3A receptors were inhibited in the presence of 50 μM PE-S by 66 ± 9% (n = 4) (Figure 4.10*C*). These results suggest that the positive modulatory effect of PE-S is subunit-selective and limited solely to GluN2 subunit-containing receptors.

For investigation of the steroid site of action, the homology model of the GluN1/GluN2B receptor (Ladislav et al., 2018) was scrutinized to identify the residues located within ~15 Å (the PE-S molecule length) from the GluN2B (Y823 and M824), the M4 helix residues whose mutations diminished the PE-S potentiation the most (Figure 4.8). As a result, the GluN1 M3 helix residues G638, I642, and S646 and the GluN2B M1 helix residue W559 were selected for further experiments (Figure 4.10*D*). Since the GluN1/GluN2B(W559A) receptors are non-functional (Figure 4.8), we used the GluN1/GluN2B(W559L) receptors that had been previously reported to be functional (Kashiwagi et al., 1997). PE-S (100 μM) inhibited the responses of GluN1/GluN2B(W559L) receptors to 1 μM glutamate by 15 ± 2% (n = 7) (Figure 4.10*E,F*). In the GluN1(G638A)/GluN2B and GluN1(I642A)/GluN2B receptors, PE-S (100 μM) potentiated the responses to glutamate (1 μM) significantly less than in WT receptors (Figure 4.10 *E,F*). The responses of GluN1(S646A)/GluN2B receptors were potentiated to the same extent as the

WT receptor responses (Figure 4.10*E,F*). The glutamate EC_{50} values for GluN1(G638A)/GluN2B, GluN1(I642A)/GluN2B, and GluN1/GluN2B(W559L) receptors were similar to those for the WT receptors (Table 4.4). These results suggest an interface formed by GluN1(G638 and I642) and GluN2B(W559, Y823, and M824) residues as a possible binding site for the steroid.

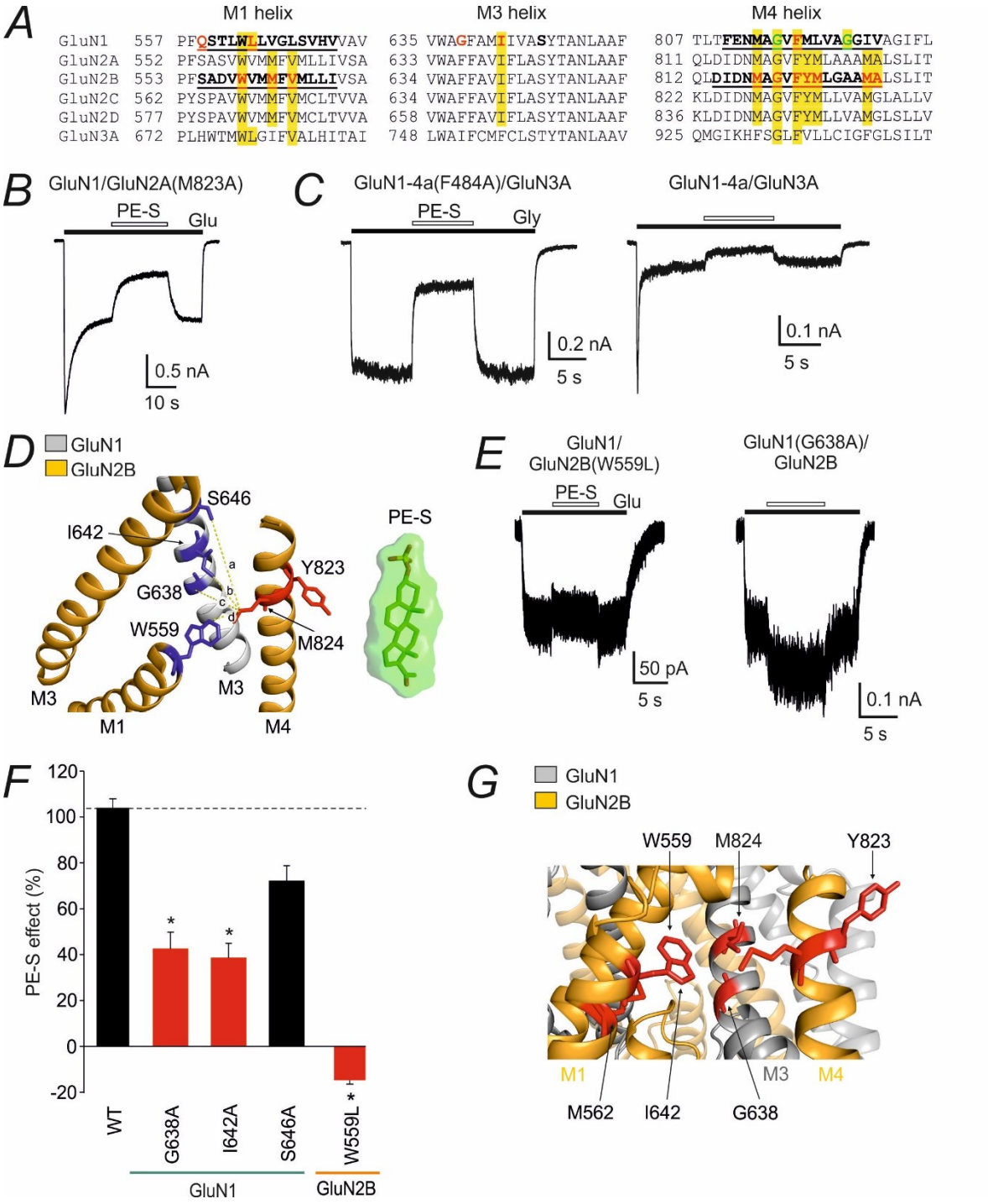

Figure 4.10. Amino-acid residues within the M3 helix of GluN1 subunit and the M1 helix of GluN2B subunit are essential for the PE-S potentiation. ***(A)*** Sequence alignment comparing

amino-acid sequences within the M1, M3, and M4 helices of GluN1, GluN2A-D, and GluN3A subunits. The amino-acid residues that were involved in the alanine scanning analysis are marked in bold and underlined. The residues whose mutations resulted in a significant reduction of the PE-S potentiation are labelled in red; the residues whose mutations resulted in significant augmentation of the PE-S potentiation are labelled in green. Homologous sequences are highlighted in light yellow. ***(B)*** Representative recordings demonstrate inhibition of the GluN1/GluN2A(M823A) receptor responses to glutamate (3 μM) in the presence of PE-S (100 μM). Duration of glutamate and PE-S application is indicated by filled and open bars, respectively. ***(C)*** Representative traces demonstrating the inhibition of the GluN1-4a(F484A)/GluN3A (left) and GluN1-4a/GluN3A (right) receptor responses to glycine (100 μM) in the presence of PE-S (100 μM). The duration of glycine and PE-S application is indicated by filled and open bars, respectively. ***(D)*** GluN1/GluN2B receptor homology model (Karakas & Furukawa, 2014; Lee et al., 2014), shown as a ribbon diagram, demonstrating the GluN1(S646, I642, G638), and GluN2B(W824) residues (blue) which are located within 12, 6, 9, and 5 Å from the M824 residue (red). The GluN1 subunit is labelled in grey; the GluN2B subunit is labelled in orange. Right, the stick model of the PE-S molecule (at the same scale). ***(E)*** Representative traces demonstrating the GluN1/GluN2B(W559L) (left) and GluN1(G638)/GluN2B (right) receptor responses to 1 μM glutamate (filled bars) before and in the presence of 100 μM PE-S (open bars). ***(F)*** Bar graph demonstrating the effect of PE-S (100 μM) on the WT and mutated GluN1/GluN2B receptors. Data are represented as mean ± SEM, n = 5-128. * indicates a significant difference from the WT receptors; statistical analysis was performed by one-way ANOVA ($p < 0.001$) followed by an unpaired t-test for single comparisons versus WT ($p < 0.050$). ***(G)*** Ribbon diagram of the GluN1/GluN2B receptor homology model (Černý et al., 2019). Location of the TMD residues essential for PE-S potentiation. Residues whose substitution diminished the PE-S effect by >50% are labelled in red. The GluN1 subunit is labelled in grey; the GluN2B subunit is labelled in orange.

4.2.5 *In silico* modelling of PE-S binding

In the unliganded state, the NMDAR displays 5- to 50- times higher affinity for PE-S than in the agonist-bound state (Horak et al., 2004). To consider this fact in PE-S binding analysis, we employed recently developed models of unliganded (closed conformation of ion channel) and agonist-bound (open and closed conformation of ion channel) GluN1/GluN2B receptor (Černý et al., 2019). Figure 4.11 (*A,B*) illustrates the rearrangements of the M1-M4 membrane helices during the receptor transition between the closed and open states.

In silico analysis of the steroid-receptor interaction was performed in two steps. First, PE-S was docked in the TMD of the unliganded model of the GluN1/GluN2B receptor. As a result, two pairs of preferential interaction sites were identified: a pair of homologous sites at the GluN1(M1/M4) interface and a pair of sites at the GluN2B(M1/M4) interface. In the next step, we used molecular dynamics (MD) to simulate PE-S interaction with the docking-predicted sites in the model lipid environment. The obtained 100 ns long MD trajectories were analysed by Molecular Mechanics Poisson-Boltzmann Surface Area (MM/PBSA)

method to estimate PE-S binding affinity. To consider the structural relaxation of the steroid/receptor complex, two separate calculations were made: one for the data from the first 30 ns of the trajectory and one for the data from the last 30 ns of the trajectory. For both stages of the MD simulation, the MM/PBSA analysis of PE-S interaction with the binding site at the GluN1(M1/M4) interface indicated the binding free energy of ∼−15 kcal mol^{-1}. The GluN1(W563; L819) residues were found to possess the greatest contribution to this binding energy by forming van der Waals contacts with PE-S (Figure 4.11*C*). For the steroid interaction with the GluN2B(M1/M4) site, the MM/PBSA analysis of the last 30 ns of MD trajectories indicated the binding free energy of −19.5 kcal mol^{-1}. The GluN2B(W559; M562; Y823) residues were shown to contribute the most to the free binding energy and form van der Waals contacts with PE-S (Figure 4.11*C*).

Next, we analysed the interaction between PE-S and the ligand-bound NMDAR with the ion channel in the open state. The results of the MD simulation indicate that the channel opening did not considerably affect PE-S binding to the GluN1(M1/M4) interface, in contrast to the GluN2B(M1/M4) interface. During receptor activation, the GluN2B M1 and M4 helices move against each other thus forming a cavity between the M1 and M4 helices of the GluN2B subunit and the M3 helix of the GluN1 subunit. The MD simulation of PE-S binding to this cavity indicates the binding free energy of −17.5 kcal mol^{-1}. The GluN1(W563; L819) and GluN2B(W559; M562; Y823) residues were shown to form van der Waals contacts with the steroid molecule (Figure 4.11*D*).

The MD simulation of the steroid interaction with the model NMDAR in the open channel configuration indicated that PE-S binding facilitates the GluN2B M4 helix rotation and tightens the contact between the GluN2B(M824) and GluN1(I642) residues of the pore-lining M3 helix (Figure 4.11*D*). In the absence of PE-S, the GluN2B(M824) residue forms contact with the GluN2B(W559) residue and therefore obstructs the entry to the cavity (Figure 4.11*D*). This finding is consistent with a lower binding affinity of PE-S for the receptor in the open state (−17.5 kcal mol^{-1}) in comparison with the closed state (−19.5 kcal mol^{-1}). Taken together, these results shed light on the mechanisms underlying the previously described disuse-dependency of the PE-S potentiation (Horak et al., 2004).

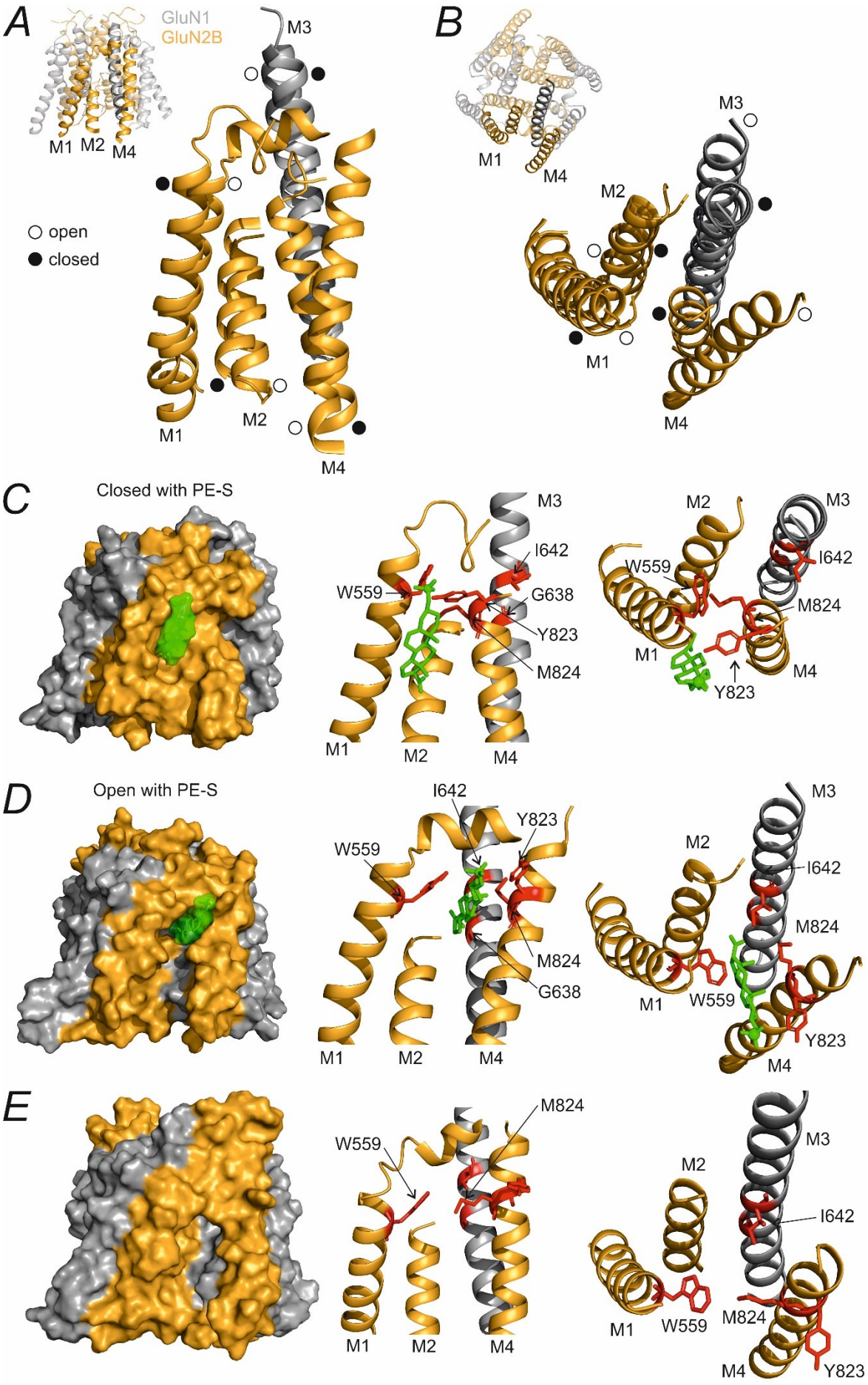
A
GluN1
GluN2B
M1 M2 M4
M3
open
closed
M1
M2
M4
B
M1
M4
M3
M2
M1
M4
C
Closed with PE-S
M3
I642
W559
G638
Y823
M824
M1
M2
M4
M2
M3
I642
W559
M824
M1
Y823
M4
D
Open with PE-S
I642
Y823
W559
M824
G638
M1
M2
M4
M3
M2
I642
M824
M1
W559
Y823
M4
E
M824
W559
M1
M2
M4
M3
M2
I642
M1
W559
M824
M4
Y823

Figure 4.11. The effect of PE-S binding on the TMD arrangement. ***(A-B)*** Side ***(A)*** and top ***(B)*** views demonstrate the structural arrangement of the TMD helices in the MD-based model of the GluN1/GluN2B receptor in the closed state (filled symbols) and open state (open symbols) (Černý et al., 2019). The GluN1 subunit is labelled in grey and the GluN2B subunit is labelled in orange. ***(C-D)*** PE-S (green) sites of action at the TMD of GluN1/GluN2B receptor in the closed state ***(C)*** and open state ***(D)*** predicted by the combination of molecular docking and 100 ns long MD simulation. Amino-acid residues experimentally identified as essential for steroid potentiation are labelled in red. ***(E)*** The model of the receptor in the closed state was simulated without the PE-S molecule bound within the TMD.

4.3 Structure requirements for potentiating neuroactive steroids

4.3.1 ω5β-pregnan-3β-yl derivatives of carboxylic acids potentiate NMDAR responses

A recent study from our laboratory demonstrated that PA-S as well as its C3-substituted analogues are NMDAR NAMs that preferentially affect tonically over phasically activated receptors (Vyklicky et al., 2016). In the current study, we aimed to explore the structural requirements for the steroid modulation of NMDAR function. For this purpose, we prepared a set of pregnane derivatives in which the ester bond was replaced with the C-C bond (Figure 4.12*A*) and screened their effect on the recombinant rat GluN1/GluN2B receptors expressed in HEK293T cells using the patch-clamp technique. The results of the study were published in *British Journal of Pharmacology* (Kysilov et al., 2022).

The results of the screening tests demonstrated that pregnane analogues with short residues at the C3 carbon of the core structure, such as PA-acetate (PA-Ace; 150 μM) and PA-carboxylate (PA-Car; 150 μM) inhibited NMDAR responses to 1 μM glutamate by 31.6 ± 3.7% (n = 7) and 51.8 ± 3.7% (n = 7), respectively (Figure 4.12*B,C*). However, the analogues with elongated residues at the C3, such as PA-propionate (PA-Pro; 10 μM) and PA-butyrate (PA-But; 15 μM) potentiated the glutamate-induced responses by 18.8 ± 6.5% (n = 6) and 82.2 ± 9.8% (n = 7), respectively (Figure 4.12*B,C*). The potentiating effect of PA-Pro and PA-But was surprising because neurosteroids with a "bent" A/B ring junction had been considered to inhibit the NMDAR responses (Korinek et al., 2011; Weaver et al., 2000). To characterize the role of stereo-configuration at the C3 chiral carbon, we have prepared the 3β-isomer of PA-But: 4-(20-oxo-5β-pregnan-3β-yl) butanoic acid (EPA-But; Figure 4.12*B,C*). EPA-But (15 μM) also produced a strong potentiation of the GluN1/GluN2B receptor response to 1 μM glutamate (190 ± 6 %; n = 7; Figure 4.12*B,C*). These results indicate that steroids with a "bent" molecular geometry, in addition to their well-known inhibitory action

(Korinek et al., 2011; Weaver et al., 2000), are able to potentiate the NMDAR; the positive modulatory effect is observed for "bent" steroids with elongated aliphatic chain at the C3 carbon.

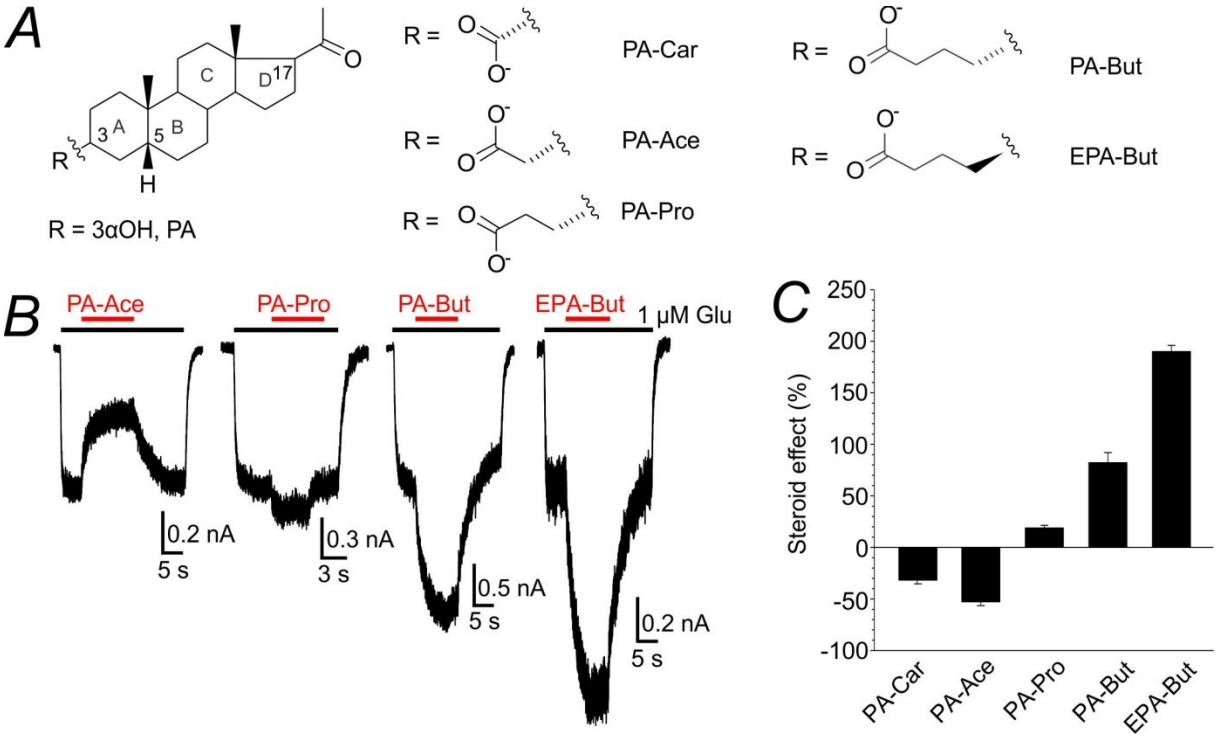

Figure 4.12 Structure-function principles underlying potentiating effect of pregnane-based steroids. ***(A)*** Structure of 3α-hydroxy-5β-pregnan-20-one (PA) and residues used as substituents at the C3 carbon: PA-carboxylate (PA-Car), PA-acetate (PA-Ace), PA-propionate (PA-Pro), PA-butyrate (PA-But), and EPA-butyrate (EPA-But). ***(B)*** Representative recordings demonstrate the effect of PA-Ace (150 μM), PA-Pro (10 μM), PA-But (15 μM), and EPA-But (15 μM) on GluN1/GluN2B receptor responses to 1 μM glutamate. Duration of glutamate and steroid application is indicated by black and red bars, respectively. ***(C)*** Bar graph shows the mean ± SEM degree of steroid-induced effect at GluN1/GluN2B receptors (n = 6-7).

4.3.2 EPA-But potentiates NMDAR responses in a disuse-dependent manner

In the following experiments, we used EPA-But as a representative potentiating steroid with a "bent" structure. For the dose-response analysis, the GluN1/GluN2B receptor responses to 1 μM glutamate were potentiated by co-application of 0.3-15 μM EPA-But. The obtained data were analysed by fitting the logistic equation 2 with the following parameters: E_{max} = 221 ± 23%; EC_{50} = 6.1 ± 0.8 μM; h = 1.4 ± 0.1 (n = 7) (Figure 4.13*A,B*). Next, we evaluated the effect of EPA-But (15 μM) on the GluN1/GluN2B receptor responses induced by 0.03-1000 μM glutamate (Figure 4.13*C-D*). The resulting data were fitted to the logistic

equation 3. In the presence of the steroid, the glutamate E_{max} value was enhanced by 35 ± 6 % (n = 7) and the EC_{50} to glutamate was reduced from 1.7 ± 0.1 μM (n = 12) to 0.4 ± 0.1 μM (n = 12) (Figure 4.13*D*). Figure 4.13*F* demonstrates the negative relationship between the concentration of glutamate co-applied with EPA-But (15 μM) and the degree of EPA-But potentiation. Moreover, the potentiating effect of EPA-But is influenced by the timing of the steroid and glutamate application. Thus, upon co-application with EPA-But (15 μM), GluN1/GluN2B receptor responses to glutamate (1 mM) were potentiated by only 35 ± 5% (n = 5) (Figure 4.13*E,F*). In contrast, 30 s pre-application of EPA-But (15 μM) potentiated the responses to subsequent glutamate (1 mM) application by 287 ± 65%**,** similar to the degree of potentiation observed when the EPA-But (15 μM) pre-application was followed by co-application of glutamate (1 mM) and the steroid (263 ± 65%; n = 6) (Figure 4.13*E*,*F*). In addition, at the holding potential of −90 mV, EPA-But (15 μM) potentiated 1 μM glutamate-induced responses of GluN1/GluN2B receptors to a similar extent as at the holding potential of +30 mV (207 ± 14% and 225 ± 28%, respectively; n = 9). Together, these results indicate that EPA-But positively modulates the NMDAR activity in a disuse-dependent and voltage-independent manner.

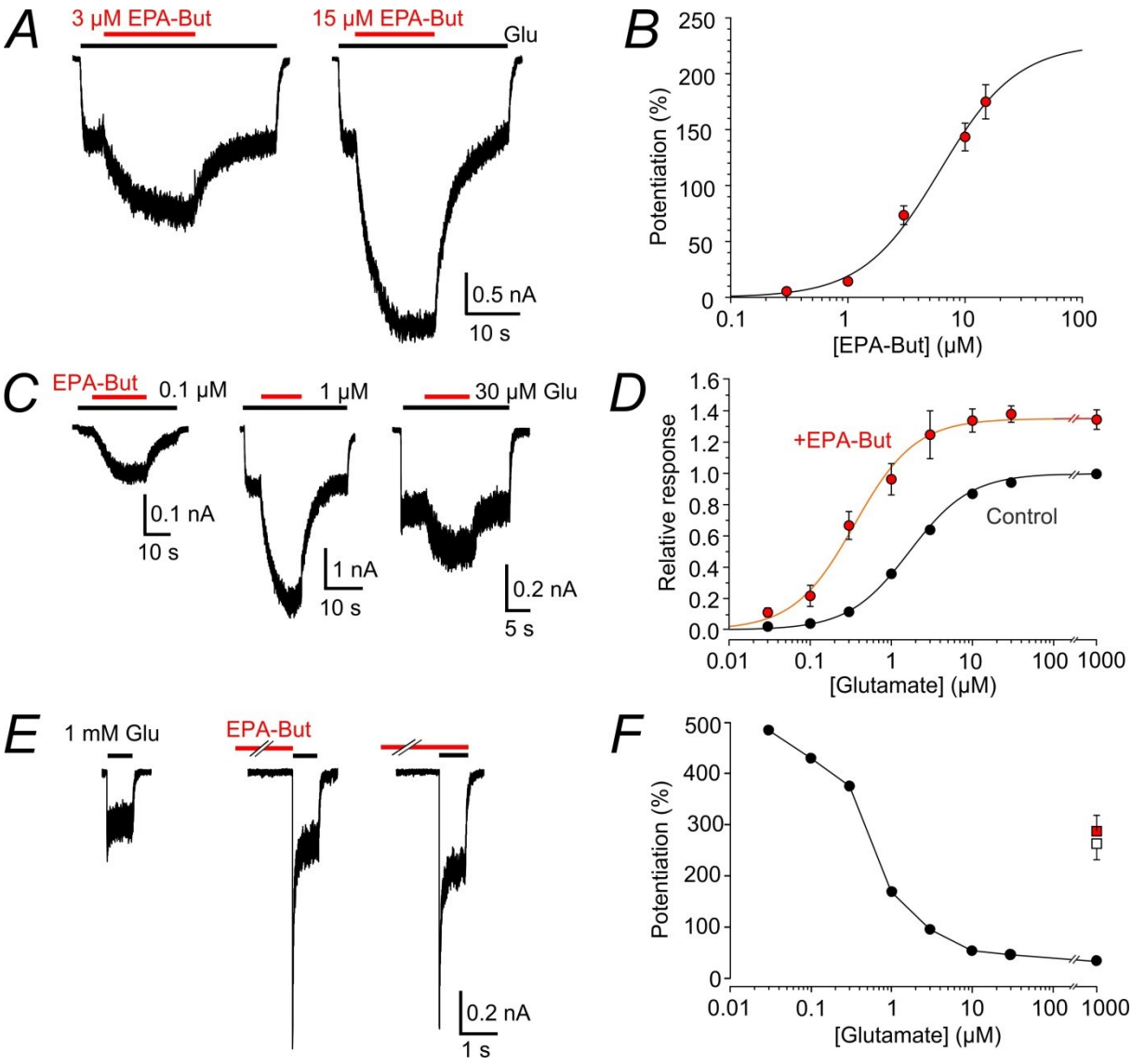

Figure 4.13 Potentiating effect of EPA-But is disuse-dependent. ***(A)*** Representative recordings of GluN1/GluN2B receptor responses to 1 μM glutamate (black bars) before and in the presence of 3 μM and 15 μM EPA-But (red bars). ***(B)*** Concentration-response curve for the EPA-But (0.3 - 15 μM) effect. The EPA-But potentiation was evaluated in HEK293 cells expressing GluN1/GluN2B receptors during the steroid co-application with 1 μM glutamate. Data points are shown as mean ± SEM; $n = 7$. ***(C)*** Representative recordings demonstrate the potentiating effect of EPA-But (15 μM) at GluN1/GluN2B receptor responses to 0.1, 1, and 30 μM glutamate. The duration of glutamate and EPA-But application is indicated by black and red bars, respectively. ***(D)*** Concentration-response curves show the glutamate (0.03-1000 μM) effect in the absence (black curve) and presence (red curve) of EPA-But (15 μM). Control and EPA-But-potentiated glutamate responses were obtained from separate sets of cells. The data were normalized to the control response to 1 mM glutamate and fitted using Equation 2. Data points show mean ± SEM; $n = 12$. ***(E)*** Representative recordings demonstrating GluN1/GluN2B receptor responses to glutamate (1 mM) in the absence and presence of EPA-But (15 μM) recorded before and after 30 s EPA-But (15 μM) pre-application. Duration of glutamate and steroid application is indicated by black and red bars, respectively. ***(F)*** The plot of the mean EPA-But-induced potentiation versus glutamate concentration. EPA-But (15 μM) was co-applied with glutamate (0.03-1000 μM) (filled

circles); the same data set as in ***(D)***. For comparison, the mean potentiation of the responses to 1 mM glutamate after 30 s pre-application of EPA-But (15 µM) (red square) and the mean potentiation of the responses to co-application of glutamate (1 mM) and EPA-But (15 µM) after 30 s EPA-But (15 µM) pre-application (white square) are included. Error bars indicate the SEM.

4.3.3 EPA-But site of action at the NMDAR is different from that for PE-S

Despite structural differences between EPA-But, which is characterized by a "bent" molecular conformation, and PE-S, which is characterized by a "planar" molecular conformation, the potentiating effects of these steroids on GluN1/GluN2B receptors are similar in terms of disuse-dependency, voltage-independency, and slow on- and off- kinetics. To examine whether the steroids act on the same site at the NMDAR, we evaluated the modulatory effect produced by the simultaneous application of a saturating concentration of EPA-But (15 µM) and PE-S (100 µM). We assumed to observe the occlusion of EPA-But and PE-S effects in case of the same site of action for both steroids (Model 1) or summation of their effects in case of different sites of action (Model 2). Simultaneous co-application of both steroids potentiated the GluN1/GluN2B receptor responses to 1 µM glutamate to a significantly greater extent than the application of EPA-But alone (by 280 ± 27% and 213 ± 17 %, respectively; $n = 9$; $p < 0.05$, paired t-test) (Figure 4.14). However, the degree of potentiation induced by the co-application of EPA-But and PE-S was smaller than that predicted by Model 2 (Figure 4.14). These results indicate distinct or partially overlapping sites of action for EPA-But and PE-S at the NMDAR.

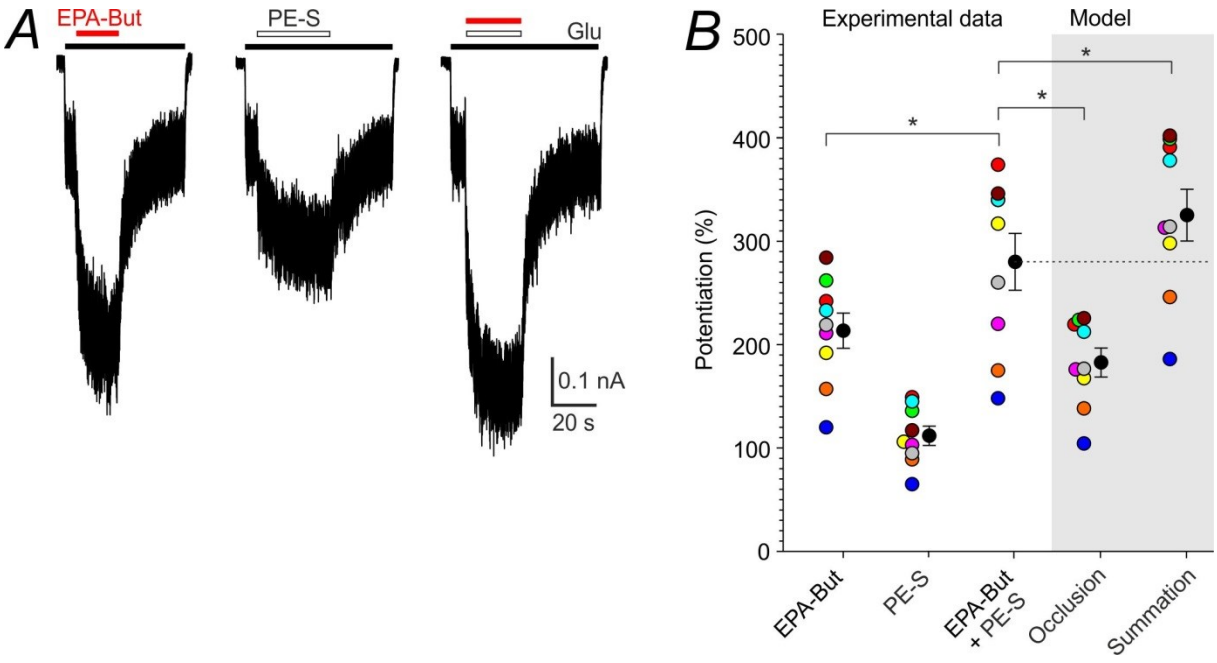

Figure 4.14. The potentiating effects of EPA-But and PE-S are additive. ***(A)*** Representative responses of GluN1/GluN2B receptor to glutamate (1 μM) alone and in the presence EPA-But (15 μM), PE-S (100 μM), or both steroids together. Duration of glutamate, EPA-But, and PE-S application is indicated by black, red, and empty bars, respectively. ***(B)*** Graph displays the degree of potentiation of the GluN1/GluN2B receptor responses to 1 μM glutamate by EPA-But (15 μM), PE-S (100 μM), and simultaneous application of both steroids. Filled circles represent colour-coded data referring to individual cells, empty circles represent mean ± SEM ($n = 9$). Right (grey square), theoretical data points generated by Model 1 (occlusion) and Model 2 (summation). * indicates a significant difference between the groups.

4.3.4 Mutations in the TMD affect the EPA-But potentiation

Using alanine scanning mutagenesis, we explored the role of the outer segment of the TMD in the positive modulation of the GluN1/GluN2B receptor by EPA-But. To allow direct compassion of the impact of amino-acid residue substitution on EPA-But and PE-S potentiation, alanine scanning analysis was performed on the same set of residues as during the identification of the site of action for PE-S (Chapter 4.2.3), i.e. (Q559-V572; G638; I642; S646; F810-V825) of the GluN1 subunit and (S555-I568; D814-A830) of the GluN2B subunit. At mutated receptors whose EC_{50} for glutamate was not significantly different from the WT (Table 4.4), the EPA-But (15 μM) effect was assessed during its co-application with 1 μM glutamate. At mutated receptors whose EC_{50} to glutamate was significantly smaller or bigger than in WT (Table 4.4), the EPA-But (15 μM) effect was evaluated at a glutamate concentration that activates the receptors to the same level as 1 μM glutamate at WT receptors (38% of the WT responses to 1 mM glutamate). This experiment showed that the substitution of the GluN1(G567; S569; V570; G638; I642; E811; N812; M813; F817) and the GluN2B(D557;V558, W559; M561; M562; V564; L566; D816; M818; G820, F822; M824; L825; A830) residues resulted in a significantly decreased EPA-But potentiation of GluN1/GluN2B receptors (one-way ANOVA, $p < 0.001$; followed by t-test) (Figure 4.15*A-C*). These results indicate the GluN1(M4)/GluN2B(M1), GluN2B(M4)/GluN1(M1), and GluN2B(M1/M4) interfaces as potential sites of action for EPA-But (Figure 4.15*D*).

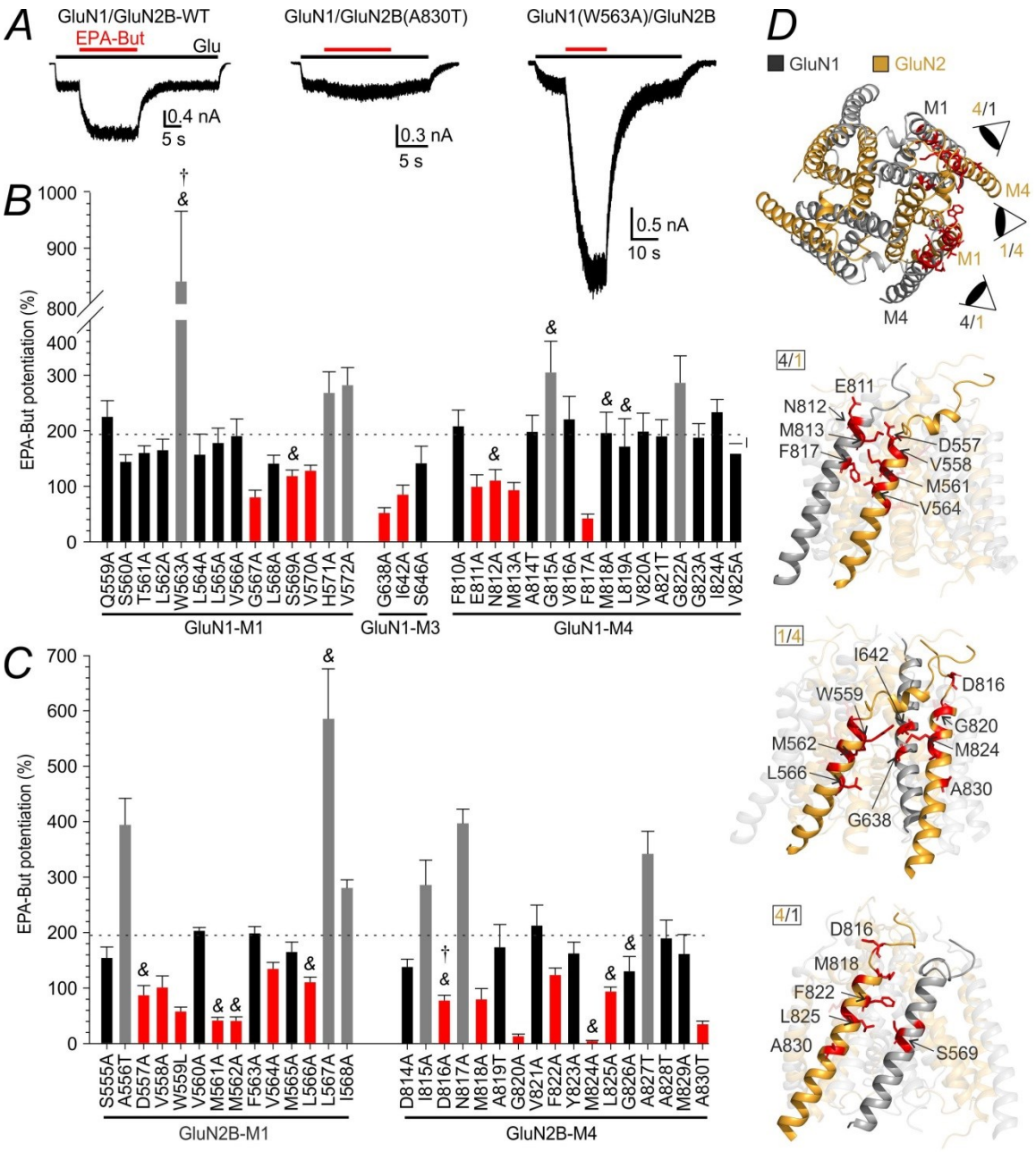

Figure 4.15. The effect of EPA-But on mutated NMDARs. ***(A)*** Representative recordings of the responses of WT, GluN1/GluN2B(A830T), and GluN1(W563A)/GluN2B receptors to 1 μM glutamate applied alone (black bars) and co-applied together with 15 μM EPA-But (red bars). ***(B-C)*** Bar graphs show the degree of EPA-But (15 μM) potentiation of glutamate-induced responses in GluN1/GluN2B receptors with mutated GluN1 ***(B)*** or GluN2B ***(C)*** subunit. The EPA-But potentiation assessments were performed at a glutamate concentration corresponding to 38% of WT receptor response to 1 mM glutamate. The mean EPA-But potentiation in WT receptors is indicated by the dashed lines. Data are presented as mean ± SEM (n = 5-126). Red bars indicate significantly decreased EPA-But potentiation; grey bars indicate significantly increased EPA-But potentiation (one-way ANOVA followed by an unpaired t-test for single comparisons versus WT). & indicate receptors whose glutamate affinity was significantly different from that in WT (Table 4.4). † indicate mutated receptors that demonstrated spontaneous activity. ***(D)*** Ribbon diagram of the TMD of non-activated rat GluN1/GluN2B receptor. The model of the non-activated receptor in the closed-

pore confirmation was taken from (Černý et al., 2019). The GluN1 subunit is coloured grey; the GluN2B subunit is coloured orange. Top, view from the extracellular side. Below, side views of the TMD with a focus on the GluN1(M4)/GluN2B(M1) interface (4/1), GluN2B(M1/M4) interface (1/4), and GluN2B(M4)/GluN1(M1) interface (4/1). Residues whose replacement resulted in a reduction of the EPA-But effect are highlighted in red.

Next, we compared the impact of the mutations on EPA-But and PE-S potentiation. No correlation was found between the effects of EPA-But and PE-S in mutated receptors exhibiting significantly decreased potentiation of the responses to 1 μM glutamate by either of the two steroids (Figure 4.16). This result supports the hypothesis that the sites of action for EPA-But and PE-S at the NMDAR are partially or completely different.

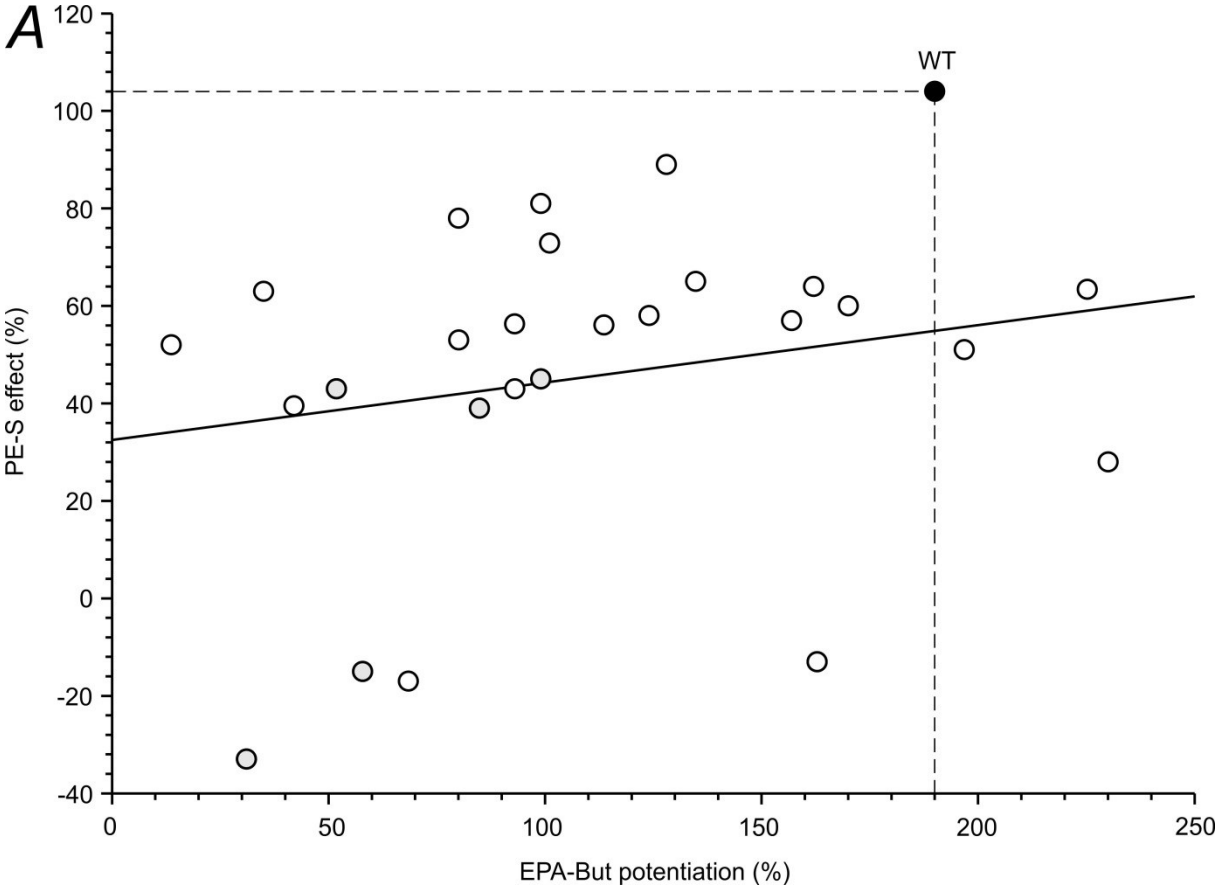

Figure 4.16. Correlation between the effects of EPA-But and PE-S on mutated NMDARs. The mean potentiating effect of EPA-But (15 μM) plotted versus that determined for PE-S (100 μM) at the mutated GluN1/GluN2B receptors where the potentiating effect of either EPA-But or PE-S was significantly diminished compared to WT. The EPA-But and PE-S effects were evaluated in the presence of 1 μM glutamate. Empty circles indicate mutations with diminished steroid effect; a filled circle indicate the WT receptors. A solid line signifies a least-squares linear regression fit. Pearson product-moment correlation analysis indicated no correlation ($p > 0.05$) between the effects of EPA-But and PE-S at mutated receptors. The

dashed lines represent the mean potentiation produced by EPA-But and PE-S in WT receptors.

4.3.5 *In silico* modelling of EPA-But binding at NMDAR

To delineate the EPA-But site of action at the NMDAR, we employed a two-step molecular modelling procedure that had been previously developed to identify the site of action for PE-S (Chapter 4.2.5). An open-state model of the rat GluN1/GluN2B receptor (Černý et al., 2019) was used for the analysis of the interaction between the receptor and EPA-But. The initial molecular docking-based analysis of the steroid-receptor interaction indicated four pairs of preferential interaction sites within the NMDAR TMD, with two pairs – a pair at the GluN1(M1/M4) interface and a pair at the GluN2B(M1/M4) interface – were similar to those previously predicted for PE-S (Chapter 4.2.5). The other two pairs of the predicted interaction sites were in the GluN1(M4)/GluN2B(M1) and GluN2B(M4)/GluN1(M1) interfaces, respectively. Subsequent analysis of the interactions between docking-predicted sites and the EPA-But molecule using MD simulation suggested the presence of three pairs of stable interaction sites within the TMD. The indicated interaction sites were formed by GluN1(M4)/GluN2B(M1), GluN2B(M4)/GluN1(M1), and GluN2B(M1/M4) interfaces (Figure 4.17*A*-*C*).

As mentioned previously (Chapter 4.2.5), the GluN2B M1 and M4 helices move against each other during the receptor activation thus spreading the cavity formed by the M1 and M4 helices of the GluN2B subunit and the M3 helix of the GluN1 subunit. The MD simulation indicated that the EPA-But binding to the GluN2B (M1/M4) interface tightens the interaction between the GluN2B M1 and M4 helices and the GluN1 M3 helix (Figure 4.17*B*), stabilizing the open state of the channel. In addition, the simulation suggested that EPA-But binding at the GluN1(M4)/GluN2B(M1) and GluN2B(M4)/GluN1(M1) interfaces results in the altered orientation of the steroid-binding residues. The side chains of these residues are oriented toward the channel pore in the absence of EPA-But. Upon EPA-But binding, these residues form van der Waals contacts with the steroid, thereby reorienting their side chains toward the steroid molecule (Figure 4.17*A,C*). Overall, the accommodation of EPA-But within the TMD leads to the stabilization of the open state and the expansion of the diameter of the ion channel (Figure 4.17).

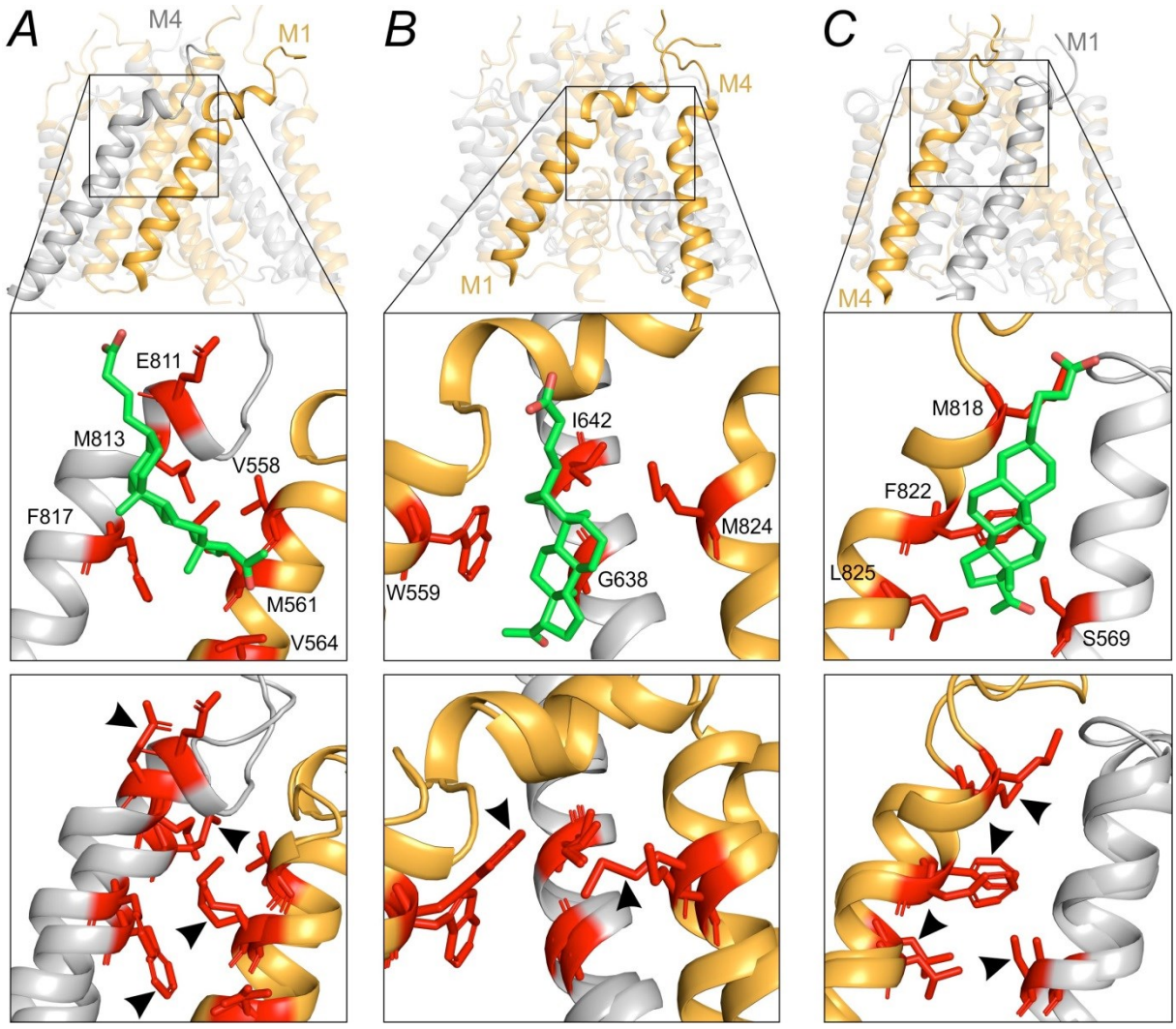

Figure 4.17. The effect of EPA-But binding on the TMD arrangement. Ribbon structure depicts the arrangement of transmembrane helices in the model of liganded GluN1/GluN2B receptor with the open channel configuration (Černý et al., 2019) in the presence and absence of EPA-But. Interaction between the receptor and EPA-But molecule (green) was analysed through molecular docking followed by a 100 ns-long MD simulation. Upper row, location of the steroid-binding GluN1(M4)/GluN2B(M1) ***(A)***, GluN2B(M1/M4) ***(B)***, and GluN2B(M4)/GluN1(M1) ***(C)*** interfaces at the NMDAR TMD. Middle row, the position of the amino-acid residues (red sticks) in direct interaction with the steroid molecule (green). Bottom row, superposition of the transmembrane helices of the NMDAR model in the open state simulated in the presence and absence of EPA-But. The orientations of residue side chains in the absence of the steroid are indicated by arrows.

4.3.6 EPA-But and PE-S effects on NMDARs with disease-related mutations

Since our previous experiments indicated that EPA-But and PE-S sites of action on the NMDAR only partially overlap, we assumed that these steroids may differently modulate the activity of human GluN1/GluN2B receptors with disease-associated mutations. We screened publicly available databases (https://www.ncbi.nlm.nih.gov/clinvar) and selected 9 *de novo*

missense mutations in the hGluN1 subunit (P557A; E662K) and hGluN2B subunit (E413G; R540H; N615I; A636P; E657G; D668N; R682C) associated with several neuropsychiatric disorders, including epilepsy, developmental delay, intellectual disability, West syndrome, intellectual disability, and autism spectrum disorders (Table 4.5). In addition, we evaluated the effects of the steroids on receptors with disease-related hGluN2B(V558I; W607C; V618G; G820A; L825V) mutations previously characterized in Chapter 4.1 (Table 4.1; 4.5). Electrophysiological assessment of WT and mutated receptor responses to 1 mM glutamate revealed a significantly lower peak current densities in HEK293T cells expressing hGluN1(P557A; E662K)/hGluN2B and hGluN1/hGluN2B(E413G; V558I; W607C; N615I; V618G; E657G; D668N; E807K; G820A) receptors in comparison to those expressing WT receptors (Figure 4.18*B*). HEK293T cells transfected with hGluN1/hGluN2B(R540H; R682C; L825V) receptors demonstrated similar current density as cells transfected with WT receptors (Figure 4.18*B*). Virtually no current responses to 1 mM glutamate (<0.1 - pA/pF) were detected in HEK293T cells transfected with hGluN1/hGluN2B(A636P) receptors (Figure 4.18*B*). Generally, prior examinations indicated various defects in the function of mutated receptors (Table 4.5).

The effects of EPA-But (15 μM) and PE-S (100 μM) at WT and mutated receptors were evaluated upon co-application with glutamate (1 μM). No significant difference was found between the degree of EPA-But potentiation in human and rat GluN1/GluN2B receptors (198 ± 9% and 190 ± 6%, respectively) (Figure 4.18*A,C*). The hGluN1/hGluN2B(E413G; N615I; E657G; L825V) receptors demonstrated significantly higher EPA-But potentiation in comparison to WT receptors (Figure 4.18*A,C*). In contrast, the hGluN1(P557R)/hGluN2B and hGluN1/hGluN2B(R540H; V558I; V618G; D668N; G820A) receptors exhibited a significantly diminished EPA-But effect (Figure 4.18*A,C*). The PE-S effect was significantly increased at the hGluN1(E662K)/hGluN2B and the hGluN1/hGluN2B(N615I; E657G; E807K; L825V) receptors and significantly reduced at the hGluN1/hGluN2B(R540H; V558I; W607C; D668N; R682C; G820A) receptors in comparison to WT (Figure 4.18*A,C*). Although significantly altered effects of either EPA-But or PE-S were observed in all tested receptor variants, a significant change in the effect of both steroids was found in only 7 out of 14 receptor variants (Figure 4.18*C*). These results indicate that steroids with a positive modulatory effect at the NMDAR may rectify the effect of loss-of-function mutations in hGluN1 and hGluN2B subunits; however, the degree of the produced potentiation depends on the steroid structure and the specific location of the mutated amino-acid residues.

Table 4.5 Selected *de novo* disease-associated mutations in GluN1 and GluN2B subunits and their phenotypic profiles

Subunit	Mutation	Genotype	Phenotype	Functional properties
hGluN1	P557R	c.1670C>G	ID [1], epi [2]	↓SE; ↓I; ↓Glu EC_{50}; ↓Gly EC_{50} [12]
hGluN1	E662K	c.1984G>A	ID, epi [3]	↑Glu EC_{50}; ↓Gly EC_{50}; ↓P_o [13]
hGluN2B	E413G	c.1238A>G	ID [4]	↓SE; ↓I; ↑Glu EC_{50} [14, 15]
hGluN2B	R540H	c.1619G>A	ID, epi [5]	↓SE; ↓Glu EC_{50}; ↓Gly EC_{50}; ↑P_o [14, 16]
hGluN2B	V558I	c.1658C>T	ID [6, 7]	↑ Glu EC_{50}, [4] but see [17]; ↓P_o [17]
hGluN2B	W607C	c.1821G>T	ID, DD [8]	↓SE; ↓I; ↑Glu EC_{50}; ↑Gly EC_{50}; ↓P_o [17]
hGluN2B	N615I	c.1844A>T	ID, WS [5]	↓I; ↑Glu EC_{50} [17] but see [16]
hGluN2B	V618G	c.1853T>G	ID, WS, epi [5]	↓I; ↓P_o [16, 17]
hGluN2B	A636P	c.1907C>T	ID [9]	↓I [4]
hGluN2B	E657G	c.1970A>G	ID, DD [4]	↓I; ↓Glu EC_{50}; ↑Gly EC_{50} [17]
hGluN2B	D668N	c.2002G>G	epi, DSLD [10]	↓P_o; [18]
hGluN2B	R682C	c.2044C>T	ID [4, 9]	↓Glu EC_{50}; ↓Gly EC_{50} [14]
hGluN2B	E807K	c.2419G>A	ID [4]	↑Glu EC_{50}; ↑Gly EC_{50}; ↓P_o [19]
hGluN2B	G820A	c.2459G>C	ID, DD, GVL, DMD, ASD, epi [4]	↓I [17]; ↓P_o [20]
hGluN2B	L825V	c.2473T>G	ASD [11]	↓P_o [17]

Note: ↓ reduced or ↑ increased surface expression (SE), peak current responses (I), glutamate EC_{50} (Glu EC_{50}), glycine EC_{50} (Gly EC_{50}), or open probability (P_o). Abbreviations: ID - intellectual disability; epi - epilepsy; DD - developmental delay; WS - West Syndrome; DSLD - delayed speech and language development; GVL - generalized cerebral volume loss; DMD - Dyskinetic Movement Disorder; ASD - Autism Spectrum Disorder. [1] (Redin et al., 2014); [2] (Ohba et al., 2015); [3] (Hamdan et al., 2011); [4] (Platzer et al., 2017); [5] (Lemke et al., 2014); [6] (Hamdan et al., 2014); [7] (Lelieveld et al., 2016); [8] (Yavarna et al., 2015); [9] (Freunscht et al., 2013); [10] ClinVar; [VCV000373930.1], https://www.ncbi.nlm.nih.gov/clinvar/variation/VCV000373930.1; [11] (Awadalla et al., 2010); [12] (Ogden et al., 2017); [13] Unpublished data: hGluN1(E662K)/hGluN2B receptors are characterized by elevated glutamate $EC_{50,}$ reduced glycine EC_{50}, and reduced open probability in comparison to WT receptors; [14] (Swanger et al., 2016); [15] (Wells et al., 2018); [16] (Mullier et al., 2017); [17] (Vyklicky et al., 2018); [18] Unpublished data: hGluN1/hGluN2B(D668N) receptors are characterized by similar glutamate EC_{50}, reduced glycine EC_{50}, and reduced open probability in comparison to WT receptors; [19] Unpublished data: hGluN1/hGluN2B(E807K) receptors are characterized by elevated glutamate and glycine EC_{50}, and reduced open probability in comparison to WT receptors; [20] (Amin et al., 2018).

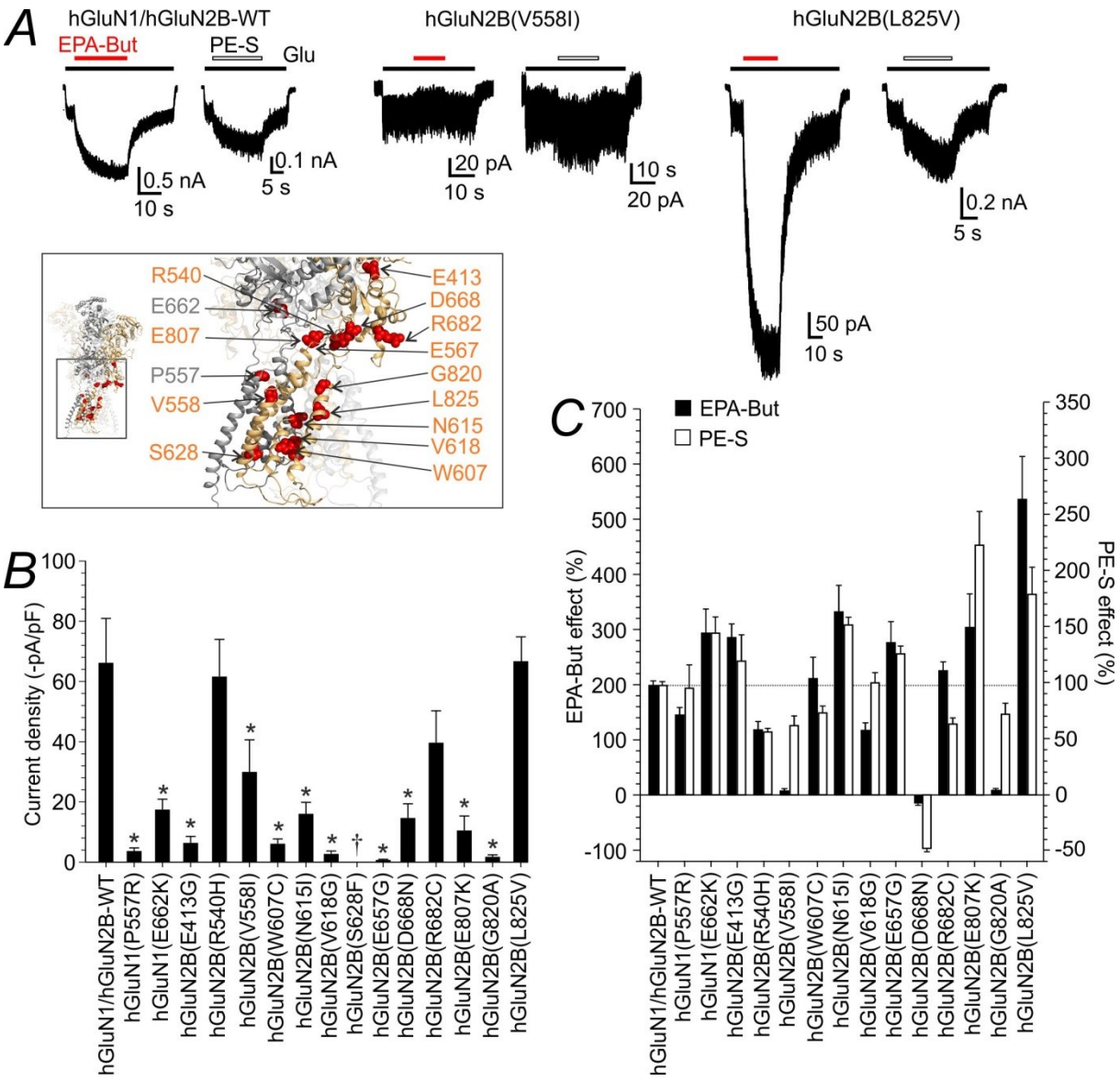

Figure 4.18. Glutamate and steroid effects on hGluN1/hGluN2B receptors with disease-associated mutations. ***(A)*** Representative responses of WT, hGluN1/hGluN2B(V558I), and hGluN1/hGluN2B(L825V) receptors to glutamate (1 μM) alone and in the presence EPA-But (15 μM) or PE-S (100 μM). Duration of glutamate, EPA-But, and PE-S application is indicated by black, red, and empty bars, respectively. The inset shows the location of mutated amino-acid residues. ***(B)*** Bar graph shows the mean current density ± SEM of WT and mutated receptors. † signifies the receptors that exhibited no detectable currents; * signifies a statistical difference compared to WT receptors (one-way ANOVA followed by Mann–Whitney rank sum test for single comparisons versus WT). ***(C)*** Bar graph represents steroid effects on glutamate-induced responses of WT and mutated receptors. 15 μM EPA-But (filled bar) or 100 μM PE-S (empty bar) was applied in the presence of 1 μM glutamate. Data are presented as mean ± SEM. The dotted line represents the mean EPA-But and PE-S effect in WT receptors.

5 Discussion

5.1 Functional and pharmacological properties of disease-associated *de novo* mutations in the hGluN2B subunit

Thanks to recent advances in high-throughput DNA sequencing, numerous mutations in *GRIN* genes were associated with various neuropsychiatric disorders (Burnashev & Szepetowski, 2015; Hu et al., 2016; Soto et al., 2014). However, the impact of disease-associated *GRIN* mutation on the receptor function is often unknown or has been analysed only partially (Ogden et al., 2017; Platzer et al., 2017; Swanger et al., 2016; Yuan et al., 2014). In the current study, we studied 10 *de novo* hGRIN2B mutations found in patients with intellectual disability, developmental delay, autism spectrum disorder, West syndrome, and epilepsy. We explored several mechanisms underlying the dysregulation of mutated receptors, including changes in receptor surface expression, agonist sensitivity, desensitization, and P_o. In addition, we demonstrated the potential of neuroactive steroids PE-S and AND-hSuc to relieve the negative consequences of certain mutations. Investigation of the effect of disease-associated hGluN2B mutations on the receptor surface expression and function is crucial to the understanding of the role of these mutations in the pathology of neuropsychiatric disorders (McRae et al., 2017). Since the GluN2B subunit predominates during early development, GluN2B mutations may have a profound effect on embryonic neurogenesis and neuronal circuit formation. Therefore, establishing a direct connection between the effect of a mutation on receptor function and its clinical outcome may be complicated.

The GluN2B(P553; V558) residues are located within the pre-M1 and M1 helices, respectively (Figure 4.1; 5.1*A*) (Karakas & Furukawa, 2014; Sobolevsky et al., 2009). These regions are structurally coupled with the LBD and have been suggested to play an important role in channel gating (Alsaloum et al., 2016; Lee et al., 2014). Despite the fact that the P553 and V558 residues are located close to each other in the GluN2B subunit, the consequences of mutations in these residues on the receptor function differed widely. Thus, hGluN1/hGluN2B(P553L) receptors showed virtually no response to glutamate (Figure 4.2*B*). In contrast, hGluN1/hGluN2B(V558I) receptors responded to 1 mM glutamate with a current amplitude similar to WT even though these receptors demonstrated increased desensitization and reduced P_o (Figure 4.2*B*; 4.4*E*). Since the hGluN2B(P553L) mutation does not change (Figure 4.2*D*) or only moderately decreases receptor surface expression (Ogden et al., 2017), it is clear that the absence of responses to 1 mM glutamate in receptors with this mutation is a result of disturbed functional properties rather than impaired surface expression. Likely, the

absence of glutamate currents in hGluN1/hGluN2B(P553L) receptors is a consequence of profound desensitization. Thus, the P553 residue is part of the so-called “hydrophobic box”, a highly conserved motif that is of critical importance for the control of NMDAR desensitization (Alsaloum et al., 2016). Consistent with this, profound (98.5%) desensitization was observed in rat NMDAR with GluN2A(P552R) mutation (Ogden et al., 2017), which is homologous in position to the P553 residue in the hGluN2B subunit. In addition, the comparison of the responses of hGluN1-4a/hGluN2B and hGluN1-4a/hGluN2B(P553L) receptors also indicated that the hGluN2B(P553L) mutation leads to greater receptor desensitization (Fedele et al., 2018). Enhanced desensitization in hGluN1/hGluN2B(V558I) receptors is in line with the results of previous studies that showed that the pre-M1 and M1 regions play a key role in fast glycine- and Ca^{2+}-independent desensitization of NMDARs (Krupp et al., 1998; Thomas et al., 2006; Alvaro Villarroel et al., 1998). In addition, this region has been demonstrated to affect the receptor P_o (Ogden et al., 2017).

To assess the structural effects of disease-associated mutations, we employed the homology model of the liganded NMDAR in the pre-open state (Vyklicky et al., 2015), based on the crystal structures of the GluN1/GluN2B receptor (Karakas & Furukawa, 2014; Lee et al., 2014). In the pre-open state, the pre-M1 helix is located in the space between the extracellular ends of the M1 and M4 helices (Figure 5.1*A*). Upon receptor activation, the pre-M1 helix is involved in the transduction of the mechanical signal from the conformational change in the ligand-bound LBD to the pore-lining M3 helix, and then to the M1 and M4 helices. This mechanism implicates the interaction between hGluN2B(P553) and the M3 residues hGluN2B(L650; F653). The structural model proposed by (Fedele et al., 2018) complements our model and suggests the interaction between hGluN2B(P553) and hGluN2B(N549). The MD simulation indicates that the hGluN2B(P553L) mutation leads to the elimination of the pre-M1 linker resulting in the formation of a near-continuous M1 helix (Figure 5.1*B*). The hGluN2B(V558) residue interacts with nearby hydrophobic residues of the M3 helix. The MD-based prediction indicates that the hGluN2B(V558I) mutation stabilizes the interaction between these residues and promotes the reorientation of the pre-M1 helix, therefore weakening the interaction between the M1 and M4 helices (Figure 5.1*C*).

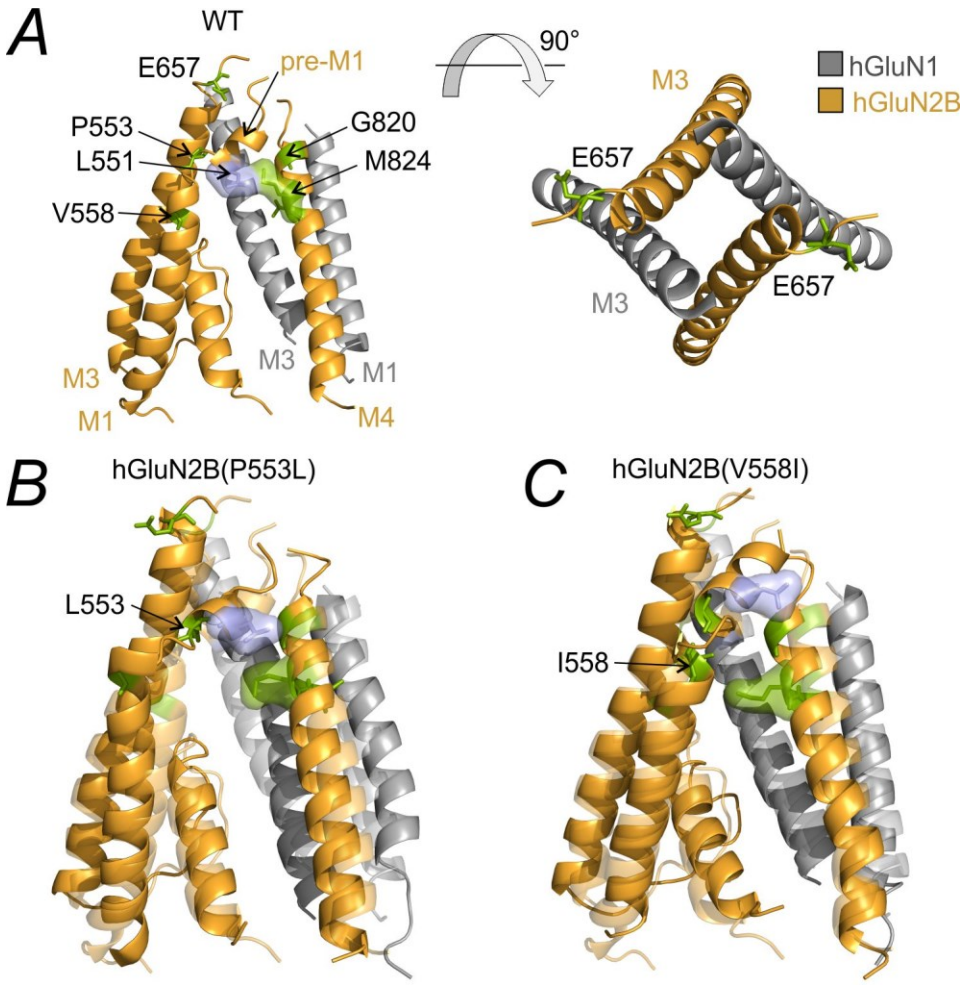

Figure 5.1. Effects of the GluN2B(P553L; V558I) mutations on the TMD structure. ***(A)*** Side view on the homology model of the TMD of the hGluN1/hGluN2B receptor. The homology model was created based on the available NMDAR crystal structures (Karakas & Furukava, 2014; Lee et al., 2014). Amino-acid residues in this study are labelled in green. The van der Waals bond between hGluN2B residues L551 and M824 which is essential for the proper structural organisation of the pre-M1, M1 and M4 helices, is depicted in light green. Right, top view from the extracellular side. ***(B)*** The helical organisation of the TMD in WT (light colours) and GluN1/hGluN2B(P553L) receptors (deep colours). MD analysis indicates that the hGluN2B(P553L) mutation leads to the disruption of the contact between the hGluN2B residues L551 and M824 resulting in the prolongation of the helical structure in the pre-M1 domain. ***(C)*** The helical organisation of the TMD in WT (light colours) and GluN1/hGluN2B(V558I) receptors (deep colours).

The substituted cysteine accessibility method (SCAM) analysis of the M2 helix indicated that the hGluN2B(W607; V618) residues are exposed to the central vestibule of the NMDAR (Kuner et al., 1996). Our results indicated that both hGluN2B(W607C) and hGluN2B(V618G) mutations result in reduced responses to 1 mM glutamate and lower P_o. In addition, hGluN1/hGluN2B(W607C) receptors exhibited reduced surface expression and

lower affinity to both agonists (Figures 4.2*B,F*; Table 4.2). Since the W607 and V618 residues are part of the selectivity filter region, they are believed to be involved in Mg^{2+} binding (Williams et al., 1998). This hypothesis was supported by the results of our experiments that indicated a considerably decreased Mg^{2+} sensitivity in both hGluN1/hGluN2B(W607C) and hGluN1/hGluN2B(V618G) receptors (Vyklicky et al., 2018). These results are in line with the results reported by other studies (Fedele et al., 2018; Mullier et al., 2017).

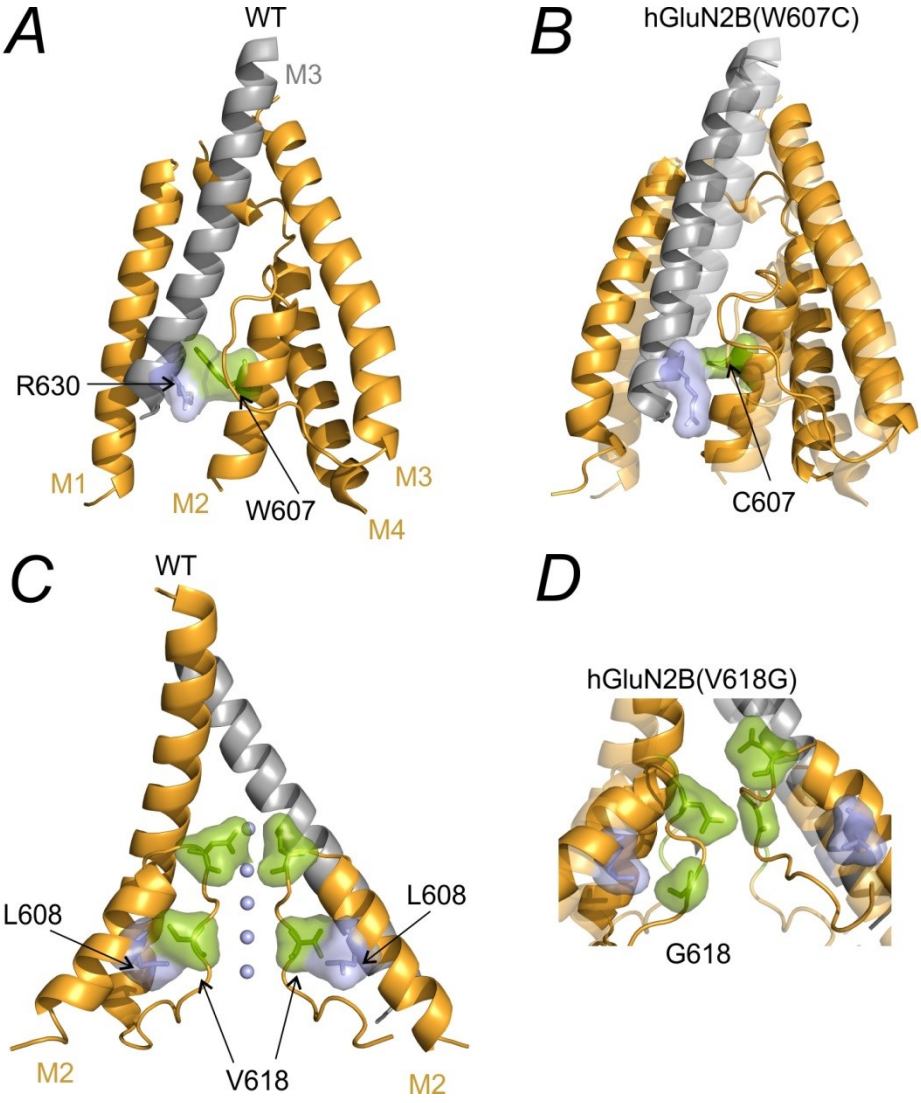

Figure 5.2. Effects of the GluN2B(W607C; V618G) mutations on the TMD structure. ***(A)*** The helical organisation of the TMD of WT hGluN1/hGluN2B receptors. The van der Waals contact between the residues W607 and R630 is indicated in light green. ***(B)*** MD prediction of the TMD organization in WT (light colours) and hGluN1/hGluN2B(W607C) (deep colours) receptors. The hGluN2B(W607C) mutation leads to a weakening of the interaction between the residues V618 and R630 of the GluN2B, therefore affecting the arrangement of the GluN2B M2 and M3 helices. ***(C)*** The homology model of the GluN1/hGluN2B receptor ion permeation pathway was based on the crystal structure of the KcsA potassium channel (Zhou

et al., 2001). The van der Waals contact between the hGluN2B residues L608 and V618 (light green) stabilizes the orientation of the hGluN2B(M2) helix in the permeation pathway. ***(D)*** MD prediction of the TMD organization in WT (light colours) and hGluN1/hGluN2B(V618G) (deep colours) receptors. The hGluN2B(V618G) mutation disrupts the interaction between hGluN2B(V618) and hGluN2B(R630) therefore altering the orientation of the M2 helix.

To reveal the structural consequences of these mutations, we employed our previously developed model for the GluN1/GluN2B receptor with an open extracellular vestibule (Vyklicky et al., 2015). The comparison of NMDAR models in the pre-open and open states indicated no considerable differences in the structures of the selectivity filter and extracellular parts of the M1, M3, and M4 helices (Figure 5.2*A*). Our NMDAR model is in line with previous studies estimating the selectivity filter diameter as 6.0 Å (Vyklicky et al., 1988), 5.5 Å (Villarroel et al., 1995), and 4.5 × 5.7 Å (Zarei & Dani, 1995) and agrees with the estimates for the extracellular vestibule diameter of 7.3 Å (Villarroel et al., 1995). The hGluN2B(W607) residue was indicated to interact with the M1 residue hGluN1(R630) (Figure 5.2*B*). The van der Waals interaction between these residues supports the proper orientation of the M2 helices with respect to their surroundings. The MD simulation predicted that the hGluN2B(W607C) mutation leads to a weakening of this interresidual interaction resulting in an altered orientation of the M2 helix (Figure 5.2*B*). The hGluN2B(V618) residue interacts with hGluN2B(L608), supporting the correct orientation of the adjacent carboxyl groups within the selectivity filter (Figure 5.2C). In turn, the hGluN2B(V618G) mutation results in the reorientation of the backbone carboxyl groups and hence is likely to impair ion selectivity and the effectiveness of ion conduction (Figure 5.2*D*).

The absence of current responses to 1 mM glutamate in hGluN1/hGluN2B(S628F) receptors was accompanied by, and likely resulted from, a severe reduction in the surface expression (Figure 4.1*F*). The hGluN2B(S628) residue is conserved in all GluN2 subunits and is located within the intracellular part of the M3 helix (Figures 4.1; 5.2*A*). A previous study by our laboratory demonstrated that the GluN2B M3 residues (W635; S645; Y646; and T647) are involved in the control of NMDAR surface expression (Kaniakova et al., 2012). Based on this, it can be speculated that the reduction in surface expression of hGluN1/hGluN2B(S628F) receptors may be controlled by the same or similar mechanisms as those for the indicated M3 residues.

The MD analysis of the hGluN2B(S628F) mutation indicates that the substitution of a polar and relatively small serine with a bulky and non-polar phenylalanine results in steric

hindrance affecting the interaction with the M1 helix and altering the structural organization of the TMD (Figure 5.3*B*). These structural distortions may be the reason behind the exclusion of hGluN1/hGluN2B(S628F) receptors from surface expression.

Despite normal surface expression, hGluN1/GluN2B(E567G) receptors displayed decreased current responses to 1 mM glutamate (Figure 4.1*B*). These results imply that the mutation leads to severe impairments in receptor function. The GluN2B(E567) residue is located within the M3-S2 linker and is conserved among the GluN2, GluK, and GluA subunits. The M3-S2 linker couples agonist-binding induced structural changes in the LBD with the M3 helix and therefore plays a crucial role in channel gating (Sobolevsky et al., 2004). Because of this, mutations in the M3-S2 linker may have a dramatic impact on receptor function and can result in impaired transmission of the signal from agonist binding to receptor activation leading to reduced Po (Kazi et al., 2014). Due to the lack of information about electron density in the available crystal structures (Karakas & Furukawa, 2014; Lee et al., 2014), the data about the location of residues within the linker regions are not available. Hence, we simulated the structure of the M3-S2 linker with computational methods. The obtained results indicate the mutation GluN2B(E567G) leads to the closing of the ion channel due to the interactions between the GluN2B(G567) and adjacent residues from the M3 helix (Figure 5.3*C*).

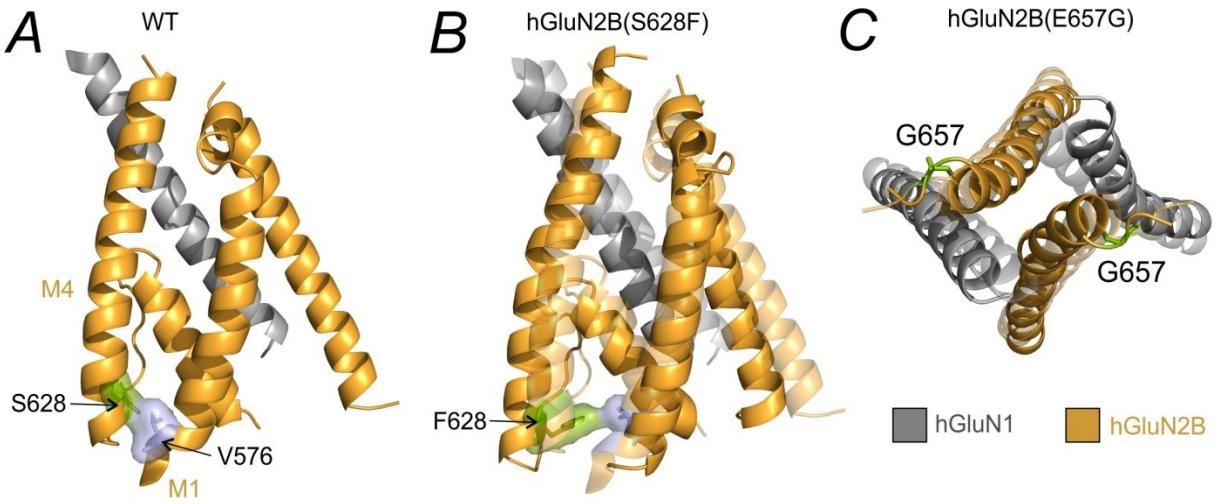

Figure 5.3. Effects of the hGluN2B(S628F; E657G) mutations on the TMD structure. ***(A)*** The homology model shows the helical organisation of the TMD in hGluN1/hGluN2B receptors. The homology model was based on the NMDAR crystal structures (Karakas & Furukava, 2014; Lee et al., 2014). MD simulation indicates several interhelical interactions that resemble a leucine zipper-like motif. A van der Waals contact between the V576 and S628 residues of hGluN2B is indicated in light green. ***(B)*** The arrangement of the TMD in WT (light colours) and hGluN1/hGluN2B(S628F) receptors (deep colours). MD indicates that the hGluN2B(S628F) mutation leads to an increase in the distance between the M1 and M4

helices. ***(C)*** The arrangement of the TMD in WT (light colours) and hGluN1/hGluN2B(E657G) receptors (deep colours). MD simulation indicates that the hGluN2B(E657G) mutation leads to a shrinking of the ion permeation pathway as a result of disrupted interaction along the M3-S2 linker of the hGluN2B subunit.

Despite the fact that the surface expression of hGluN1/ hGluN2B(G820A; G820E; and M824R) receptors was similar to or even higher than that of WT, the responses of these receptors to 1 mM glutamate were reduced dramatically **(**Figure 4.1*B,F*). These results indicate severe functional impairments; however, the negligible amplitude or absence of current responses of these receptors precluded a detailed analysis of the functional consequences of indicated mutations. A more recent study (Amin et al., 2018) reported that GluN1/hGluN2B(G820A) receptors have a dramatically reduced P_o and accelerated deactivation. The hGluN1/hGluN2B(L825V) receptors responded to 1 mM glutamate with the same current amplitude as WT receptors even though their P_o was 7-fold lower (Figures 4.1*B*; 4.4).

The hGluN2B(G820; M824; and L825) residues are located in the upper part of the M4 helix and are conserved across all GluN2 subunits (Figure 4.1; 5.4*A*). Several studies imply an important role of the M4 helix in the control of NMDAR gating (Amin et al., 2021; Premo et al., 2021). Our model indicates interaction between the hGluN2B(L825) and hGluN1(M639) residues upon receptor liganding (Figure 5.4*B*). The hGluN2B(L825V) mutation impairs the interaction between these residues. However, the structural consequences of this mutation are not clear (Figure 5.4*B*). In fully liganded receptors, the hGluN2B(M824) residue interacts with the pre-M1 residue hGluN2B(L551) (Figure 5.4*E*). In mutated hGluN1/hGluN2B(M824R) receptors, this interaction is disrupted (Figure 5.4*E*), resulting in a mutual displacement of the M1 and M4 helices that is likely to make the transduction of the mechanical signal from the LBD to the TMD less effective. The hGluN2B(G820) is located at the very end of the M4 helix and plays a role as a hinge providing structural flexibility to the M4 helix allowing the extension of the S2-M4 linker during receptor activation (Figure 5.4*C-D*). When the channel is open, hGluN2B(G820) is located in proximity to the pre-M1 residue GluN2B(L547) and is likely to interact with this residue (Amin et al., 2018). The hGluN2B(G820A) and hGluN2B(G820E) mutations decrease the flexibility of the upper part of the M4 helix preventing the structural rearrangements necessary for the channel opening (Figure 5.4*C-D*).

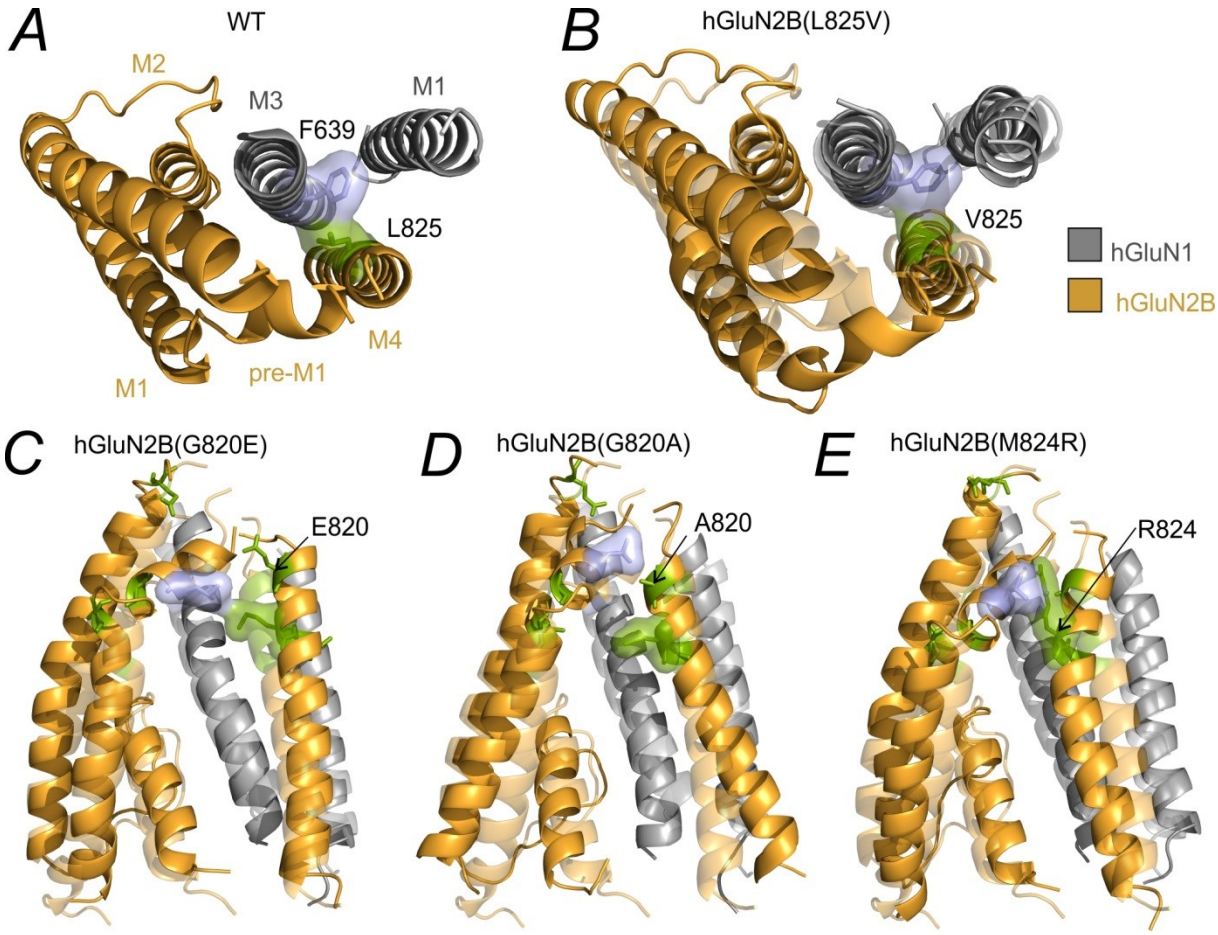

Figure 5.4. Effects of the GluN2B(L825V; G820E; G820A; and G824R) mutations on the TMD structure. ***(A)*** The homology model shows the structural organisation of the hGluN1/hGluN2B receptor TMD. The homology model was based on the NMDAR crystal structures (Karakas & Furukava, 2014; Lee et al., 2014). MD simulation indicated that a van der Waals contact between the hGluN1(F639) and hGluN2B(L825V) residues stabilizes the interaction between the helices hGluN1 M3 and hGluN2B M4. ***(B)*** The arrangement of the TMD in WT (light colours) and hGluN1/hGluN2B(L825V) receptors (deep colours). The hGluN2B(L825V) mutation weakens the van der Waals contact with hGluN1(F639) resulting in increased distance between hGluN1 M3 and hGluN2B M4. ***(C-D)*** The arrangement of the TMD in WT (light colours), hGluN1/hGluN2B(G820E) (***C***, deep colours), and GluN1/hGluN2B(G820A) receptors (***D***, deep colours). As the last residue of the M4 helix, G820 is important for the extension of the S2-M4 linker upon the LBD reorientation. ***(E)*** The arrangement of the TMD in WT (light colours) and hGluN1/hGluN2B(M824R) receptors (deep colours). Upon ligand binding, the hGluN2B(M824) residue forms contact with the pre-M1 residue hGluN2B(L551). The hGluN2B(M824R) mutation leads to the disruption of the contact with hGluN2B(L551) inducing a mutual displacement of the M1 and M4 helices and decreasing the efficiency of transduction of the mechanical signal from the LBD.

Compounds that enhance the NMDAR $P_{o,}$ such as the potentiating neurosteroid PE-S (Horak et al., 2004), appear to be promising therapeutics to compensate for the effect of loss-of-function mutations associated with the reduction of the receptor P_o. In this study, we

explored the potential of PE-S and its more potent synthetic analogue AND-hSuc to correct the impaired function of hGluN1/hGluN2B receptors harbouring the disease-associated hGluN2B mutations described above. The steroids potentiated glutamate-evoked responses of hGluN1/hGluN2B(V558I; W607C; V618G; and G820A) receptors to approximately the same extent as the responses of WT receptors. In hGluN1/hGluN2B(L825V) receptors, the degree of potentiation produced by the steroids was significantly higher than that in WT receptors. These results indicate the potential of PE-S and AND-hSuc as personalized medicine to treat the negative effects of this loss-of-function mutation. Moreover, it is credible that the potentiating effect is not limited to mutations in the TMD, since the responses of NMDARs with LBD mutations, such as GluN2A(V685G) and GluN2A(D731N), have been also shown to be potentiated by PE-S (Swanger et al., 2016).

For the full manifestation of mutation-induced impairments in receptor function, patients must be homozygous for the given mutation. However, this situation is very unlikely for *de novo* mutations, so the majority of patients are heterozygous for the mutation. If only one allele is mutated, 50% of all expressed GluN2B subunits will be mutated; in these circumstances 25% of hGluN1/hGluN2B receptors will be unmutated, 50% of hGluN1/hGluN2B receptors will harbour a mutation in one hGluN2B subunit, and 25% of hGluN1/hGluN2B receptors will harbour a mutation in both GluN2B subunits.

To estimate the effect of a mutation on receptor activity, we may use as an example a GluN2 mutation that reduces the receptor P_o from 10% (in WT receptors) to 1% (in receptors with both GluN2 subunits mutated). Using Mendel's law of dominance and uniformity, we may approximate that the overall activity of receptors will be reduced to 77.5, 55.0, and 32.5%, respectively. These results indicate that for the full compensation for the mutation-induced impairments, a pharmacological agent may potentiate the receptor responses 1.3-fold, 1.8-fold, and 3.1-fold, respectively. However, these are only rough approximations of the effect of mutations on receptor function, which do not take into account the fact that a significant portion of NMDARs in the brain are triheteromers containing different types of GluN2 or/and GluN3 subunits (Monyer et al., 1994; Pérez-Otaño et al., 2016; Stroebel et al., 2018). Therefore, further studies are needed for a better understanding of the association between loss-of-function mutations in the NMDAR and their clinical outcomes.

5.2 Identification of the site of action for pregnenolone sulfate at the NMDAR

In the current study, we identified a particular group of residues within the TMD of the GluN1/GluN2B receptor that comprise the positive allosteric modulatory site for PE-S. A

variety of compounds from different structural groups produce positive allosteric modulation of NMDARs by increasing the receptor agonist sensitivity and/or by improving their efficacy (Hackos & Hanson, 2017). Several steroids with structural similarity to PE-S, such as androst-5-ene and pregn-5-ene dicarboxylic acid esters, have been demonstrated to potentiate NMDAR currents 0.5-4.5-fold with the binding affinity varying in the range of 2-151 μM (Krausova et al., 2018). Supposing that charged potentiating steroids act at the same or overlapping site, it is probable that this site of action can accommodate steroids with large substituents without clear structural preferences for the residues at the C3 and C17 carbons of the core structure.

Despite the similarity in the molecular structure of various naturally-occurring sulfated neurosteroids and sterols, these compounds differently modulate NMDAR function. PE-S produces mixed effects at the NMDAR: a disuse-dependent potentiating effect and a use-dependent inhibitory effect; however, the potentiating effect of the steroid predominates at GluN1/GluN2A and GluN1/GluN2B receptors (Bowlby, 1993; Gibbs et al., 2006; Horak et al., 2004, 2006; Malayev et al., 2002; Wu et al., 1991). In contrast, PA-S is a use-dependent NMDAR NAM whose site of action is located at the outer vestibule of the ion channel (Park-Chung et al., 1994; Petrović et al., 2005; Vyklicky et al., 2015). Although the site of action for sterols at the NMDAR is not clear, it is likely to be located within the TMD (Hackos & Hanson, 2017; Korinek et al., 2015; Paul et al., 2013). The inability of PE-S treatment to compensate for the consequences of cholesterol depletion (Figure 4.7*D*) as well as the fact that 24(S)-HC and PE-S effects do not occlude (Linsenbardt et al., 2014) suggest that PE-S and sterols act at different sites at the NMDAR. In addition, experiments on chimeric receptors combining different NMDAR and KAR domains indicated distinct domain demands for PE-S- and 24(S)-HC-induced potentiation. Whereas the availability of both the TMD and LBD from the NMDAR was needed for PE-S potentiation, the 24(S)-HC potentiation required only the NMDAR TMD (Wilding et al., 2016).

Our experiments showed that alanine substitutions of the GluN1(G638; I642) and GluN2B(W559; M562; Y823; M824) residues result in a substantial reduction of PE-S potentiation (Figure 4.8; 4.10), indicating that these residues are likely to comprise the steroid-binding site. This assumption is supported by several findings. First, these residues are co-located at the GluN2B M1/M4 interface in proximity to each other and were predicted by MD simulation to form van der Waals interactions with the PE-S molecule (Figure 4.10; 4.11). Second, the comparative analysis of the NMDAR models in an open and closed channel state (Figure 4.11) suggests that, upon channel opening, the GluN2B M1/M4

interface is subjected to structural rearrangements leading to a reduction in PE-S binding affinity, in line with the disuse-dependent action of PE-S (Horak et al., 2004). Finally, the indicated GluN2B subunit residues are conserved among GluN2 subunits but share almost no homology to the GluN3A subunit (Figure 4.10*A*). This finding is in line with the fact that PE-S potentiates the responses of conventional NMDARs but not the GluN3A subunit-containing NMDARs (Horak et al., 2006; Jang et al., 2004; Kostakis et al., 2011; Malayev et al., 2002).

The suggested steroid-binding site within the cavity enclosed by the GluN1 M3 and GluN2B (M1; M4) helices is subjected to conformational rearrangements upon channel opening. The MD simulation indicated that the steroid binding affects these conformational rearrangements facilitating the GluN2B M4 helix rotation during the receptor activation (Figure 4.11). In addition, the interaction with the PE-S molecule leads to a tightening of the interaction between the GluN1(I642) and GluN2B(W559) residues (Figure 4.11). Since the GluN1(I642) residue is located within the pore-lining M3 helix, it seems reasonable to assume that this interaction underlies the mechanism by which PE-S increases the NMDAR P_o (Černý et al., 2019; Horak et al., 2004). Upon the steroid unbinding, the GluN2B M4 helix returns to its ordinary position moving the GluN2B(M824) residue closer to the GluN2B(W559) residue (Figure 4.11). As a result, these residues form a van der Waals contact with each other therefore impeding proper accommodation of the steroid molecule in the binding pocket. This mechanism sheds light on the disuse-dependent potentiating effect of PE-S (Horak et al., 2004).

Several lines of evidence indicate that the negative allosteric modulatory site is likely to be distinct from the site characterized above. Thus, the potentiating and inhibitory effects of PE-S differ in their mechanisms: whereas PE-S potentiation is disuse-dependent, PE-S inhibition is use-dependent (Horak et al., 2004). Moreover, alanine substitution of GluN2B(Y823; M824) residues abolishes the potentiating but not the inhibitory effect of PE-S (Figure 4.11). The results of a recent alanine-scanning study indicated that the GluN1 M4 helix is a potential negative allosteric modulatory site for PE-S (Langer et al., 2021). In addition, the previously identified binding site for inhibitory steroids at the extracellular vestibule of the ion channel is also likely to be a negative allosteric modulatory site for PE-S (Vyklicky et al., 2015). However, additional experiments may be required to clarify the site(s) and mechanisms of NAM action of PE-S.

Numerous neuropsychiatric disorders are linked to NMDAR hypofunction, including ASD, epilepsy, schizophrenia, intellectual disability, and developmental delay (Hansen et al., 2021). For example, several *de novo* disease-associated mutations were associated with

decreased NMDAR expression or impaired function of the receptors (Kehoe et al., 2013; Ogden et al., 2017; Platzer et al., 2017; Vyklicky et al., 2018; Wells et al., 2018). Therefore, there is considerable interest in NMDAR PAMs, such as PE-S, as pharmacological tools to correct NMDAR hypofunction. Thus, the evaluation of the PE-S effect on human NMDARs with disease-associated hGluN2A(V685G; D731N) and hGluN2B (L825V) mutations demonstrated that the steroid produces a much stronger potentiation of mutated receptors in comparison to WT, suggesting the potential of PE-S for use in personalized medicine (Swanger et al., 2016; Vyklicky et al., 2018). Moreover, the identification of sites of action for PE-S and better understanding of mechanisms underlying the potentiating effect of the steroid is pivotal for further design of novel potentiating neurosteroid-like compounds to treat disorders associated with NMDAR hypofunction.

5.3 Structure requirements for potentiating neuroactive steroids

In this study, we demonstrated that C3-substituted derivatives of pregnanolone exhibit a positive allosteric modulatory effect at NMDAR. Despite the common structural features and similarities in the on- and off-kinetics of EPA-But and PE-S, the potentiating effects of these steroids at GluN1/GluN2B receptors are additive. In addition, no correlation was observed between the effects of EPA-But and PE-S on receptors with the TMD mutations that decreased the potentiation of either of the two steroids and the steroids differently modulated the activity of hGluN1/hGluN2B receptors with different disease-associated mutations. The results of alanine screening mutagenesis and *in silico* modelling indicated three interaction interfaces for EPA-But at the GluN1/GluN2B receptor. These interaction interfaces are formed by residues at the upper parts of the GluN1(M4)/GluN2B(M1), GluN2B(M4)/GluN1(M1), and GluN2B(M1/M4) helices.

Although the structural principles determining the modulatory effect of steroids at the NMDAR are not fully understood, several studies indicated that steroids with a “planar” molecule potentiate the NMDAR function, whereas steroids with a “bent” molecule inhibit the NMDAR function (Borovska et al., 2012; Korinek et al., 2011; Kudova et al., 2015; Park-Chung et al., 1994; Stastna et al., 2009; Weaver et al., 2000; Wu et al., 1991). However, our results demonstrated that derivatives of the endogenous inhibitory steroid PA-S, such as PA-But and EPA-But, can potentiate NMDAR function despite the “bent” shape of the steroid molecule (Wu et al., 1991). Interestingly, EPA-But was similar to the “planar” neurosteroid

PE-S in terms of a disuse-dependent positive allosteric effect at the NMDAR (Horak et al., 2004).

Our findings indicated that the NMDAR harbours several separate sites of action for different steroids. The site of action for inhibitory steroids, such as PA-S, is within the outer vestibule of the ion channel (Vyklicky et al., 2015), whereas the site of action for PE-S is located at the interface formed by transmembrane GluN2B(M1/M4) helices (Krausova et al., 2020). The results of mutagenesis experiments together with MD simulation indicated that in addition to the site of action at the GluN2B(M1/M4) interface, the TMD contains two extra pairs of sites of action for EPA-But, which are distinct from those for PE-S (Krausova et al., 2020). Despite the site of action at the GluN2B(M1/M4) interface being generally similar for EPA-But and PE-S, binding modes and predicted mechanisms of action differ between the steroids (Figure 5.5). PE-S firmly interacts with and supports the rotation of the GluN2B(M4) helix. In addition, PE-S tightens the interaction between the GluN2B(M4) and GluN1(M3) helices by direct interaction with M3 residues and through GluN2B(M824)-mediated contacts. In contrast to EPA-But, PE-S forms contact with the GluN2B(Y823) residue. The EPA-But molecule intercalates between the residue GluN2B(W559) of the M1 helix and the residue GluN2B(M824) of the M4 helix (Figure 5.5*A*). The C-17 acetyl group of EPA-But interacts with the GluN1(M634) and GluN2B(W610) residues (Figure 5.5*A*).

It is necessary to mention that the experimental and *in silico* characterization of the EPA-But binding site is challenging because of several technical issues. GRIN genes have a low residual variation intolerance score, which indicates a very low tolerance to mutations of NMDARs (Petrovski et al., 2013; Traynelis et al., 2017). Hence, it is not surprising that even a single amino-acid substitution in the NMDAR often dramatically affects receptor function. Moreover, even substitutions in the same residue may result in distinct functional and structural consequences. On the other hand, the identification of specific residues involved in EPA-But binding with *in silico* analysis is also arduous, since the predicted EPA-But binding site is constituted by mostly hydrophobic residues and the van der Waals forces involved in the steroid binding are not directional and the side-chain confirmation can dynamically change. Nevertheless, the residues that are predicted to be within 4 Å of the steroid molecule include a substantial fraction of the experimentally identified residues (Figure 4.10; 5.5*A*). In general, *in silico* analysis explains the results of alanine scanning mutagenesis well, including the distinctions between the effects of residue substitution on EPA-But and PE-S potentiation. For example, the GluN2B(L566) residue was experimentally shown to be important for EPA-But potentiation (Figure 4.10) but is too remote from the binding site to interact with the

steroid directly. The results of *in silico* analysis indicated that the interaction between the GluN2B(L566) and the steroid is mediated by the GluN2B(W610) residue. Nonetheless, the analysis of the role of the residues within pre-M1 and M2 helices is complicated due to the severe adverse effects of mutation in these regions on receptor function.

The divergence in the EPA-But and PE-S binding sites results in a considerable difference in the effects of the steroids in ceratin disease-related receptor variants. Thus, hGluN1/hGluN2B(E413G) receptors demonstrated increased EPA-But potentiation, but the PE-S effect in these receptors was not changed. In contrast, hGluN1(E662K) and GluN2B(E807K) mutations resulted in enhanced PE-S potentiation but did not change the degree of EPA-But potentiation significantly (Figure 4.7). These findings indicate the development of novel steroid-based PAMs as a promising approach to revert NMDAR hypofunction in specific disease-associated variants.

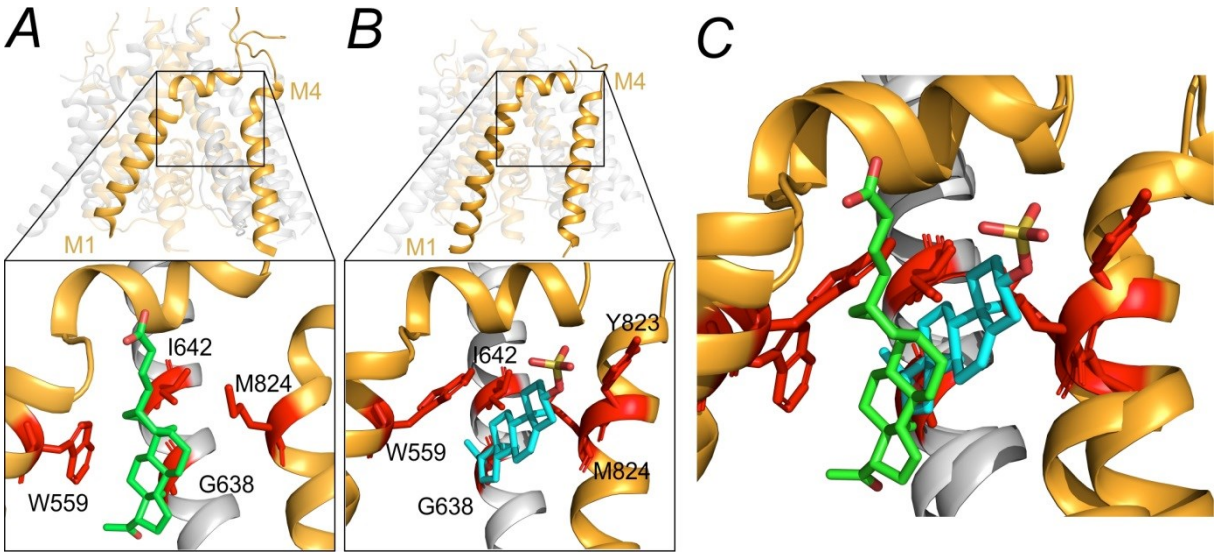

Figure 5.5. Binding modes for EPA-But and PE-S at the GluN2B(M1/M4) interface. Ribbon structure shows the arrangement of M1-M4 helices in the model of the GluN1/GluN2B receptor in the open state (Černý et al., 2019). The GluN1 subunit is labelled in grey colour and the GluN2B subunit is labelled in orange colour. The EPA-But (green) ***(A)*** and PE-S (cyan) ***(B)*** binding were modelled by docking followed by MD simulation. Residues which have been experimentally identified as important for the steroid-induced potentiation are labelled in red colour. ***(C)*** Superimposition of the orientation of EPA-But and PE-S molecules within the GluN2B(M1/M4) interface. The Y823 residue does not interact with EPA-But but interacts with PE-S.

The EPA-But binding site is likely to be in proximity to or even overlap with that for tetrahydroisoquinolines. Thus, the proposed binding site for CIQ, a tetrahydroisoquinoline derivative that acts as PAM at GluN2C- and GluN2D- containing NMDARs, is located at the GluN2D(M1) helix (Mullasseril et al., 2010; Ogden & Traynelis, 2013). Alanine substitution

of GluN2D(V582; W583; V588; L591) residues resulted in a diminished CIQ potentiation (Ogden & Traynelis, 2013); similarly, the substitution of homologous GluN2B residues (V558; W559; V564; L567) decreased the degree of EPA-But-induced potentiation (Figure 4.10). The binding site for another tetrahydroisoquinoline NMDAR PAM, EU1180–55, is located at the GluN1(M4)/GluN2D(M1) interface (Strong et al., 2021). The GluN1(G567A; V572A) and GluN2B(A556T; V558A; L567A) mutations shifted the EU1180–55 and EPA-But potentiating effects in the same direction (Kysilov et al., 2022; Strong et al., 2021). However, the substitution of the GluN1(L562; L564; L565) residues that were shown to be important for the EU1180–55 effect did not significantly affect EPA-But potentiation. Vice versa, alanine substitution of the GluN1(V570) and GluN2B(M562; V564) residues enhanced the EU1180–55 effect but decreased the EPA-But effect (Kysilov et al., 2022; Strong et al., 2021).

The location of binding sites for other classes of NMDAR PAMs seems to be distinct from those for steroids. Pyrrolidinones, which are selective PAMs of GluN1/GluN2C receptors, bind to the pocket formed between the ATD and LBD of the GluN2C subunit (Kaiser et al., 2018; Khatri et al., 2014; Zimmerman et al., 2014). The binding sites for naphthalenes and phenanthrenes, which comprise another class of subunit-selective NMDAR PAMs, are located within the LBD (Costa et al., 2010; Irvine et al., 2012). The proposed positive allosteric modulatory site for polyamines is located at the interface between the lower lobes of GluN1 and GluN2B ATDs (Mony et al., 2011; Tomitori et al., 2012; Traynelis et al., 1995). A thiazolopyrimidinone derivative GNE-9278 is an NMDAR PAM that enhances glycine and glutamate potencies and slows receptor deactivation. Mutagenesis experiments suggested that the binding site for GNE-9278 is located at the extracellular region of the pre-M1/M1 helices of the GluN1 subunit (Wang et al., 2017).

Discovering the principles underlying steroid-receptor interaction is pivotal for understanding the mechanisms of NMDAR modulation by steroids and the development of neurosteroid-like drugs to treat neuropsychiatric disorders associated with abnormal NMDAR function. Further systematic research is needed to enable predictions of the steroid effects on certain disease-associated NMDAR variants and allow the rational design of novel neurosteroid-like drugs specific for these receptor variants.

6 Conclusion

Hypofunction of the NMDAR has been implicated in the pathogenesis of multiple neuropsychiatric diseases, including epilepsy, schizophrenia, intellectual disability, and autism spectrum disorders. Because of this, there is considerable interest in developing new compounds that can potentiate NMDARs as a pharmacological tool to treat neuropsychiatric diseases. When designing new NMDAR-enhancing drugs, it should be taken into account that exaggerated NMDAR activation can lead to excitotoxic effects. In this regard, special attention should be paid to NMDAR PAMs. In contrast to agonists, PAMs are unable to activate NMDARs but only enhance the responses of receptors activated by naturally released glutamate; therefore, PAMs demonstrate reduced risk of NMDAR overstimulation (Yao & Zhou, 2017). Among the NMDAR PAMs are compounds of different classes, including neuroactive steroids; however, the mechanisms underlying steroid potentiation are not well understood.

This dissertation focuses on the mechanisms of interaction between NMDARs and potentiating neuroactive steroids. In this study, we identified novel sites of action for naturally occurring and synthetic potentiating steroids at the TMD of NMDARs and suggested the mechanisms by which steroids enhance NMDAR function. Moreover, we uncovered the structural determinants for the positive modulatory effect of neurosteroids on NMDARs. In addition, this study explores the functional consequences of selected *de novo* disease-associated mutations in NMDAR subunits and indicates the potential of potentiating steroids as pharmacological tools to compensate for the effects of these mutations.

The results given in this dissertation contribute to a deeper understanding of the mechanisms underlying allosteric modulation of NMDARs and offer new possibilities for *in silico* development of new neurosteroid-like drugs for the treatment of neuropsychiatric disorders associated with NMDAR hypofunction.

7 Summary

7.1 Functional and pharmacological properties of disease-associated *de novo* mutations in the hGluN2B subunit

- The hGluN2B(W607C; S628F) mutations decreased the surface expression of the receptors. In contrast, the hGluN2B(G820E) mutation increased the surface expression of the receptors.
- The hGluN1/hGluN2B(P553L; S628F; G820E; M824R) receptors showed no glutamate-induced currents and the hGluN1/hGluN2B(W607C; V618G; E657G; G820A) receptors exhibited significantly decreased peak current responses to a saturating concentration of glutamate (1 mM). The absence of glutamate-evoked response in hGluN2B(S628F) receptors and reduced responses of hGluN2B(G820A) receptors are likely to be a consequence of low surface expression.
- The hGluN2B(W607C) mutation profoundly decreased receptor glutamate affinity. In contrast, the hGluN2B(E657G) mutation enhanced NMDAR affinity to glutamate. The hGluN2B(W607C; E657G) mutations led to reduced affinity to glycine.
- The hGluN2B(V558I) mutation led to a 4.6-fold increase in receptor desensitization. In contrast, the hGluN2B(V618G) mutation led to a 4.0-fold reduction in receptor desensitization. The analysis of the effect of hGluN2B(E657G; G820A) mutations on receptor desensitization was precluded by the low amplitude of current responses.
- The hGluN2B(V558I; W607C; V618G; L825V) mutations resulted in the considerable reduction of receptor P_o. The analysis of the effect of hGluN2B(E657G; G820A) mutations on receptor P_o was precluded by the low amplitude of current responses.
- The responses of hGluN1/hGluN2B(L825V) receptors were potentiated by PE-S and AND-hSuc to a significantly greater extent than the responses of WT and hGluN1/hGluN2B(V558; W607C; V618G; G820A) receptors.

7.2 Identification of the site of action for pregnenolone sulfate at the NMDAR

- The site of action for PE-S at GluN1/GluN2B receptors is different from those of 24(S)-HC and cholesterol.
- PE-S acts at the TMD of the GluN1/GluN2B receptor. The site of action for PE-S is located at the interface formed by residues from the GluN2B(M1; M4) and GluN1(M3)

helices.

- Upon binding to the receptor, PE-S facilitates the rotation of the GluN2B M4 helix promoting a switch to the open channel conformation. In addition, PE-S tightens the interaction between the GluN1(I642) and GluN2B(W559) residues, stabilizing the pore-lining GluN1 M3 helix in the open-state position. These conformational effects of PE-S binding underlie the mechanism by which the steroid positively modulates the NMDAR function.

7.3 Structure requirements for potentiating neuroactive steroids

- 5β-pregnane 3α-substituted carboxy analogues with short C3 residues, such as PA-Ace and PA-Car inhibit the responses of GluN1/GluN2B receptors, whereas analogues with longer C3 residues, such as PA-But and EPA-But, potentiate the responses. These results demonstrate that steroids with a "bent" structure can potentiate NMDAR responses similarly to steroids with a "planar" structure
- EPA-But is a disuse-dependent PAM of GluN1/GluN2B receptors.
- Potentiating effects of EPA-But and PE-S are additive. No correlation was observed between the EPA-But and PE-S effects at mutated receptors with significantly decreased potentiation by either of the two steroids. In addition, the magnitudes of the effects of these steroids at hGluN1/hGluN2B receptors harbouring different disease-associated mutations were considerably different. Together, these results indicate that EPA-But and PE-S act at distinct/partially overlapping sites at the NMDAR.
- EPA-But acts at the TMD of the GluN1/GluN2B receptor. The sites of action for EPA-But are located within the GluN1(M4)/GluN2B(M1), GluN2B(M4)/GluN1(M1), and GluN2B(M1/M4) interfaces.
- EPA-But binding results in the stabilization of the channel in the open state and the expansion of the channel diameter.

8 Souhrn

8.1 Funkční a farmakologické vlastnosti NMDAR s *de novo* mutacemi v podjednotce hGluN2B spojenými s onemocněními

- Mutace hGluN2B(W607C; S628F) snížila povrchovou expresi NMDA receptorů. Naproti tomu mutace hGluN2B(G820E) zvýšila povrchovou expresi receptorů.
- Receptory hGluN1/hGluN2B(P553L; S628F; G820E; M824R) nevykazovaly žádné proudy indukované glutamátem a receptory hGluN1/hGluN2B(W607C; V618G; E657G; G820A) vykazovaly významně sníženou amplitudu proudové odpovědi na saturující koncentraci glutamátu (1 mM). Absence glutamátem vyvolané odpovědi u hGluN2B(S628F) stejně jako snížená proudová odpověď hGluN2B(G820A) jsou pravděpodobně důsledkem nízké povrchové exprese.
- Mutace hGluN2B(W607C) silně snížila afinitu receptoru ke glutamátu. Naproti tomu mutace hGluN2B(E657G) zvýšila afinitu NMDAR ke glutamátu. Mutace hGluN2B(W607C; E657G) vedly ke snížení afinity ke glycinu.
- Mutace hGluN2B(V558I) vedla ke 4,6 násobnému zvýšení desenzitizace receptoru. Naproti tomu mutace hGluN2B(V618G) vedla ke 4,0 násobnému snížení desenzitizace receptoru. Analýza vlivu mutací hGluN2B(E657G; G820A) na desenzitizaci receptoru byla znemožněna nízkou amplitudou proudových odpovědí.
- Mutace hGluN2B(V558I; W607C; V618G; L825V) vedly ke značnému snížení pravděpodobnosti otevření receptoru. Analýza vlivu mutací hGluN2B(E657G; G820A) na P_o receptoru byla znemožněna nízkou amplitudou proudových odpovědí.
- Odpovědi receptorů hGluN1/hGluN2B(L825V) byly potencovány steroidy PE-S a AND-hSuc ve významně větší míře než odpovědi receptorů WT a hGluN1/hGluN2B(V558; W607C; V618G; G820A).

8.2 Identifikace místa působení pregnenolon sulfátu na NMDAR

- Místo působení PE-S na receptory GluN1/GluN2B se liší od místa působení 24(S)-HC a cholesterolu.
- PE-S působí v transmembránové doméně receptoru GluN1/GluN2B. Místo působení PE-S se nachází na rozhraní tvořeném aminokyselinovými zbytky v šroubovicích GluN2B(M1; M4) a GluN1(M3).

- Po navázání na receptor PE-S usnadňuje rotaci šroubovice GluN2B(M4) a podporuje přechod do konformace s otevřeným iontovým kanálem. Kromě toho PE-S posiluje interakci mezi zbytky GluN1(I642) a GluN2B(W559), čímž stabilizuje šroubovici GluN1(M3), která lemuje póry, v otevřeném stavu. Tyto účinky vazby PE-S na konformaci jsou podstatou mechanismu, kterým steroid pozitivně moduluje funkci NMDAR.

8.3 Strukturní požadavky na strukturu neuroaktivních steroidů s potencionálním účinkem

- Analogy 5β-pregnanu substituovaného karboxylu s krátkými C3 zbytky, jako jsou pregnanolon acetát a pregnanolon karboxylát, inhibují odpovědi receptorů GluN1/GluN2B, zatímco analogy s delšími C3 zbytky, jako jsou PA-But a EPA-But, odpovědi potencují. Tyto výsledky ukazují, že steroidy s "ohnutou" strukturou mohou potencovat odpovědi NMDAR podobně jako steroidy s "planární" strukturou.
- EPA-But je pozitivní alosterický modulátor receptorů GluN1/GluN2B, který je „disuse-dependentní“, tedy váže se nejlépe na neaktivovaný receptor.
- Potenciační účinky EPA-But a PE-S jsou aditivní. Nebyla pozorována žádná korelace mezi účinky EPA-But a PE-S na mutovaných receptorech s výrazně sníženou potenciací kterýmkoli z obou steroidů. Kromě toho se velikost účinků těchto steroidů na receptory hGluN1/hGluN2B, které nesou mutace spojené s onemocněním, značně lišila. Tyto výsledky společně naznačují, že EPA-But a PE-S působí na NMDAR na odlišných/částečně se překrývajících místech.
- EPA-But působí v transmembránové doméně receptoru GluN1/GluN2B, konkrétně na rozhraní šroubovic GluN1(M4)/GluN2B(M1), GluN2B(M4)/GluN1(M1) a GluN2B(M1/M4).
- Vazba EPA-But vede ke stabilizaci kanálu v otevřeném stavu a k rozšíření průměru kanálu.

9 References

Adell, A. (2020). Brain NMDA receptors in schizophrenia and depression. *Biomolecules*, *10*(6), 1–27. https://doi.org/10.3390/biom10060947

Akazawa, C., Shigemoto, R., Bessho, Y., Nakanishi, S., & Mizuno, N. (1994). Differential expression of five N-methyl-D-aspartate receptor subunit mRNAs in the cerebellum of developing and adult rats. *The Journal of Comparative Neurology*, *347*(1), 150–160. https://doi.org/10.1002/cne.903470112

Alsaloum, M., Kazi, R., Gan, Q., Amin, J., & Wollmuth, L. P. (2016). A molecular determinant of subtype-specific desensitization in ionotropic glutamate receptors. *Journal of Neuroscience*, *36*(9), 2617–2622. https://doi.org/10.1523/JNEUROSCI.2667-15.2016

Amador, A., Bostick, C. D., Olson, H., Peters, J., Camp, C. R., Krizay, D., Chen, W., Han, W., Tang, W., Kanber, A., Kim, S., Teoh, J. J., Sah, M., Petri, S., Paek, H., Kim, A., Lutz, C. M., Yang, M., Myers, S. J., … Frankel, W. N. (2020). Modelling and treating GRIN2A developmental and epileptic encephalopathy in mice. *Brain*, *143*(7), 2039–2057. https://doi.org/10.1093/brain/awaa147

Amico-Ruvio, S. a, Paganelli, M. a, Myers, J. M., & Popescu, G. K. (2012). Ifenprodil effects on GluN2B-containing glutamate receptors. *Molecular Pharmacology*, *82*(6), 1074–1081. https://doi.org/10.1124/mol.112.078998

Amin, J. B., Gochman, A., He, M., Certain, N., & Wollmuth, L. P. (2021). NMDA Receptors Require Multiple Pre-opening Gating Steps for Efficient Synaptic Activity. *Neuron*, *109*(3), 488-501.e4. https://doi.org/10.1016/j.neuron.2020.11.009

Amin, J. B., Leng, X., Gochman, A., Zhou, H. X., & Wollmuth, L. P. (2018). A conserved glycine harboring disease-associated mutations permits NMDA receptor slow deactivation and high Ca2+ permeability. *Nature Communications*, *9*(1). https://doi.org/10.1038/s41467-018-06145-w

Auerbach, A., & Zhou, Y. (2005). Gating Reaction Mechanisms for NMDA Receptor Channels. *The Journal of Neuroscience*, *25*(35), 7914–7923. https://doi.org/10.1523/JNEUROSCI.1471-05.2005

Awadalla, P., Gauthier, J., Myers, R. A., Casals, F., Hamdan, F. F., Griffing, A. R., Côté, M., Henrion, E., Spiegelman, D., Tarabeux, J., Piton, A., Yang, Y., Boyko, A., Bustamante, C., Xiong, L., Rapoport, J. L., Addington, A. M., Delisi, J. L. E., Krebs, M. O., … Rouleau, G. A. (2010). Direct measure of the de novo mutation rate in autism and schizophrenia cohorts. *American Journal of Human Genetics*, *87*(3), 316–324. https://doi.org/10.1016/j.ajhg.2010.07.019

Bading, H. (2017). Therapeutic targeting of the pathological triad of extrasynaptic NMDA receptor signaling in neurodegenerations. *The Journal of Experimental Medicine*, *214*(3), 569–578. https://doi.org/10.1084/jem.20161673

Balu, D. T. (2016). The NMDA Receptor and Schizophrenia: From Pathophysiology to Treatment. *Advances in Pharmacology*, *76*, 351–382. https://doi.org/10.1016/bs.apha.2016.01.006.The

Banke, T. G. (2005). Protons Trap NR1/NR2B NMDA Receptors in a Nonconducting State. *Journal of Neuroscience*, *25*(1), 42–51. https://doi.org/10.1523/JNEUROSCI.3154-04.2005

Banke, Tue G, & Traynelis, S. F. (2003). Activation of NR1/NR2B NMDA receptors. *Nature Neuroscience*, *6*(2), 144–152. https://doi.org/10.1038/nn1000

Bekkers, J. M., & Stevens, C. F. (1989). NMDA and non-NMDA receptors are co-localized at individual excitatory synapses in cultured rat hippocampus. *Nature*, *341*(6239), 230–233. https://doi.org/10.1038/341230a0

Belforte, J. E., Zsiros, V., Sklar, E. R., Jiang, Z., Yu, G., Li, Y., Quinlan, E. M., & Nakazawa, K. (2010). Postnatal NMDA receptor ablation in corticolimbic interneurons confers schizophrenia-like phenotypes. *Nature Neuroscience*, *13*(1), 76–83. https://doi.org/10.1038/nn.2447

Benveniste, B. Y. M., Clements, J., Jrt, L. V., & Mayer, M. L. (1990). A kinetic analysis of the modulation of N-methyl-D-aspartic acid receptors by glycine in mouse cultured hippocampal neurones. *The Journal of Physiology*, *428*, 333–357.

Benveniste, M., Clements, J., Vyklický, L., & Mayer, M. L. (1990). A kinetic analysis of the modulation of N-methyl-D-aspartic acid receptors by glycine in mouse cultured hippocampal neurones. *The Journal of Physiology*, *428*(1), 333–357. https://doi.org/10.1113/jphysiol.1990.sp018215

Bertocchi, I., Eltokhi, A., Rozov, A., Chi, V. N., Jensen, V., Bus, T., Pawlak, V., Serafino, M., Sonntag, H., Yang, B., Burnashev, N., Li, S. Bin, Obenhaus, H. A., Both, M., Niewoehner, B., Single, F. N., Briese, M., Boerner, T., Gass, P., … Sprengel, R. (2021). Voltage-independent GluN2A-type NMDA receptor Ca2+ signaling promotes audiogenic seizures, attentional and cognitive deficits in mice. *Communications Biology*, *4*(1), 1–21. https://doi.org/10.1038/s42003-020-01538-4

Birch, P. J., Grossman, C. J., & Hayes, A. G. (1988). Kynurenic acid antagonises responses to NMDA via an action at the strychnine-insensitive glycine receptor. *European Journal of Pharmacology*, *154*(1), 85–87. https://doi.org/10.1016/0014-2999(88)90367-6

Blanpied, T. A. (2005). Amantadine Inhibits NMDA Receptors by Accelerating Channel Closure during Channel Block. *Journal of Neuroscience*, *25*(13), 3312–3322. https://doi.org/10.1523/JNEUROSCI.4262-04.2005

Blanpied, T. a, Boeckman, F. a, Aizenman, E., & Johnson, J. W. (1997). Trapping channel block of NMDA-activated responses by amantadine and memantine. *Journal of Neurophysiology*, *77*(1), 309–323.

Blaustein, M., Wirth, S., Saldaña, G., Piantanida, A. P., Bogetti, M. E., Martin, M. E., Colman-Lerner, A., & Uchitel, O. D. (2020). A new tool to sense pH changes at the neuromuscular junction synaptic cleft. *Scientific Reports*, *10*(1), 1–7. https://doi.org/10.1038/s41598-020-77154-3

Bolshakov, K. V., Gmiro, V. E., Tikhonov, D. B., & Magazanik, L. G. (2003). Determinants of trapping block of N-methyl-D-aspartate receptor channels. *Journal of Neurochemistry*, *87*(1), 56–65. https://doi.org/10.1046/j.1471-4159.2003.01956.x

Borovska, J., Vyklicky, V., Stastna, E., Kapras, V., Slavikova, B., Horak, M., Chodounska,

H., & Vyklicky, L. (2012). Access of inhibitory neurosteroids to the NMDA receptor. *British Journal of Pharmacology*, *166*(3), 1069–1083. https://doi.org/10.1111/j.1476-5381.2011.01816.x

Borschel, W. F., Cummings, K. A., Tindell, L. K., & Popescu, G. K. (2015). Kinetic contributions to gating by interactions unique to N-methyl-D-aspartate (NMDA) receptors. *Journal of Biological Chemistry*, *290*(44), 26846–26855. https://doi.org/10.1074/jbc.M115.678656

Bowlby, M. R. (1993). Pregnenolone sulfate potentiation of N-methyl-D-aspartate receptor channels in hippocampal neurons. *Molecular Pharmacology*, *43*, 813–819.

Bowling, K. M., Thompson, M. L., Amaral, M. D., Finnila, C. R., Hiatt, S. M., Engel, K. L., Cochran, J. N., Brothers, K. B., East, K. M., Gray, D. E., Kelley, W. V., Lamb, N. E., Lose, E. J., Rich, C. A., Simmons, S., Whittle, J. S., Weaver, B. T., Nesmith, A. S., Myers, R. M., … Cooper, G. M. (2017). Genomic diagnosis for children with intellectual disability and/or developmental delay. *Genome Medicine*, *9*(1), 1–11. https://doi.org/10.1186/s13073-017-0433-1

Boyce-Rustay, J. M., & Holmes, A. (2006). Genetic inactivation of the NMDA receptor NR2A subunit has anxiolytic- and antidepressant-like effects in mice. *Neuropsychopharmacology*, *31*(11), 2405–2414. https://doi.org/10.1038/sj.npp.1301039

Brodie, M. J., Wroe, S. J., Dean, A. D. P., Holdich, T. A. H., Whitehead, J., & Stevens, J. W. (2002). Efficacy and safety of remacemide versus carbamazepine in newly diagnosed epilepsy: Comparison by sequential analysis. *Epilepsy and Behavior*, *3*(2), 140–146. https://doi.org/10.1006/ebeh.2002.0337

Burnashev, N., & Szepetowski, P. (2015). NMDA receptor subunit mutations in neurodevelopmental disorders. *Current Opinion in Pharmacology*, *20*, 73–82. https://doi.org/10.1016/j.coph.2014.11.008

Cais, O., Sedlacek, M., Horak, M., Dittert, I., & Vyklicky, L. (2008). Temperature dependence of NR1/NR2B NMDA receptor channels. *Neuroscience*, *151*(2), 428–438. https://doi.org/10.1016/j.neuroscience.2007.11.002

Calabrese, F., Guidotti, G., Molteni, R., Racagni, G., Mancini, M., & Riva, M. A. (2012). Stress-induced changes of hippocampal NMDA receptors: Modulation by duloxetine treatment. *PLoS ONE*, *7*(5), 3–10. https://doi.org/10.1371/journal.pone.0037916

Carter, C., Rivy, J. P., & Scatton, B. (1989). Ifenprodil and SL 82.0715 are antagonists at the polyamine site of the N-methyl-D-aspartate (NMDA) receptor. *European Journal of Pharmacology*, *164*(3), 611–612. https://doi.org/10.1016/0014-2999(89)90275-6

Castillo, P. E., Malenka, R. C., & Nicoll, R. A. (1997). Kainate receptors mediate a slow postsynaptic current in hippocampal CA3 neurons. *Nature*, *388*(6638), 182–186. https://doi.org/10.1038/40645

Ceccon, M., Rumbaugh, G., & Vicini, S. (2001). Distinct effect of pregnenolone sulfate on NMDA receptor subtypes. *Neuropharmacology*, *40*(4), 491–500. https://doi.org/10.1016/S0028-3908(00)00197-0

Černý, J., Božíková, P., Balík, A., Marques, S. M., & Vyklický, L. (2019). NMDA receptor opening and closing-Transitions of a molecular machine revealed by molecular

dynamics. *Biomolecules*, *9*(10), 1–17. https://doi.org/10.3390/biom9100546

Chandrasekar, R. (2013). Alcohol and NMDA receptor: current research and future direction. *Front Mol Neurosci*, *6*(May), 14. https://doi.org/10.3389/fnmol.2013.00014

Cheon, Y., Park, J., Joe, K. H., & Kim, D. J. (2008). The effect of 12-week open-label memantine treatment on cognitive function improvement in patients with alcohol-related dementia. *International Journal of Neuropsychopharmacology*, *11*(7), 971–983. https://doi.org/10.1017/S1461145708008663

Choi, D. W. (2020). Excitotoxicity: Still Hammering the Ischemic Brain in 2020. *Frontiers in Neuroscience*, *14*(October). https://doi.org/10.3389/fnins.2020.579953

Christian, M. A., Haynes, M. P., Phillips, M. C., & George, H. (1997). Use of cyclodextrins for manipulating cellular cholesterol content. *Journal Lipid Research*, *38*(11), 2264–2272. https://doi.org/10.1016/S0022-2275(20)34940-3

Clements, J. D. (1996). Transmitter timecourse in the synaptic cleft: Its role in central synaptic function. *Trends in Neurosciences*, *19*(5), 163–171. https://doi.org/10.1016/S0166-2236(96)10024-2

Clements, J. D., Lester, R. A. J., Tong, G., Jahr, C. E., & Westbrook, G. L. (1992). The Time Course of Glutamate in the Synaptic Cleft The Time Course of Glutamate in the Synaptic Cleft. *Science*, *258*(5087), 1498–1501.

Corpechot, C., Robel, P., Axelson, M., Sjövall, J., & Baulieu, E. E. (1981). Characterization and measurement of dehydroepiandrosterone sulfate in rat brain. *Proceedings of the National Academy of Sciences of the United States of America*, *78*(8 I), 4704–4707. https://doi.org/10.1073/pnas.78.8.4704

Correll, C. U., & Schooler, N. R. (2020). Negative Symptoms in Schizophrenia: A Review and Clinical Guide for Recognition, Assessment, and Treatment. *Neuropsychiatr Dis Treat.*, *16*, 519–534.

Cossart, R., Epsztein, J., Tyzio, R., Becq, H., Hirsch, J., Ben-Ari, Y., & Crépel, V. (2002). Quantal release of glutamate generates pure kainate and mixed AMPA/kainate EPSCs in hippocampal neurons. *Neuron*, *35*(1), 147–159. https://doi.org/10.1016/S0896-6273(02)00753-5

Costa, B. M., Irvine, M. W., Fang, G., Eaves, R. J., Mayo-Martin, M. B., Skifter, D. A., Jane, D. E., & Monaghan, D. T. (2010). A novel family of negative and positive allosteric modulators of NMDA receptors. *Journal of Pharmacology and Experimental Therapeutics*, *335*(3), 614–621. https://doi.org/10.1124/jpet.110.174144

Coyle, J. T. (2006). Glutamate and schizophrenia: beyond the dopamine hypothesis. *Cellular and Molecular Neurobiology*, *26*(4–6), 365–384. https://doi.org/10.1007/s10571-006-9062-8

Dai, J., & Zhou, H. X. (2013). An NMDA receptor gating mechanism developed from MD simulations reveals molecular details underlying subunit-specific contributions. *Biophysical Journal*, *104*(10), 2170–2181. https://doi.org/10.1016/j.bpj.2013.04.013

de Ligt, J., Willemsen, M. H., van Bon, B. W. M., Kleefstra, T., Yntema, H. G., Kroes, T., Vulto-van Silfhout, A. T., Koolen, D. A., de Vries, P., Gilissen, C., del Rosario, M.,

Hoischen, A., Scheffer, H., de Vries, B. B. A., Brunner, H. G., Veltman, J. A., & Vissers, L. E. L. M. (2012). Diagnostic Exome Sequencing in Persons with Severe Intellectual Disability. *New England Journal of Medicine*, *367*(20), 1921–1929. https://doi.org/10.1056/nejmoa1206524

DeVries, S. H., & Schwartz, E. A. (1999). Kainate receptors mediate synaptic transmission between cones and "Off" bipolar cells in a mammalian retina. *Nature*, *397*(6715), 157–160. https://doi.org/10.1038/16462

Dingledine, R., Traynelis, S. F. F., Borges, K., Bowie, D., & Traynelis, S. F. . (1999). The glutamate receptor ion channels. *Pharmacological Reviews*, *51*(1), 7–61. https://doi.org/10049997

Dong, X. X., Wang, Y., & Qin, Z. H. (2009). Molecular mechanisms of excitotoxicity and their relevance to pathogenesis of neurodegenerative diseases. *Acta Pharmacologica Sinica*, *30*(4), 379–387. https://doi.org/10.1038/aps.2009.24

Doss, S., Wandinger, K.-P., Hyman, B. T., Panzer, J. A., Synofzik, M., Dickerson, B., Mollenhauer, B., Scherzer, C. R., Ivinson, A. J., Finke, C., Schols, L., Muller Vom Hagen, J., Trenkwalder, C., Jahn, H., Holtje, M., Biswal, B. B., Harms, L., Ruprecht, K., Buchert, R., … Prüss, H. (2014). High prevalence of NMDA receptor IgA/IgM antibodies in different dementia types. *Annals of Clinical and Translational Neurology*, *1*(10), 822–832. https://doi.org/10.1002/acn3.120

Edman, S., McKay, S., MacDonald, L. J., Samadi, M., Livesey, M. R., Hardingham, G. E., & Wyllie, D. J. A. (2012). TCN 201 selectively blocks GluN2A-containing NMDARs in a GluN1 co-agonist dependent but non-competitive manner. *Neuropharmacology*, *63*(3), 441–449. https://doi.org/10.1016/j.neuropharm.2012.04.027

Endele, S., Rosenberger, G., Geider, K., Popp, B., Tamer, C., Stefanova, I., Milh, M., Kortüm, F., Fritsch, A., Pientka, F. K., Hellenbroich, Y., Kalscheuer, V. M., Kohlhase, J., Moog, U., Rappold, G., Rauch, A., Ropers, H.-H., von Spiczak, S., Tönnies, H., … Kutsche, K. (2010). Mutations in GRIN2A and GRIN2B encoding regulatory subunits of NMDA receptors cause variable neurodevelopmental phenotypes. *Nature Genetics*, *42*(11), 1021–1026. https://doi.org/10.1038/ng.677

Erhardt, S., Schwieler, L., Nilsson, L., Linderholm, K., & Engberg, G. (2007). The kynurenic acid hypothesis of schizophrenia. *Physiology and Behavior*, *92*(1–2), 203–209. https://doi.org/10.1016/j.physbeh.2007.05.025

Erreger, K., Dravid, S. M., Banke, T. G., Wyllie, D. J. A., & Traynelis, S. F. (2005). Subunit-specific gating controls rat NR1/NR2A and NR1/NR2B NMDA channel kinetics and synaptic signalling profiles. *Journal of Physiology*, *563*(2), 345–358. https://doi.org/10.1113/jphysiol.2004.080028

Fagg, G. E., Olpe, H. R., Pozza, M. F., Baud, J., Steinmann, M., Schmutz, M., Portet, C., Baumann, P., Thedinga, K., & Bittiger, H. (1990). CGP 37849 and CGP 39551: novel and potent competitive N-methyl-D-aspartate receptor antagonists with oral activity. *British Journal of Pharmacology*, *99*(4), 791–797. https://doi.org/10.1111/j.1476-5381.1990.tb13008.x

Fedele, L., Newcombe, J., Topf, M., Gibb, A., Harvey, R. J., & Smart, T. G. (2018). Disease-associated missense mutations in GluN2B subunit alter NMDA receptor ligand binding

and ion channel properties. *Nature Communications*, *9*(1). https://doi.org/10.1038/s41467-018-02927-4

Frederickson, C. J., Giblin, L. J., Rengarajan, B., Masalha, R., Frederickson, C. J., Zeng, Y., Lopez, E. V., Koh, J. Y., Chorin, U., Besser, L., Hershfinkel, M., Li, Y., Thompson, R. B., & Krezel, A. (2006). Synaptic release of zinc from brain slices: Factors governing release, imaging, and accurate calculation of concentration. *Journal of Neuroscience Methods*, *154*(1–2), 19–29. https://doi.org/10.1016/j.jneumeth.2005.11.014

Frerking, M., & Ohliger-Frerking, P. (2002). AMPA receptors and kainate receptors encode different features of afferent activity. *Journal of Neuroscience*, *22*(17), 7434–7443. https://doi.org/10.1523/jneurosci.22-17-07434.2002

Freunscht, I., Popp, B., Blank, R., Endele, S., Moog, U., Petri, H., Prott, E. C., Reis, A., Rübo, J., Zabel, B., Zenker, M., Hebebrand, J., & Wieczorek, D. (2013). Behavioral phenotype in five individuals with de novo mutations within the GRIN2B gene. *Behavioral and Brain Functions*, *9*(1). https://doi.org/10.1186/1744-9081-9-20

Fujikawa, D. G., Daniels, A. H., & Kim, J. S. (1994). The competitive NMDA receptor antagonist CGP 40116 protects against status epilepticus-induced neuronal damage. *Epilepsy Research*, *17*(3), 207–219. https://doi.org/10.1016/0920-1211(94)90051-5

Ghasemi, M., Phillips, C., Trillo, L., De Miguel, Z., Das, D., & Salehi, A. (2014). The role of NMDA receptors in the pathophysiology and treatment of mood disorders. *Neuroscience and Biobehavioral Reviews*, *47*, 336–358. https://doi.org/10.1016/j.neubiorev.2014.08.017

Ghasemi, M., & Schachter, S. C. (2011). The NMDA receptor complex as a therapeutic target in epilepsy: A review. *Epilepsy and Behavior*, *22*(4), 617–640. https://doi.org/10.1016/j.yebeh.2011.07.024

Gibb, A. J., & Colquhoun, D. (1991). Glutamate activation of a single NMDA receptor-channel produces a cluster of channel openings. *Proceedings of the Royal Society B: Biological Sciences*, *243*(1306), 39–45. https://doi.org/10.1098/rspb.1991.0007

Gibbs, T. T., Russek, S. J., & Farb, D. H. (2006). Sulfated steroids as endogenous neuromodulators. *Pharmacology Biochemistry and Behavior*, *84*(4), 555–567. https://doi.org/10.1016/j.pbb.2006.07.031

Giffard, R. G., Monyer, H., Christine, C. W., & Choi, D. W. (1990). Acidosis reduces NMDA receptor activation, glutamate neurotoxicity, and oxygen-glucose deprivation neuronal injury in cortical cultures. *Brain Research*, *506*(2), 339–342. https://doi.org/10.1016/0006-8993(90)91276-M

Gladding, C. M., & Raymond, L. A. (2011). Mechanisms underlying NMDA receptor synaptic/extrasynaptic distribution and function. *Molecular and Cellular Neuroscience*, *48*(4), 308–320. https://doi.org/10.1016/j.mcn.2011.05.001

Gutnikov, S. A., & Gaffan, D. (1996). Systemic NMDA receptor antagonist CGP-40116 does not impair memory acquisition but protects against NMDA neurotoxicity in rhesus monkeys. *Journal of Neuroscience*, *16*(12), 4041–4045. https://doi.org/10.1523/jneurosci.16-12-04041.1996

Hackos, D. H., & Hanson, J. E. (2017). Diverse modes of NMDA receptor positive allosteric

modulation: Mechanisms and consequences. *Neuropharmacology*, *112*, 34–45. https://doi.org/10.1016/j.neuropharm.2016.07.037

Hamdan, F. F., Gauthier, J., Araki, Y., Lin, D. T., Yoshizawa, Y., Higashi, K., Park, A. R., Spiegelman, D., Dobrzeniecka, S., Piton, A., Tomitori, H., Daoud, H., Massicotte, C., Henrion, E., Diallo, O., Shekarabi, M., Marineau, C., Shevell, M., Maranda, B., … Michaud, J. L. (2011). Excess of de novo deleterious mutations in genes associated with glutamatergic systems in nonsyndromic intellectual disability. *American Journal of Human Genetics*, *88*(3), 306–316. https://doi.org/10.1016/j.ajhg.2011.02.001

Hamdan, F. F., Srour, M., Capo-Chichi, J. M., Daoud, H., Nassif, C., Patry, L., Massicotte, C., Ambalavanan, A., Spiegelman, D., Diallo, O., Henrion, E., Dionne-Laporte, A., Fougerat, A., Pshezhetsky, A. V., Venkateswaran, S., Rouleau, G. A., & Michaud, J. L. (2014). De Novo Mutations in Moderate or Severe Intellectual Disability. *PLoS Genetics*, *10*(10). https://doi.org/10.1371/journal.pgen.1004772

Hansen, K. B., Wollmuth, L. P., Bowie, D., Furukawa, H., Menniti, F. S., Sobolevsky, A. I., Swanson, G. T., Swanger, S. A., Greger, I. H., Nakagawa, T., McBain, C. J., Jayaraman, V., Low, C. M., Dell'Acqua, M. L., Diamond, J. S., Camp, C. R., Perszyk, R. E., Yuan, H., & Traynelis, S. F. (2021). Structure, Function, and Pharmacology of Glutamate Receptor Ion Channels. *Pharmacological Reviews*, *73*(4), 298–487. https://doi.org/doi.org/10.1124/pharmrev.120.000131

Hansen, Kasper B., Ogden, K. K., & Traynelis, S. F. (2012). Subunit-selective allosteric inhibition of glycine binding to NMDA receptors. *Journal of Neuroscience*, *32*(18), 6197–6208. https://doi.org/10.1523/JNEUROSCI.5757-11.2012

Hansen, Kasper B., Tajima, N., Risgaard, R., Perszyk, R. E., Jorgensen, L., Vance, K. M., Ogden, K. K., Clausen, R. P., Furukawa, H., & Traynelis, S. F. (2013). Structural determinants of agonist efficacy at the glutamate binding site of n-methyl-d-Aspartate receptorss. *Molecular Pharmacology*, *84*(1), 114–127. https://doi.org/10.1124/mol.113.085803

Hansen, Kasper B., Yi, F., Perszyk, R. E., Furukawa, H., Wollmuth, L. P., Gibb, A. J., & Traynelis, S. F. (2018). Structure, function, and allosteric modulation of NMDA receptors. *Journal of General Physiology*, *150*(8), 1081–1105. https://doi.org/10.1085/jgp.201812032

Hardingham, G. E., & Bading, H. (2010). Synaptic versus extrasynaptic NMDA receptor signalling: implications for neurodegenerative disorders. *Nature Reviews Neuroscience*, *11*(10), 682–696. https://doi.org/10.1038/nrn2911

Hashimoto, K., Sawa, A., & Iyo, M. (2007). Increased Levels of Glutamate in Brains from Patients with Mood Disorders. *Biological Psychiatry*, *62*(11), 1310–1316. https://doi.org/10.1016/j.biopsych.2007.03.017

Hayashi, T. (1954). Effects of sodium glutamate on the nervous system. *The Keio Journal of Medicine*, *3*(4), 183–192. https://doi.org/10.2302/kjm.3.183

Henson, M. A., Roberts, A. C., Pérez-Otaño, I., & Philpot, B. D. (2010). Influence of the NR3A subunit on NMDA receptor functions. *Progress in Neurobiology*, *91*(1), 23–37. https://doi.org/10.1016/j.pneurobio.2010.01.004

Herman, M. A., & Jahr, C. E. (2007). Extracellular glutamate concentration in hippocampal slice. *The Journal of Neuroscience : The Official Journal of the Society for Neuroscience*, *27*(36), 9736–9741. https://doi.org/10.1523/JNEUROSCI.3009-07.2007

Hollmann, M. (1994). Cloned Glutamate Receptors. *Annual Review of Neuroscience*, *17*(1), 31–108. https://doi.org/10.1146/annurev.neuro.17.1.31

Horak, M., Vlcek, K., Chodounska, H., & Vyklicky, L. (2006). Subtype-dependence of N-methyl-D-aspartate receptor modulation by pregnenolone sulfate. *Neuroscience*, *137*(1), 93–102. https://doi.org/10.1016/j.neuroscience.2005.08.058

Horak, M., Vlcek, K., Petrovic, M., Chodounska, H., & Vyklicky, L. (2004). Molecular Mechanism of Pregnenolone Sulfate Action at NR1/NR2B Receptors. *Journal of Neuroscience*, *24*(46), 10318–10325. https://doi.org/10.1523/JNEUROSCI.2099-04.2004

Horak, Martin, & Wenthold, R. J. (2009). Different roles of C-terminal cassettes in the trafficking of full-length NR1 subunits to the cell surface. *Journal of Biological Chemistry*, *284*(15), 9683–9691. https://doi.org/10.1074/jbc.M807050200

Howe, J. R., Cull-Candy, S. G., & Colquhoun, D. (1991). Currents through single glutamate receptor channels in outside-out patches from rat cerebellar granule cells. *The Journal of Physiology*, *432*(1), 143–202. https://doi.org/10.1113/jphysiol.1991.sp018381

Hu, C., Chen, W., Myers, S. J., Yuan, H., & Traynelis, S. F. (2016). Human GRIN2B variants in neurodevelopmental disorders. In *Journal of Pharmacological Sciences* (Vol. 132, Issue 2, pp. 115–121). https://doi.org/10.1016/j.jphs.2016.10.002

Huettner, J. E., & Bean, B. P. (1988). Block of N-methyl-D-aspartate-activated current by the anticonvulsant MK-801: Selective binding to open channels (excitatory amino acid receptors/visual cortex/cell culture/single channels). *Neurobiology*, *85*(February), 1307–1311.

Irvine, M. W., Costa, B. M., Volianskis, A., Fang, G., Ceolin, L., Collingridge, G. L., Monaghan, D. T., & Jane, D. E. (2012). Coumarin-3-carboxylic acid derivatives as potentiators and inhibitors of recombinant and native N-methyl-d-aspartate receptors. *Neurochemistry International*, *61*(4), 593–600. https://doi.org/10.1016/j.neuint.2011.12.020

Ishchenko, Y., Carrizales, M. G., & Koleske, A. J. (2021). Regulation of the NMDA receptor by its cytoplasmic domains: (How) is the tail wagging the dog? *Neuropharmacology*, *195*(February), 108634. https://doi.org/10.1016/j.neuropharm.2021.108634

Jadi, M., Behrens, M., & Sejnowski, T. (2016). Abnormal gamma oscillations in NMDAR hypofunction models of schizophrenia. *Biol Psychiatry*, *79*(9), 716–726. https://doi.org/10.1016/j.biopsych.2015.07.005.Abnormal

Jahr, C. E. (1992). High probability opening of NMDA receptor channels by L-glutamate. *Science*, *255*(5043), 470–472. https://doi.org/10.1126/science.1346477

Jang, M.-K., Mierke, D. F., Russek, S. J., & Farb, D. H. (2004). A steroid modulatory domain on NR2B controls N-methyl-D-aspartate receptor proton sensitivity. *Proceedings of the National Academy of Sciences of the United States of America*, *101*(21), 8198–8203. https://doi.org/10.1073/pnas.0401838101

Jensen, P. J., Millan, N., & Mack, K. J. (1997). Cortical NMDAR-1 gene expression is rapidly upregulated after seizure. *Molecular Brain Research*, *44*(1), 157–162. https://doi.org/10.1016/S0169-328X(96)00262-8

Jessa, M., Nazar, M., Bidzinski, A., & Plaznik, A. (1996). The effects of repeated administration of diazepam, MK-801 and CGP 37849 on rat behavior in two models of anxiety. *European Neuropsychopharmacology*, *6*(1), 55–61. https://doi.org/10.1016/0924-977X(95)00068-Z

Jonas, P. (2000). The time course of signaling at central glutamatergic synapses. *News in Physiological Sciences*, *15*(2), 83–89. https://doi.org/10.1152/physiologyonline.2000.15.2.83

Kaiser, T. M., Kell, S. A., Kusumoto, H., Shaulsky, G., Bhattacharya, S., Epplin, M. P., Strong, K. L., Miller, E. J., Cox, B. D., Menaldino, D. S., Liotta, D. C., Traynelis, S. F., & Burger, P. B. (2018). The bioactive protein-ligand conformation of GluN2C-selective positive allosteric modulators bound to the NMDA receptor. *Molecular Pharmacology*, *93*(2), 141–156. https://doi.org/10.1124/mol.117.110940

Kalbaugh, T. L., Zhang, J., & Diamond, J. S. (2009). Coagonist release modulates NMDA receptor subtype contributions at synaptic inputs to retinal ganglion cells. *Journal of Neuroscience*, *29*(5), 1469–1479. https://doi.org/10.1523/JNEUROSCI.4240-08.2009

Kaniakova, M., Krausova, B., Vyklicky, V., Korinek, M., Lichnerova, K., Vyklicky, L., & Horak, M. (2012). Key amino acid residues within the third membrane domains of NR1 and NR2 subunits contribute to the regulation of the surface delivery of N-methyl-D-aspartate receptors. *Journal of Biological Chemistry*, *287*(31), 26423–26434. https://doi.org/10.1074/jbc.M112.339085

Karakas, E, & Furukava, H. (2014). Crystal structure ofa heterotetrameric NMDA receptor ion channel. *Science*, *344*(6187), 992–997.

Karakas, Erkan, & Furukawa, H. (2014). Crystal structure of a heterotetrameric NMDA receptor ion channel. *Science*, *48*(Suppl 2), 1–6. https://doi.org/10.1097/MPG.0b013e3181a15ae8.Screening

Kashiwagi, K., Pahk, A. J., Masuko, T., Igarashi, K., & Williams, K. (1997). Block and modulation of N-methyl-D-aspartate receptors by polyamines and protons: Role of amino acid residues in the transmembrane and pore-forming regions of NR1 and NR2 subunits. *Molecular Pharmacology*, *52*(4), 701–713. https://doi.org/10.1124/mol.52.4.701

Kavalali, E. T., & Monteggia, L. M. (2018). The Ketamine Metabolite 2R,6R-Hydroxynorketamine Blocks NMDA Receptors and Impacts Downstream Signaling Linked to Antidepressant Effects. *Neuropsychopharmacology*, *43*(1), 221–222. https://doi.org/10.1038/npp.2017.210

Kay, A. R., & Tóth, K. (2008). Is zinc a neuromodulator? *Science Signaling*, *1*(19), 1–7. https://doi.org/10.1126/stke.119re3

Kazi, R., Dai, J., Sweeney, C., Zhou, H.-X., & Wollmuth, L. P. (2014). Mechanical coupling maintains the fidelity of NMDA receptor-mediated currents. *Nature Neuroscience*, *17*(7), 914–922. https://doi.org/10.1038/nn.3724

Kehoe, L. A., Bernardinelli, Y., & Muller, D. (2013). GluN3A: An NMDA receptor subunit with exquisite properties and functions. *Neural Plasticity*, *2013*(January 2013). https://doi.org/10.1155/2013/145387

Kessler, M., Terramani, T., Lynch, G., & Baudry, M. (1989). A Glycine Site Associated with N-Methyl-d-Aspartic Acid Receptors: Characterization and Identification of a New Class of Antagonists. *Journal of Neurochemistry*, *52*(4), 1319–1328. https://doi.org/10.1111/j.1471-4159.1989.tb01881.x

Khatri, A., Burger, P. B., Swanger, S. A., Hansen, K. B., Zimmerman, S., Karakas, E., Liotta, D. C., Furukawa, H., Snyder, J. P., & Traynelis, S. F. (2014). Structural determinants and mechanism of action of a GluN2C-selective NMDA receptor positive allosteric modulator. *Molecular Pharmacology*, *86*(5), 548–560. https://doi.org/10.1124/mol.114.094516

Kidd, F. L., & Isaac, J. T. R. (1999). Developmental and activity-dependent regulation of kainate receptors at thalamocortical synapses. *Nature*, *400*(6744), 569–573. https://doi.org/10.1038/23040

Kidd, F. L., & Isaac, J. T. R. (2001). Kinetics and activation of postsynaptic kainate receptors at thalamocortical synapses: Role of glutamate clearance. *Journal of Neurophysiology*, *86*(3), 1139–1148. https://doi.org/10.1152/jn.2001.86.3.1139

Kikuchi, S., Iwasa, H., & Sato, T. (2000). Lasting changes in NMDAR1 mRNA level in various regions of cerebral cortex in epileptogenesis of amygdaloid-kindled rat. *Psychiatry and Clinical Neurosciences*, *54*(5), 573–577. https://doi.org/10.1046/j.1440-1819.2000.00755.x

Kiss, J. P., Szasz, B. K., Fodor, L., Mike, A., Lenkey, N., Kurkó, D., Nagy, J., & Vizi, E. S. (2012). GluN2B-containing NMDA receptors as possible targets for the neuroprotective and antidepressant effects of fluoxetine. *Neurochemistry International*, *60*(2), 170–176. https://doi.org/10.1016/j.neuint.2011.12.005

Korinek, M., Kapras, V., Vyklicky, V., Adamusova, E., Borovska, J., Vales, K., Stuchlik, A., Horak, M., Chodounska, H., & Vyklicky, L. (2011a). Neurosteroid modulation of N-methyl-d-aspartate receptors: Molecular mechanism and behavioral effects. *Steroids*, *76*(13), 1409–1418. https://doi.org/10.1016/j.steroids.2011.09.002

Korinek, M., Vyklicky, V., Borovska, J., Lichnerova, K., Kaniakova, M., Krausova, B., Krusek, J., Balik, A., Smejkalova, T., Horak, M., & Vyklicky, L. (2015). Cholesterol modulates open probability and desensitization of NMDA receptors. *Journal of Physiology*, *593*(10), 2279–2293. https://doi.org/10.1113/jphysiol.2014.288209

Kostakis, E., Jang, M. K., Russek, S. J., Gibbs, T. T., & Farb, D. H. (2011). A steroid modulatory domain in NR2A collaborates with NR1 exon-5 to control NMDAR modulation by pregnenolone sulfate and protons. *Journal of Neurochemistry*, *119*(3), 486–496. https://doi.org/10.1111/j.1471-4159.2011.07442.x

Kotermanski, S. E., & Johnson, J. W. (2009). Mg2+ Imparts NMDA Receptor Subtype Selectivity to the Alzheimer's Drug Memantine. *Journal of Neuroscience*, *29*(9), 2774–2779. https://doi.org/10.1523/JNEUROSCI.3703-08.2009

Kotermanski, S. E., Wood, J. T., & Johnson, J. W. (2009). Memantine binding to a superficial

site on NMDA receptors contributes to partial trapping. *Journal of Physiology*, *587*(19), 4589–4604. https://doi.org/10.1113/jphysiol.2009.176297

Kozak, R., Campbell, B. M., Strick, C. A., Horner, W., Hoffmann, W. E., Kiss, T., Chapin, D. S., McGinnis, D., Abbott, A. L., Roberts, B. M., Fonseca, K., Guanowsky, V., Young, D. A., Seymour, P. A., Dounay, A., Hajos, M., Williams, G. V., & Castner, S. A. (2014). Reduction of brain kynurenic acid improves cognitive function. *Journal of Neuroscience*, *34*(32), 10592–10602. https://doi.org/10.1523/JNEUROSCI.1107-14.2014

Hrcka Krausova, B. H., Kysilov, B., Cerny, J., Vyklicky, V., Smejkalova, T., Ladislav, M., Balik, A., Korinek, M., Chodounska, H., Kudova, E., & Vyklicky, L. (2020). Site of action of brain neurosteroid pregnenolone sulfate at the N-methyl-D-aspartate receptor. *Journal of Neuroscience*, *40*(31), 5922–5936. https://doi.org/10.1523/JNEUROSCI.3010-19.2020

Krausova, B., Slavikova, B., Nekardova, M., Hubalkova, P., Vyklicky, V., Chodounska, H., Vyklicky, L., & Kudova, E. (2018). Positive Modulators of the N-Methyl- d -aspartate Receptor: Structure-Activity Relationship Study of Steroidal 3-Hemiesters [Research-article]. *Journal of Medicinal Chemistry*, *61*(10), 4505–4516. https://doi.org/10.1021/acs.jmedchem.8b00255

Krizay, D., Chen, W., Han, W., Tang, W., Kanber, A., Teoh, J. J., Petri, S., Paek, H., Kim, A., Lutz, C. M., & Yang, M. (2019). *Modeling and treating GRIN2A developmental and epileptic encephalopathy in mice*. 1–33.

Krupp, J. J., Vissel, B., Heinemann, S. F., & Westbrook, G. L. (1998). N-terminal domains in the NR2 subunit control desensitization of NMDA receptors. *Neuron*, *20*(2), 317–327. https://doi.org/10.1016/S0896-6273(00)80459-6

Krystal, J. H., D'Souza, D. C., Mathalon, D., Perry, E., Belger, A., & Hoffman, R. (2003). NMDA receptor antagonist effects, cortical glutamatergic function, and schizophrenia: Toward a paradigm shift in medication development. *Psychopharmacology*, *169*(3–4), 215–233. https://doi.org/10.1007/s00213-003-1582-z

Kudova, E., Chodounska, H., Slavikova, B., Budesinsky, M., Nekardova, M., Vyklicky, V., Krausova, B., Svehla, P., & Vyklicky, L. (2015). A New Class of Potent N-Methyl- d -Aspartate Receptor Inhibitors: Sulfated Neuroactive Steroids with Lipophilic D-Ring Modifications. *Journal of Medicinal Chemistry*, *58*(15), 5950–5966. https://doi.org/10.1021/acs.jmedchem.5b00570

Kuner, T., Wollmuth, L. P., Karlin, A., Seeburg, P. H., & Sakmann, B. (1996). Structure of the NMDA receptor channel M2 segment inferred from the accessibility of substituted cysteines. *Neuron*, *17*(2), 343–352. https://doi.org/10.1016/S0896-6273(00)80165-8

Kussius, C. L., Kaur, N., & Popescu, G. K. (2009). Pregnanolone sulfate promotes desensitization of activated NMDA receptors. *The Journal of Neuroscience : The Official Journal of the Society for Neuroscience*, *29*(21), 6819–6827. https://doi.org/10.1523/JNEUROSCI.0281-09.2009

Kysilov, B., Hrcka Krausova, B., Vyklicky, V., Smejkalova, T., Korinek, M., Horak, M., Chodounska, H., Kudova, E., Cerny, J., & Vyklicky, L. (2022). Pregnane-based steroids are novel positive NMDA receptor modulators that may compensate for the effect of loss-of-function disease-associated GRIN mutations. *British Journal of Pharmacology*,

February, 3970–3990. https://doi.org/10.1111/bph.15841

Ladislav, M., Cerny, J., Krusek, J., Horak, M., Balik, A., & Vyklicky, L. (2018). The LILI motif of M3-S2 linkers is a component of the NMDA receptor channel gate. *Frontiers in Molecular Neuroscience*, *11*(April), 1–16. https://doi.org/10.3389/fnmol.2018.00113

Lahti, A. C., Weiler, M. A., Michaelidis, T., Parwani, A., & Tamminga, C. A. (2001). Effects of ketamine in normal and schizophrenic volunteers. *Neuropsychopharmacology*, *25*(4), 455–467. https://doi.org/10.1016/S0893-133X(01)00243-3

Langer, K., Müller-Längle, A., Wempe, J., & Laube, B. (2021). Analysis of M4 Transmembrane Segments in NMDA Receptor Function: A Negative Allosteric Modulatory Site at the GluN1 M4 is Determining the Efficiency of Neurosteroid Modulation. *Frontiers in Pharmacology*, *12*(October), 1–16. https://doi.org/10.3389/fphar.2021.769046

Lapchak, P. A. (2006). 3α-OL-5-β-pregnan-20-one hemisuccinate, a steroidal low-affinity NMDA receptor antagonist improves clinical rating scores in a rabbit multiple infarct ischemia model: Synergism with tissue plasminogen activator. *Experimental Neurology*, *197*(2), 531–537. https://doi.org/10.1016/j.expneurol.2005.10.025

Larkin, J. R., Foo, L. S., Sutherland, B. A., Khrapitchev, A., & Tee, Y. K. (2022). Magnetic Resonance pH Imaging in Stroke – Combining the Old With the New. *Frontiers in Physiology*, *12*(February), 1–8. https://doi.org/10.3389/fphys.2021.793741

Laube, B., Hirai, H., Sturgess, M., Betz, H., & Kuhse, J. (1997). Molecular determinants of agonist discrimination by NMDA receptor subunits: Analysis of the glutamate binding site on the NR2B subunit. *Neuron*, *18*(3), 493–503. https://doi.org/10.1016/S0896-6273(00)81249-0

Le Meur, K., Galante, M., Angulo, M. C., & Audinat, E. (2007). Tonic activation of NMDA receptors by ambient glutamate of non-synaptic origin in the rat hippocampus. *The Journal of Physiology*, *580*(Pt. 2), 373–383. https://doi.org/10.1113/jphysiol.2006.123570

Lee, C.-H., Lü, W., Michel, J. C., Goehring, A., Du, J., Song, X., & Gouaux, E. (2014). NMDA receptor structures reveal subunit arrangement and pore architecture. *Nature*, *511*(7508), 191–197. https://doi.org/10.1038/nature13548

Lee, E. J., Choi, S. Y., & Kim, E. (2015). NMDA receptor dysfunction in autism spectrum disorders. *Current Opinion in Pharmacology*, *20*, 8–13. https://doi.org/10.1016/j.coph.2014.10.007

Lelieveld, S. H., Reijnders, M. R. F., Pfundt, R., Yntema, H. G., Kamsteeg, E. J., De Vries, P., De Vries, B. B. A., Willemsen, M. H., Kleefstra, T., Löhner, K., Vreeburg, M., Stevens, S. J. C., Van Der Burgt, I., Bongers, E. M. H. F., Stegmann, A. P. A., Rump, P., Rinne, T., Nelen, M. R., Veltman, J. A., … Gilissen, C. (2016). Meta-analysis of 2,104 trios provides support for 10 new genes for intellectual disability. *Nature Neuroscience*, *19*(9), 1194–1196. https://doi.org/10.1038/nn.4352

Lemke, J. R., Geider, K., Helbig, K. L., Heyne, H. O., Schütz, H., Hentschel, J., Courage, C., Depienne, C., Nava, C., Heron, D., Møller, R. S., Hjalgrim, H., Lal, D., Neubauer, B. A., Nürnberg, P., Thiele, H., Kurlemann, G., Arnold, G. L., Bhambhani, V., … Syrbe, S.

(2016). Delineating the GRIN1 phenotypic spectrum: A distinct genetic NMDA receptor encephalopathy. *Neurology*, *86*(23), 2171–2178. https://doi.org/10.1212/WNL.0000000000002740

Lemke, J. R., Hendrickx, R., Geider, K., Laube, B., Schwake, M., Harvey, R. J., James, V. M., Pepler, A., Steiner, I., Hörtnagel, K., Neidhardt, J., Ruf, S., Wolff, M., Bartholdi, D., Caraballo, R., Platzer, K., Suls, A., De Jonghe, P., Biskup, S., & Weckhuysen, S. (2014). GRIN2B mutations in west syndrome and intellectual disability with focal epilepsy. *Annals of Neurology*, *75*(1), 147–154. https://doi.org/10.1002/ana.24073

Lester, R. A., & Jahr, C. E. (1992). NMDA channel behavior depends on agonist affinity. *The Journal of Neuroscience : The Official Journal of the Society for Neuroscience*, *12*(2), 635–643. http://www.ncbi.nlm.nih.gov/pubmed/1346806

Lester, R. A., Tong, G., & Jahr, C. E. (1993). Interactions between the glycine and glutamate binding sites of the NMDA receptor. *The Journal of Neuroscience : The Official Journal of the Society for Neuroscience*, *13*(3), 1088–1096. http://www.ncbi.nlm.nih.gov/pubmed/8095067

Li, H., Rajani, V., Han, L., Chung, D., Cooke, J. E., Sengar, A. S., & Salter, M. W. (2021). Alternative splicing of GluN1 gates glycine site-dependent nonionotropic signaling by NMDAR receptors. *Proceedings of the National Academy of Sciences of the United States of America*, *118*(27). https://doi.org/10.1073/pnas.2026411118

Lichnerova, K., Kaniakova, M., Skrenkova, K., Vyklicky, L., & Horak, M. (2014). Distinct regions with in the GluN2C subunit regulate the surface delivery of NMDA receptors. *Frontiers in Cellular Neuroscience*, *8*(November), 1–12. https://doi.org/10.3389/fncel.2014.00375

Linsenbardt, A. J., Taylor, A., Emnett, C. M., Doherty, J. J., Krishnan, K., Covey, D. F., Paul, S. M., Zorumski, C. F., & Mennerick, S. (2014). Different oxysterols have opposing actions at N-methyl-d-aspartate receptors. *Neuropharmacology*, *85*, 232–242. https://doi.org/10.1016/j.neuropharm.2014.05.027

Lipton, S. (2005). The Molecular Basis of Memantine Action in Alzheimers Disease and Other Neurologic Disorders: Low-affinity, Uncompetitive Antagonism. *Current Alzheimer Research*, *2*(2), 155–165. https://doi.org/10.2174/1567205053585846

Lozovaya, N., Melnik, S., Tsintsadze, T., Grebenyuk, S., Kirichok, Y., & Krishtal, O. (2004). Protective cap over CA1 synapses: Extrasynaptic glutamate does not reach the postsynaptic density. *Brain Research*, *1011*(2), 195–205. https://doi.org/10.1016/j.brainres.2004.03.023

Maki, B. a, & Popescu, G. K. (2014). Extracellular Ca2+ ions reduce NMDA receptor conductance and gating. *The Journal of General Physiology*, *144*(5), 379–392. https://doi.org/10.1085/jgp.201411244

Malayev, A., Gibbs, T. T., & Farb, D. H. (2002). Inhibition of the NMDA response by pregnenolone sulphate reveals subtype selective modulation of NMDA receptors by sulphated steroids. *British Journal of Pharmacology*, *135*(4), 901–909. https://doi.org/10.1038/sj.bjp.0704543

Marsman, A., Van Den Heuvel, M. P., Klomp, D. W. J., Kahn, R. S., Luijten, P. R., &

Hulshoff Pol, H. E. (2013). Glutamate in schizophrenia: A focused review and meta-analysis of 1H-MRS studies. *Schizophrenia Bulletin*, *39*(1), 120–129. https://doi.org/10.1093/schbul/sbr069

Martineau, M., Parpura, V., & Mothet, J. P. (2014). Cell-type specific mechanisms of D-serine uptake and release in the brain. *Frontiers in Synaptic Neuroscience*, *6*(MAY), 1–9. https://doi.org/10.3389/fnsyn.2014.00012

Masrour, F. F., Peeri, M., Azarbayjani, M. A., & Hosseini, M. J. (2018). Voluntary Exercise During Adolescence Mitigated Negative the Effects of Maternal Separation Stress on the Depressive-Like Behaviors of Adult Male Rats: Role of NMDA Receptors. *Neurochemical Research*, *43*(5), 1067–1074. https://doi.org/10.1007/s11064-018-2519-6

Mathews, D. C., Henter, I. D., & Zarate, C. A. (2012). Targeting the Glutamatergic System to Treat Major Depressive Disorder. *Drugs*, *72*(10), 1313–1333. https://doi.org/10.2165/11633130-000000000-00000

Matveychuk, D., Thomas, R. K., Swainson, J., Khullar, A., MacKay, M.-A., Baker, G. B., & Dursun, S. M. (2020). Ketamine as an antidepressant: overview of its mechanisms of action and potential predictive biomarkers. *Therapeutic Advances in Psychopharmacology*, *10*, 204512532091665. https://doi.org/10.1177/2045125320916657

Mayer ML, Vyklicky L Jr, C. J. (1989). Regulation of NMDA receptor desensitization in mouse hippocampal neurons by glycine. *Nature*, *338*(6214), 425–427.

McClymont, D. W., Harris, J., & Mellor, I. R. (2012). Open-channel blockade is less effective on GluN3B than GluN3A subunit-containing NMDA receptors. *European Journal of Pharmacology*, *686*(1–3), 22–31. https://doi.org/10.1016/j.ejphar.2012.04.036

McGurk, J. F., Bennett, M. V. L., & Zukin, R. S. (1990). Polyamines potentiate responses of N-methyl-D-aspartate receptors expressed in Xenopus oocytes. *Proceedings of the National Academy of Sciences of the United States of America*, *87*(24), 9971–9974. https://doi.org/10.1073/pnas.87.24.9971

McNaught, A. D., & Wilkinson, A. (1997). IUPAC. Compendium of Chemical Terminology, 2nd ed. (the "Gold Book. *Blackwell Scientific Publications, Oxford*, 135–151. https://doi.org/10.1002/9783527626854.ch7

McRae, J. F., Clayton, S., Fitzgerald, T. W., Kaplanis, J., Prigmore, E., Rajan, D., Sifrim, A., Aitken, S., Akawi, N., Alvi, M., Ambridge, K., Barrett, D. M., Bayzetinova, T., Jones, P., Jones, W. D., King, D., Krishnappa, N., Mason, L. E., Singh, T., … Hurles, M. E. (2017). Prevalence and architecture of de novo mutations in developmental disorders. *Nature*, *542*(7642), 433–438. https://doi.org/10.1038/nature21062

Mealing, G. A. R., Lanthorn, T. H., Small, D. L., Murray, R. J., Mattes, K. C., Comas, T. M., & Morley, P. (2001). Structural modifications to an N-methyl-D-aspartate receptor antagonist result in large differences in trapping block. *Journal of Pharmacology and Experimental Therapeutics*, *297*(3), 906–914.

Meldrum, B., Millan, M., Patel, S., & de Sarro, G. (1988). Anti-epileptic effects of focal micro-injection of excitatory amino acid antagonists. *Journal of Neural Transmission*, *72*(3), 191–200. https://doi.org/10.1007/BF01243419

Mendes, P. (1993). Dynamics , Steady States and Control of Biochemical and Other Systems. *Cabios*, *9*(5), 563–571.

Mendes, Pedro. (1997). Biochemistry by numbers: Simulation of biochemical pathways with Gepasi 3. *Trends in Biochemical Sciences*, *22*(9), 361–363. https://doi.org/10.1016/S0968-0004(97)01103-1

Mendes, Pedro, & Kell, D. B. (1998). Non-linear optimization of biochemical pathways: Applications to metabolic engineering and parameter estimation. *Bioinformatics*, *14*(10), 869–883. https://doi.org/10.1093/bioinformatics/14.10.869

Moghaddam, B. (1993). Stress Preferentially Increases Extraneuronal Levels of Excitatory Amino Acids in the Prefrontal Cortex: Comparison to Hippocampus and Basal Ganglia. *Journal of Neurochemistry*, *60*(5), 1650–1657. https://doi.org/10.1111/j.1471-4159.1993.tb13387.x

Moldavski, A., Behr, J., Bading, H., & Bengtson, C. P. (2020). A novel method using ambient glutamate for the electrophysiological quantification of extrasynaptic NMDA receptor function in acute brain slices. *Journal of Physiology*, *598*(4), 633–650. https://doi.org/10.1113/JP278362

Mony, L., Zhu, S., Carvalho, S., & Paoletti, P. (2011). Molecular basis of positive allosteric modulation of GluN2B NMDA receptors by polyamines. *EMBO Journal*, *30*(15), 3134–3146. https://doi.org/10.1038/emboj.2011.203

Monyer, H., Burnashev, N., Laurie, D. J., Sakmann, B., & Seeburg, P. H. (1994). Developmental and regional expression in the rat brain and functional properties of four NMDA receptors. *Neuron*, *12*(3), 529–540. https://doi.org/0896-6273(94)90210-0 [pii]

Mott, D. D., Doherty, J. J., Zhang, S., Washburn, M. S., Fendley, M. J., Lyuboslavsky, P., Traynelis, S. F., & Dingledine, R. (1998). Phenylethanolamines inhibit NMDA receptors by enhancing proton inhibition. *Nature Neuroscience*, *1*(8), 659–667. https://doi.org/10.1038/3661

Moussawi, K., Riegel, A., Nair, S., & Kalivas, P. W. (2011). Extracellular Glutamate: Functional Compartments Operate in Different Concentration Ranges. *Frontiers in Systems Neuroscience*, *5*(November), 94. https://doi.org/10.3389/fnsys.2011.00094

Mullasseril, P., Hansen, K. B., Vance, K. M., Ogden, K. K., Yuan, H., Kurtkaya, N. L., Santangelo, R., Orr, A. G., Le, P., Vellano, K. M., Liotta, D. C., & Traynelis, S. F. (2010). A subunit-selective potentiator of NR2C- and NR2D-containing NMDA receptors. *Nature Communications*, *1*(7). https://doi.org/10.1038/ncomms1085

Mullier, B., Wolff, C., Sands, Z. A., Ghisdal, P., Muglia, P., Kaminski, R. M., & André, V. M. (2017). GRIN2B gain of function mutations are sensitive to radiprodil, a negative allosteric modulator of GluN2B-containing NMDA receptors. *Neuropharmacology*, *123*, 322–331. https://doi.org/10.1016/j.neuropharm.2017.05.017

Musazzi, L., Tornese, P., Sala, N., & Popoli, M. (2018). What acute stress protocols can tell us about PTSD and stress-related neuropsychiatric disorders. *Frontiers in Pharmacology*, *9*(JUN), 1–13. https://doi.org/10.3389/fphar.2018.00758

Neill, J. C., Harte, M. K., Haddad, P. M., Lydall, E. S., & Dwyer, D. M. (2014). Acute and chronic effects of NMDA receptor antagonists in rodents, relevance to negative

symptoms of schizophrenia: A translational link to humans. *European Neuropsychopharmacology*, *24*(5), 822–835. https://doi.org/10.1016/j.euroneuro.2013.09.011

Nowak, L., Bregestovski, P., Ascher, P., Herbet, A., & Prochiantz, A. (1984). Magnesium gates glutamate-activated channels in mouse central neurones. *Nature*, *307*(5950), 462–465. https://doi.org/10.1038/307462a0

Nozaki, K., & Beal, M. F. (1992). Neuroprotective effects of L-kynurenine on hypoxia-ischemia and NMDA lesions in neonatal rats. *Journal of Cerebral Blood Flow and Metabolism*, *12*(3), 400–407. https://doi.org/10.1038/jcbfm.1992.57

Ogden, K. K., Chen, W., Swanger, S. A., McDaniel, M. J., Fan, L. Z., Hu, C., Tankovic, A., Kusumoto, H., Kosobucki, G. J., Schulien, A. J., Su, Z., Pecha, J., Bhattacharya, S., Petrovski, S., Cohen, A. E., Aizenman, E., Traynelis, S. F., & Yuan, H. (2017). Molecular Mechanism of Disease-Associated Mutations in the Pre-M1 Helix of NMDA Receptors and Potential Rescue Pharmacology. In *PLoS Genetics* (Vol. 13, Issue 1). https://doi.org/10.1371/journal.pgen.1006536

Ogden, K. K., & Traynelis, S. F. (2013). Contribution of the M1 transmembrane helix and pre-M1 region to positive allosteric modulation and gating of N-methyl-D-aspartate receptors. *Molecular Pharmacology*, *83*(5), 1045–1056. https://doi.org/10.1124/mol.113.085209

Ohba, C., Shiina, M., Tohyama, J., Haginoya, K., Lerman-Sagie, T., Okamoto, N., Blumkin, L., Lev, D., Mukaida, S., Nozaki, F., Uematsu, M., Onuma, A., Kodera, H., Nakashima, M., Tsurusaki, Y., Miyake, N., Tanaka, F., Kato, M., Ogata, K., … Matsumoto, N. (2015). GRIN1 mutations cause encephalopathy with infantile-onset epilepsy, and hyperkinetic and stereotyped movement disorders. *Epilepsia*, *56*(6), 841–848. https://doi.org/10.1111/epi.12987

Ohtani, Y., Irie, T., Uekama, K., Fukunaga, K., & Pitha, J. (1989). Differential effects of alpha-, beta- and gamma-cyclodextrins on human erythrocytes. *European Journal of Biochemistry*, *186*(1–2), 17–22. http://www.ncbi.nlm.nih.gov/pubmed/2598927

Olney, J. W. (1969). Brain lesions, obesity, and other disturbances in mice treated with monosodium glutamate. *Science*, *164*(3880), 719–721. https://doi.org/10.1126/science.164.3880.719

Orser, B. A., Pennefather, P. S., & MacDonald, J. F. (1997). Multiple mechanisms of ketamine blockade of N-methyl-D-aspartate receptors. *Anesthesiology*, *86*(4), 903–917. https://doi.org/doi.org/10.1097/00000542-199704000-00021

Pachernegg, S., Strutz-Seebohm, N., & Hollmann, M. (2012). GluN3 subunit-containing NMDA receptors: Not just one-trick ponies. *Trends in Neurosciences*, *35*(4), 240–249. https://doi.org/10.1016/j.tins.2011.11.010

Pahk, A. J., & Williams, K. (1997). Influence of extracellular pH on inhibition by ifenprodil at N-methyl-D-aspartate receptors in Xenopus oocytes. *Neuroscience Letters*, *225*(1), 29–32. https://doi.org/10.1016/S0304-3940(97)00176-6

Paoletti, P., Bellone, C., & Zhou, Q. (2013). NMDA receptor subunit diversity: impact on receptor properties, synaptic plasticity and disease. *Nature Reviews. Neuroscience*, *14*(6),

383–400. https://doi.org/10.1038/nrn3504

Papouin, T., Ladépêche, L., Ruel, J., Sacchi, S., Labasque, M., Hanini, M., Groc, L., Pollegioni, L., Mothet, J. P., & Oliet, S. H. R. (2012). Synaptic and extrasynaptic NMDA receptors are gated by different endogenous coagonists. *Cell*, *150*(3), 633–646. https://doi.org/10.1016/j.cell.2012.06.029

Papp, M., & Moryl, E. (1994). Antidepressant activity of non-competitive and competitive NMDA receptor antagonists in a chronic mild stress model of depression. *European Journal of Pharmacology*, *263*(1–2), 1–7. https://doi.org/10.1016/0014-2999(94)90516-9

Park-Chung, M., Wu, F. S., & Farb, D. H. (1994). 3α-Hydroxy-5β-pregnan-20-one sulfate: A negative modulator of the NMDA- induced current in cultured neurons. *Molecular Pharmacology*, *46*(1), 146–150.

Park-Chung, M., Wu, F. S., Purdy, R. H., Malayev, a a, Gibbs, T. T., & Farb, D. H. (1997). Distinct sites for inverse modulation of N-methyl-D-aspartate receptors by sulfated steroids. *Molecular Pharmacology*, *52*, 1113–1123. https://doi.org/10.1124/mol.52.6.1113

Parsons, C. G., Danysz, W., & Quack, G. (1999). Memantine is a clinically well tolerated. *Pharmacological Research*, *38*, 735–767.

Patel, K. R., Cherian, J., Gohil, K., & Atkinson, D. (2014). Schizophrenia: Overview and treatment options. *P and T*, *39*(9), 638–645.

Paul, S M, Doherty, J. J., Robichaud, A. J., Belfort, G. M., Chow, B. Y., Hammond, R. S., Crawford, D. C., Linsenbardt, A. J., Shu, H. J., Izumi, Y., Mennerick, S. J., & Zorumski, C. F. (2013). The major brain cholesterol metabolite 24(s)-hydroxycholesterol is a potent allosteric modulator of N-methyl-d-aspartate receptors. *J Neurosci*, *33*(44), 17290–17300. https://doi.org/10.1523/JNEUROSCI.2619-13.2013

Paul, Steven M., & Purdy, R. H. (1992). Neuroactive steroids. *FASEB Journal*, *6*(6), 2311–2322. https://doi.org/10.1096/fasebj.6.6.1347506

Pegasiou, C. M., Zolnourian, A., Gomez-Nicola, D., Deinhardt, K., Nicoll, J. A. R., Ahmed, A. I., Vajramani, G., Grundy, P., Verhoog, M. B., Mansvelder, H. D., Perry, V. H., Bulters, D., & Vargas-Caballero, M. (2020). Age-dependent changes in synaptic NMDA receptor composition in adult human cortical neurons. *Cerebral Cortex*, *30*(7), 4246–4256. https://doi.org/10.1093/CERCOR/BHAA052

Peng, F. Z., Fan, J., Ge, T. T., Liu, Q. Q., & Li, B. J. (2020). Rapid anti-depressant-like effects of ketamine and other candidates: Molecular and cellular mechanisms. *Cell Proliferation*, *53*(5), 1–13. https://doi.org/10.1111/cpr.12804

Pérez-Otaño, I., Larsen, R. S., & Wesseling, J. F. (2016). Emerging roles of GluN3-containing NMDA receptors in the CNS. *Nature Reviews Neuroscience*, *17*(10), 623–635. https://doi.org/10.1038/nrn.2016.92

Petrovic, M. (2005). 20-Oxo-5 -Pregnan-3 -yl Sulfate Is a Use-Dependent NMDA Receptor Inhibitor. *Journal of Neuroscience*, *25*(37), 8439–8450. https://doi.org/10.1523/JNEUROSCI.1407-05.2005

Petrović, M., Horák, M., Sedlácek, M., & Vyklický, L. (2005). Physiology and pathology of

NMDA receptors. *Prague Medical Report*, *106*(2), 113–136.

Petrovski, S., Wang, Q., Heinzen, E. L., Allen, A. S., & Goldstein, D. B. (2013). Genic Intolerance to Functional Variation and the Interpretation of Personal Genomes. *PLoS Genetics*, *9*(8). https://doi.org/10.1371/journal.pgen.1003709

Platzer, K., Yuan, H., Schütz, H., Winschel, A., Chen, W., Hu, C., Kusumoto, H., Heyne, H. O., Helbig, K. L., Tang, S., Willing, M. C., Tinkle, B. T., Adams, D. J., Depienne, C., Keren, B., Mignot, C., Frengen, E., Strømme, P., Biskup, S., … Lemke, J. R. (2017). GRIN2B encephalopathy: Novel findings on phenotype, variant clustering, functional consequences and treatment aspects. *Journal of Medical Genetics*, *54*(7), 460–470. https://doi.org/10.1136/jmedgenet-2016-104509

Plitman, E., Iwata, Y., Caravaggio, F., Nakajima, S., Chung, J. K., Gerretsen, P., Kim, J., Takeuchi, H., Chakravarty, M. M., Remington, G., & Graff-Guerrero, A. (2017). Kynurenic Acid in Schizophrenia: A Systematic Review and Meta-analysis. *Schizophrenia Bulletin*, *43*(4), 764–777. https://doi.org/10.1093/schbul/sbw221

Poot, M. (2019). Phenotypic Spectrum and Severity of Disease Depending on the Mutated Protein Domain of NMDA Receptor-Encoding Genes. *Molecular Syndromology*, *10*(3), 127–129. https://doi.org/10.1159/000500004

Premo, H., Liu, B., Iacobucci, G. J., & Popescu, G. K. (2021). Direct M3-M4 Interactions Control NMDA Receptor Gating and Desensitization. *Biophysical Journal*, *120*(3), 58a. https://doi.org/10.1016/j.bpj.2020.11.583

Preskorn, S. H., Baker, B., Kolluri, S., Menniti, F. S., Krams, M., & Landen, J. W. (2008). An Innovative design to establish proof of concept of the antidepressant effects of the NR2B subunit selective n-methyl-d-aspartate antagonist, CP-101,606, in patients with treatment-refractory major depressive disorder. *Journal of Clinical Psychopharmacology*, *28*(6), 631–637. https://doi.org/10.1097/JCP.0b013e31818a6cea

Ransom, R. W., & Deschenes, N. L. (1990). Polyamines regulate glycine interaction with the N-methyl-D-aspartate receptor. *Synapse*, *5*(4), 294–298. https://doi.org/10.1002/syn.890050406

Ratner, M. H., Kumaresan, V., & Farb, D. H. (2019). Neurosteroid actions in memory and neurologic/neuropsychiatric disorders. *Frontiers in Endocrinology*, *10*(APR), 1–37. https://doi.org/10.3389/fendo.2019.00169

Redin, C., Gérard, B., Lauer, J., Herenger, Y., Muller, J., Quartier, A., Masurel-Paulet, A., Willems, M., Lesca, G., El-Chehadeh, S., Gras, S. Le, Vicaire, S., Philipps, M., Dumas, M., Geoffroy, V., Feger, C., Haumesser, N., Alembik, Y., Barth, M., … Piton, A. (2014). Efficient strategy for the molecular diagnosis of intellectual disability using targeted high-throughput sequencing. *Journal of Medical Genetics*, *51*(11), 724–736. https://doi.org/10.1136/jmedgenet-2014-102554

Reynolds, I. J., & Miller, R. J. (1988). Tricyclic antidepressants block N-methyl-D-aspartate receptors: similarities to the action of zinc. *British Journal of Pharmacology*, *95*(1), 95–102. https://doi.org/10.1111/j.1476-5381.1988.tb16552.x

Rodríguez-Muñoz, M., Sánchez-Blázquez, P., Callado, L. F., Meana, J. J., & Garzón-Niño, J. (2017). Schizophrenia and depression, two poles of endocannabinoid system

deregulation. *Translational Psychiatry*, *7*(12). https://doi.org/10.1038/s41398-017-0029-y

Rosenmund, C., Feltz, a, & Westbrook, G. L. (1995). Synaptic NMDA receptor channels have a low open probability. *The Journal of Neuroscience : The Official Journal of the Society for Neuroscience*, *15*(April), 2788–2795.

Rundfeldt, C., Wlaź, P., & Löscher, W. (1994). Anticonvulsant activity of antagonists and partial agonists for the NMDA receptor-associated glycine site in the kindling model of epilepsy. *Brain Research*, *653*(1–2), 125–130. https://doi.org/10.1016/0006-8993(94)90380-8

Sengar, A. S., Li, H., Zhang, W., Leung, C., Ramani, A. K., Saw, N. M., Wang, Y., Tu, Y. S., Ross, P. J., Scherer, S. W., Ellis, J., Brudno, M., Jia, Z., & Salter, M. W. (2019). Control of Long-Term Synaptic Potentiation and Learning by Alternative Splicing of the NMDA Receptor Subunit GluN1. *Cell Reports*, *29*(13), 4285-4294.e5. https://doi.org/10.1016/j.celrep.2019.11.087

Sheng, M., Cummings, J., Roldan, L. A., Jan, Y. N., & Jan, L. Y. (1994). Changing subunit composition of heteromeric NMDA receptors during development of rat cortex. *Nature*, *368*(6467), 144–147. https://doi.org/10.1038/368144a0

Smothers, C. T., & Woodward, J. J. (2009). Expression of glycine-activated diheteromeric NR1/NR3 receptors in human embryonic kidney 293 cells Is NR1 splice variant-dependent. *The Journal of Pharmacology and Experimental Therapeutics*, *331*(3), 975–984. https://doi.org/10.1124/jpet.109.158493

Sobolevsky, A. I., Rosconi, M. P., & Gouaux, E. (2009). X-ray structure, symmetry and mechanism of an AMPA-subtype glutamate receptor. *Nature*, *462*(7274), 745–756. https://doi.org/10.1038/nature08624

Sobolevsky, A. I., Yelshansky, M. V., & Wollmuth, L. P. (2004). The Outer Pore of the Glutamate Receptor Channel Has 2-Fold Rotational Symmetry. *Neuron*, *41*(3), 367–378. https://doi.org/10.1016/S0896-6273(04)00008-X

Somogyi, P., Tamás, G., Lujan, R., & Buhl, E. H. (1998). Salient features of synaptic organisation in the cerebral cortex. *Brain Research Reviews*, *26*(2–3), 113–135. https://doi.org/10.1016/S0165-0173(97)00061-1

Soto, D., Altafaj, X., Sindreu, C., & Bayés, À. (2014). *Commun Integr Biol 2014 Soto*. *January*, 1–6.

Stastna, E., Chodounska, H., Pouzar, V., Kapras, V., Borovska, J., Cais, O., & Vyklicky, L. (2009). Synthesis of C3, C5, and C7 pregnane derivatives and their effect on NMDA receptor responses in cultured rat hippocampal neurons. *Steroids*, *74*(2), 256–263. https://doi.org/10.1016/j.steroids.2008.11.011

Stephen F. Traynelis, Lonnie P. Wollmuth, Chris J. McBain, Frank S. Menniti, Katie M. Vance, Kevin K. Ogden, Kasper B. Hansen, Hongjie Yuan, Scott J. Myers, R. D. (2010). Glutamate Receptor Ion Channels: Structure, Regulation, and Function. *Pharmacological Reviews*, *62*(3), 405–496. https://doi.org/10.1124/pr.109.002451.

Stephenson, F. A. (2006). Structure and trafficking of NMDA and GABAA receptors. *Biochemical Society Transactions*, *34*(Pt 5), 877–881.

https://doi.org/10.1042/BST0340877

Stroebel, D., Casado, M., & Paoletti, P. (2018). Triheteromeric NMDA receptors: from structure to synaptic physiology. *Current Opinion in Physiology*, *2*, 1–12. https://doi.org/10.1016/j.cophys.2017.12.004

Strong, K. L., Epplin, M. P., Ogden, K. K., Burger, P. B., Kaiser, T. M., Wilding, T. J., Kusumoto, H., Camp, C. R., Shaulsky, G., Bhattacharya, S., Perszyk, R. E., Menaldino, D. S., McDaniel, M. J., Zhang, J., Le, P., Banke, T. G., Hansen, K. B., Huettner, J. E., Liotta, D. C., & Traynelis, S. F. (2021). Distinct GluN1 and GluN2 Structural Determinants for Subunit-Selective Positive Allosteric Modulation of N-Methyl-d-aspartate Receptors. *ACS Chemical Neuroscience*, *12*(1), 79–98. https://doi.org/10.1021/acschemneuro.0c00561

Sun, W., Shchepakin, D., Kalachev, L. V., & Kavanaugh, M. P. (2014). Glutamate transporter control of ambient glutamate levels. *Neurochemistry International*, *73*(1), 146–151. https://doi.org/10.1016/j.neuint.2014.04.007

Swanger, S. A., Chen, W., Wells, G., Burger, P. B., Tankovic, A., Bhattacharya, S., Strong, K. L., Hu, C., Kusumoto, H., Zhang, J., Adams, D. R., Millichap, J. J., Petrovski, S., Traynelis, S. F., & Yuan, H. (2016). Mechanistic Insight into NMDA Receptor Dysregulation by Rare Variants in the GluN2A and GluN2B Agonist Binding Domains. *American Journal of Human Genetics*, *99*(6), 1261–1280. https://doi.org/10.1016/j.ajhg.2016.10.002

Szejtli, J. (1998). Introduction and general overview of cyclodextrin chemistry. *Chemical Reviews*, *98*(5), 1743–1753. https://doi.org/10.1021/cr970022c

Tabone, C. J., & Ramaswami, M. (2012). Is NMDA Receptor-Coincidence Detection Required for Learning and Memory? *Neuron*, *74*(5), 767–769. https://doi.org/10.1016/j.neuron.2012.05.008

Tang, C. M., Dichter, M., & Morad, M. (1990). Modulation of the N-methyl-D-aspartate channel by extracellular H+. *Proceedings of the National Academy of Sciences of the United States of America*, *87*(16), 6445–6449. https://doi.org/10.1073/pnas.87.16.6445

Thomas, C. G., Krupp, J. J., Bagley, E. E., Bauzon, R., Heinemann, S. F., Vissel, B., & Westbrook, G. L. (2006). Probing N-methyl-D-aspartate receptor desensitization with the substituted-cysteine accessibility method. *Molecular Pharmacology*, *69*(4), 1296–1303. https://doi.org/10.1124/mol.105.017350

Tomitori, H., Suganami, A., Saiki, R., Mizuno, S., Yoshizawa, Y., Masuko, T., Tamura, Y., Nishimura, K., Toida, T., Williams, K., Kashiwagi, K., & Igarashi, K. (2012). Structural changes of regulatory domain heterodimer of N-methyl-D-aspartate receptor subunits GluN1 and GluN2B through the binding of spermine and ifenprodil. *Journal of Pharmacology and Experimental Therapeutics*, *343*(1), 82–90. https://doi.org/10.1124/jpet.112.192286

Traynelis, J., Silk, M., Wang, Q., Berkovic, S. F., Liu, L., Ascher, D. B., Balding, D. J., & Petrovski, S. (2017). Optimizing genomic medicine in epilepsy through a gene-customized approach to missense variant interpretation. *Genome Research*, *27*(10), 1715–1729. https://doi.org/10.1101/gr.226589.117

Traynelis, S. F., Hartley, M., & Heinemann, S. F. (1995). Control of proton sensitivity of the NMDA receptor by RNA splicing and polyamines. *Science*, *268*(5212), 873–876. https://doi.org/10.1126/science.7754371

Traynelis, S. F., Wollmuth, L. P., McBain, C. J., Menniti, F. S., Vance, K. M., Ogden, K. K., Hansen, K. B., Yuan, H., Myers, S. J., & Dingledine, R. (2010). Glutamate receptor ion channels: Structure, regulation, and function. *Pharmacological Reviews*, *62*(3), 405–496. https://doi.org/10.1124/pr.109.002451

Turecek, R., Vlcek, K., Petrovic, M., Horak, M., Vlachova, V., & Vyklicky, L. (2004). Intracellular spermine decreases open probability of N-methyl-D-aspartate receptor channels. *Neuroscience*, *125*(4), 879–887. https://doi.org/10.1016/j.neuroscience.2004.03.003

Twomey, E. C., & Sobolevsky, A. I. (2018). Structural Mechanisms of Gating in Ionotropic Glutamate Receptors. *Biochemistry*, *57*(3), 267–276. https://doi.org/10.1021/acs.biochem.7b00891

Twomey, E. C., Yelshanskaya, M. V., & Sobolevsky, A. I. (2019). Structural and functional insights into transmembrane AMPA receptor regulatory protein complexes. *Journal of General Physiology*, *151*(12), 1347–1356. https://doi.org/10.1085/JGP.201812264

Vadivelu, N., Schermer, E., Kodumudi, V., Belani, K., Urman, R. D., & Kaye, A. D. (2016). Role of ketamine for analgesia in adults and children. *Journal of Anaesthesiology Clinical Pharmacology*, *32*(3), 298–306. https://doi.org/10.4103/0970-9185.168149

van Velzen, M., & Dahan, A. (2014). Ketamine metabolomics in the treatment of major depression. *Anesthesiology, 121*(1), 4–5. https://doi.org/10.1159/000356540

Vasudevan, P., & Suri, M. (2017). A clinical approach to developmental delay and intellectual disability. *Clinical Medicine, Journal of the Royal College of Physicians of London*, *17*(6), 558–561. https://doi.org/10.7861/clinmedicine.17-6-558

Velíšek, L., Jehle, K., Asche, S., & Velíšková, J. (2007). Model of infantile spasms induced by N-methyl-D-aspartic acid in prenatally impaired brain. *Annals of Neurology*, *61*(2), 109–119. https://doi.org/10.1002/ana.21082

Vergnano, A. M., Rebola, N., Savtchenko, L. P., Pinheiro, P. S., Casado, M., Kieffer, B. L., Rusakov, D. A., Mulle, C., & Paoletti, P. (2014). Zinc dynamics and action at excitatory synapses. *Neuron*, *82*(5), 1101–1114. https://doi.org/10.1016/j.neuron.2014.04.034

Vezzani, A., Wu, H. Q., Angelico, P., Stasi, M. A., & Samanin, R. (1988). Quinolinic acid-induced seizures, but not nerve cell death, are associated with extracellular Ca2+ decrease assessed in the hippocampus by brain dialysis. *Brain Research*, *454*(1–2), 289–297. https://doi.org/10.1016/0006-8993(88)90829-3

Vieira, M. M., Jeong, J., & Roche, K. W. (2021). The role of NMDA receptor and neuroligin rare variants in synaptic dysfunction underlying neurodevelopmental disorders. *Current Opinion in Neurobiology*, *69*, 93–104. https://doi.org/10.1016/j.conb.2021.03.001

Villarroel, A., Burnashev, N., & Sakmann, B. (1995). Dimensions of the narrow portion of a recombinant NMDA receptor channel. *Biophysical Journal*, *68*(3), 866–875. https://doi.org/10.1016/S0006-3495(95)80263-8

Villarroel, Alvaro, Regalado, M. P., & Lerma, J. (1998). Glycine-independent NMDA receptor desensitization: Localization of structural determinants. *Neuron*, *20*(2), 329–339. https://doi.org/10.1016/S0896-6273(00)80460-2

Vyklicky, L., Krusek, J., & Edwards, C. (1988). Differences in the pore sizes of the N-methyl-d-aspartate and kainate cation channels. *Neuroscience Letters*, *89*(3), 313–318. https://doi.org/10.1016/0304-3940(88)90545-9

Vyklický, L., Vlachová, V., & Krůsek, J. (1990). The effect of external pH changes on responses to excitatory amino acids in mouse hippocampal neurones. *The Journal of Physiology*, *430*(1), 497–517. https://doi.org/10.1113/jphysiol.1990.sp018304

Vyklicky, V., Smejkalova, T., Krausova, B., Balik, A., Korinek, M., Borovska, J., Horak, M., Chvojkova, M., Kleteckova, L., Vales, K., Cerny, J., Nekardova, M., Chodounska, H., Kudova, E., & Vyklicky, L. (2016). Preferential Inhibition of Tonically over Phasically Activated NMDA Receptors by Pregnane Derivatives. *Journal of Neuroscience*, *36*(7), 2161–2175. https://doi.org/10.1523/JNEUROSCI.3181-15.2016

Vyklicky, V, Korinek, M., Smejkalova, T., Balik, A., Krausova, B., Kaniakova, M., Lichnerova, K., Cerny, J., Krusek, J., Dittert, I., Horak, M., & Vyklicky, L. (2014). Structure, function, and pharmacology of NMDA receptor channels. *Physiological Research / Academia Scientiarum Bohemoslovaca*, *63 Suppl 1*, S191-203. http://www.ncbi.nlm.nih.gov/pubmed/24564659

Vyklicky, Vojtech, Krausova, B., Cerny, J., Balik, A., Zapotocky, M., Novotny, M., Lichnerova, K., Smejkalova, T., Kaniakova, M., Korinek, M., Petrovic, M., Kacer, P., Horak, M., Chodounska, H., & Vyklicky, L. (2015). Block of NMDA receptor channels by endogenous neurosteroids: Implications for the agonist induced conformational states of the channel vestibule. *Scientific Reports*, *5*(November 2014), 10935. https://doi.org/10.1038/srep10935

Vyklicky, Vojtech, Krausova, B., Cerny, J., Ladislav, M., Smejkalova, T., Kysilov, B., Korinek, M., Danacikova, S., Horak, M., Chodounska, H., Kudova, E., & Vyklicky, L. (2018). Surface expression, function, and pharmacology of disease-associated mutations in the membrane domain of the human GluN2B subunit. *Frontiers in Molecular Neuroscience*, *11*(April), 1–20. https://doi.org/10.3389/fnmol.2018.00110

Wang, T. M., Brown, B. M., Deng, L., Sellers, B. D., Lupardus, P. J., Wallweber, H. J. A., Gustafson, A., Wong, E., Volgraf, M., Schwarz, J. B., Hackos, D. H., & Hanson, J. E. (2017). A novel NMDA receptor positive allosteric modulator that acts via the transmembrane domain. *Neuropharmacology*, *121*, 204–218. https://doi.org/10.1016/j.neuropharm.2017.04.041

Warming, H., Pegasiou, C. M., Pitera, A. P., Kariis, H., Houghton, S. D., Kurbatskaya, K., Ahmed, A., Grundy, P., Vajramani, G., Bulters, D., Altafaj, X., Deinhardt, K., & Vargas-Caballero, M. (2019). A primate-specific short GluN2A-NMDA receptor isoform is expressed in the human brain. *Molecular Brain*, *12*(1), 1–8. https://doi.org/10.1186/s13041-019-0485-9

Weaver, C. E., Land, M. B., Purdy, R. H., Richards, K. G., Gibbs, T. T., & Farb, D. H. (2000). *Geometry and Charge Determine Pharmacological Effects of Steroids on N - Methyl- D -aspartate Receptor-Induced Ca 2 ∂ Accumulation and Cell Death 1*. *293*(3), 747–754.

Weiss, J. N. (1997). The Hill equation revisited: uses and misuses. *The FASEB Journal*, *11*(11), 835–841. https://doi.org/10.1096/fasebj.11.11.9285481

Wells, G., Yuan, H., McDaniel, M. J., Kusumoto, H., Snyder, J. P., Liotta, D. C., & Traynelis, S. F. (2018). The GluN2B-Glu413Gly NMDA receptor variant arising from a de novo GRIN2B mutation promotes ligand-unbinding and domain opening. *Proteins: Structure, Function and Bioinformatics*, *86*(12), 1265–1276. https://doi.org/10.1002/prot.25595

Wilding, T. J., Lopez, M. N., & Huettner, J. E. (2016). Chimeric glutamate receptor subunits reveal the transmembrane domain is sufficient for NMDA receptor pore properties but some positive allosteric modulators require additional domains. *Journal of Neuroscience*, *36*(34), 8815–8825. https://doi.org/10.1523/JNEUROSCI.0345-16.2016

Williams, K. (1997). Modulation and block of ion channels: a new biology of polyamines. *Cellular Signalling, 9*(1), 1–13. https://doi.org/10.1007/BF01282048

Williams, K., Russell, S. L., Shen, Y. M., & Molinoff, P. B. (1993). Developmental switch in the expression of NMDA receptors occurs in vivo and in vitro. *Neuron*, *10*(2), 267–278. https://doi.org/10.1016/0896-6273(93)90317-K

Wu, F. S., Gibbs, T. T., & Farb, D. H. (1991). Pregnenolone sulfate: A positive allosteric modulator at the N-methyl-D-aspartate receptor. *Molecular Pharmacology*, *40*(3), 333–336.

Xia, P., Chen, H. V., Zhang, D., & Lipton, S. A. (2010). Memantine preferentially blocks extrasynaptic over synaptic NMDA receptor currents in hippocampal autapses. *The Journal of Neuroscience : The Official Journal of the Society for Neuroscience*, *30*(33), 11246–11250. https://doi.org/10.1523/JNEUROSCI.2488-10.2010

Xu, X. X., & Luo, J. H. (2018). Mutations of N-Methyl-D-Aspartate Receptor Subunits in Epilepsy. *Neuroscience Bulletin*, *34*(3), 549–565. https://doi.org/10.1007/s12264-017-0191-5

Yaksh, T. L., Schwarcz, R., & Snodgrass, H. R. (2017). Characterization of the Effects of L-4-Chlorokynurenine on Nociception in Rodents. *Journal of Pain*, *18*(10), 1184–1196. https://doi.org/10.1016/j.jpain.2017.03.014

Yang, Yang, & Xu-Fried, M. A. (2015). Different pools of glutamate receptors mediate sensitivity to ambient glutamate in the cochlear nucleus. *Journal of Neurophysiology*, *113*(10), 3634–3645. https://doi.org/10.1152/jn.00693.2014

Yang, Yunlei, Ge, W., Chen, Y., Zhang, Z., Shen, W., Wu, C., Poo, M., & Duan, S. (2003). Contribution of astrocytes to hippocampal long-term potentiation through release of D-serine. *Proceedings of the National Academy of Sciences of the United States of America*, *100*(25), 15194–15199. https://doi.org/10.1073/pnas.2431073100

Yao, L., & Zhou, Q. (2017). Enhancing NMDA Receptor Function: Recent Progress on Allosteric Modulators. *Neural Plasticity*, *2017*. https://doi.org/10.1155/2017/2875904

Yavarna, T., Al-Dewik, N., Al-Mureikhi, M., Ali, R., Al-Mesaifri, F., Mahmoud, L., Shahbeck, N., Lakhani, S., AlMulla, M., Nawaz, Z., Vitazka, P., Alkuraya, F. S., & Ben-Omran, T. (2015). High diagnostic yield of clinical exome sequencing in Middle Eastern patients with Mendelian disorders. *Human Genetics*, *134*(9), 967–980. https://doi.org/10.1007/s00439-015-1575-0

Yi, F., Zachariassen, L. G., Dorsett, K. N., & Hansen, K. B. (2018). Properties of triheteromeric N-methyl-D-aspartate receptors containing two distinct GluN1 isoforms. *Molecular Pharmacology*, *93*(5), 453–467. https://doi.org/10.1124/mol.117.111427

Yuan, H., Hansen, K. B., Zhang, J., Pierson, T. M., Markello, T. C., Fajardo, K. V. F., Holloman, C. M., Golas, G., Adams, D. R., Boerkoel, C. F., Gahl, W. a, & Traynelis, S. F. (2014). Functional analysis of a de novo GRIN2A missense mutation associated with early-onset epileptic encephalopathy. *Nature Communications*, *5*, 3251. https://doi.org/10.1038/ncomms4251

Yuzaki, M., & Aricescu, A. R. (2017). A GluD Coming-Of-Age Story. *Trends in Neurosciences*, *40*(3), 138–150. https://doi.org/10.1016/j.tins.2016.12.004

Zanos, P., Moaddel, R., Morris, P. J., Georgiou, P., Fischell, J., Elmer, G. I., Alkondon, M., Yuan, P., Pribut, H. J., Singh, N. S., Dossou, K. S. S., Fang, Y., Huang, X. P., Mayo, C. L., Wainer, I. W., Albuquerque, E. X., Thompson, S. M., Thomas, C. J., Zarate, C. A., & Gould, T. D. (2016). NMDAR inhibition-independent antidepressant actions of ketamine metabolites. *Nature*, *533*(7604), 481–486. https://doi.org/10.1038/nature17998

Zanos, P., Piantadosi, S. C., Wu, H. Q., Pribut, H. J., Dell, M. J., Can, A., Snodgrass, H. R., Zarate, C. A., Schwarcz, R., & Gould, T. D. (2015). The prodrug 4-chlorokynurenine causes ketamine-like antidepressant effects, but not side effects, by NMDA/glycineB-site inhibitionS. *Journal of Pharmacology and Experimental Therapeutics*, *355*(1), 76–85. https://doi.org/10.1124/jpet.115.225664

Zarei, M. M., & Dani, J. A. (1995). Structural basis for explaining open-channel blockade of the NMDA receptor. *Journal of Neuroscience*, *15*(2), 1446–1454. https://doi.org/10.1523/jneurosci.15-02-01446.1995

Zhou, Y., Morais-Cabral, J. H., Kaufman, A., & Mackinnon, R. (2001). Chemistry of ion coordination and hydration revealed by a K+ channel-Fab complex at 2.0 Å resolution. *Nature*, *414*(6859), 43–48. https://doi.org/10.1038/35102009

Zhu, S., & Paoletti, P. (2015). Allosteric modulators of NMDA receptors: Multiple sites and mechanisms. *Current Opinion in Pharmacology*, *20*, 14–23. https://doi.org/10.1016/j.coph.2014.10.009

Zimmerman, S. S., Khatri, A., Garnier-Amblard, E. C., Mullasseril, P., Kurtkaya, N. L., Gyoneva, S., Hansen, K. B., Traynelis, S. F., & Liotta, D. C. (2014). Design, synthesis, and structure-activity relationship of a novel series of GluN2C-selective potentiators. *Journal of Medicinal Chemistry*, *57*(6), 2334–2356. https://doi.org/10.1021/jm401695d

Zivanovic, D., Susic, V., & Stanojlovic, O. (1999). Inhibition of metaphit-induced audiogenic seizures by APV in rats. In *Physiological Research* (Vol. 48, Issue 2, pp. 149–156).

10 List of publications

This dissertation is based on the following publications:

1) **Kysilov, B**., Hrcka Krausova, B., Vyklicky, V., Smejkalova, T., Korinek, M., Horak, M., Chodounska, H., Kudova, E., Cerny, J., & Vyklicky, L. (2022). Pregnane-based steroids are novel positive NMDA receptor modulators that may compensate for the effect of loss-of-function disease-associated GRIN mutations. *British Journal of Pharmacology*, *179*(15), 3970–3990. https://doi.org/10.1111/bph.15841\. IF = 9.473 (2021).

2) Hrcka Krausova, B., **Kysilov, B**., Cerny, J., Vyklicky, V., Smejkalova, T., Ladislav, M., Balik, A., Korinek, M., Chodounska, H., Kudova, E., & Vyklicky, L. (2020). Site of Action of Brain Neurosteroid Pregnenolone Sulfate at the N-Methyl-D-Aspartate Receptor. *The Journal of Neuroscience*, 5922–5936. https://doi.org/10.1523/JNEUROSCI.3010-19.2020. IF = 6.167 (2020).

3) Vyklicky, V., Krausova, B., Cerny, J., Ladislav, M., Smejkalova, T., **Kysilov, B**., Korinek, M., Danacikova, S., Horak, M., Chodounska, H., Kudova, E., & Vyklicky, L. (2018). Surface Expression, Function, and Pharmacology of Disease-Associated Mutations in the Membrane Domain of the Human GluN2B Subunit. *Frontiers in Molecular Neuroscience*, *11*, 110. https://doi.org/10.3389/fnmol.2018.00110. IF = 3.72 (2018).

Other scientific publications:

1) Štefková-Mazochová, K., Danda, H., Dehaen, W., Jurásek, B., Šíchová, K., Pinterová-Leca, N., Mazoch, V., Krausová, B. H., Kysilov, B., Smejkalová, T., Vyklický, L., Kohout, M., Hájková, K., Svozil, D., Horsley, R. R., Kuchař, M., & Páleníček, T. (2022). Pharmacokinetic, pharmacodynamic, and behavioural studies of deschloroketamine in Wistar rats. *British Journal of Pharmacology*, *179*(1), 65–83. https://doi.org/10.1111/bph.15680. IF = 9.473 (2021).

2) Hubalkova, P., Ladislav, M., Vyklicky, V., Smejkalova, T., Hrcka Krausova, B., Kysilov, B., Krusek, J., Naimová, Z., Korinek, M., Chodounska, H., Kudova, E., Cerny, J., & Vyklicky, L., Jr (2021) . *The Journal of Neuroscience*, Palmitoylation Controls NMDA Receptor Function and Steroid Sensitivity, *41*(10), 2119–2134. https://doi.org/10.1523/JNEUROSCI.2654-20.2021. IF = 6.709.

3) Tumanovska, L. V., Swanson, R. J., Serebrovska, Z. O., Portnichenko, G. V., Goncharov, S. V., Kysilov, B. A., Moibenko, O. O., & Dosenko, V. E. (2019). Cholesterol enriched diet suppresses ATF6 and PERK and upregulates the IRE1 pathways of the unfolded protein response in spontaneously hypertensive rats: Relevance to pathophysiology of atherosclerosis in the setting of hypertension. *Pathophysiology 26*(3-4), 219–226. https://doi.org/10.1016/j.pathophys.2019.05.005. No IF.

11 Appendices

1) **Kysilov, B**., Hrcka Krausova, B., Vyklicky, V., Smejkalova, T., Korinek, M., Horak, M., Chodounska, H., Kudova, E., Cerny, J., & Vyklicky, L. (2022). Pregnane-based steroids are novel positive NMDA receptor modulators that may compensate for the effect of loss-of-function disease-associated GRIN mutations. *British Journal of Pharmacology*, *179*(15), 3970–3990. https://doi.org/10.1111/bph.15841\

2) Hrcka Krausova, B., **Kysilov, B**., Cerny, J., Vyklicky, V., Smejkalova, T., Ladislav, M., Balik, A., Korinek, M., Chodounska, H., Kudova, E., & Vyklicky, L. (2020). Site of Action of Brain Neurosteroid Pregnenolone Sulfate at the N-Methyl-D-Aspartate Receptor. *The Journal of Neuroscience :*, *40*(31), 5922–5936. https://doi.org/10.1523/JNEUROSCI.3010-19.2020

3) Vyklicky, V., Krausova, B., Cerny, J., Ladislav, M., Smejkalova, T., **Kysilov, B**., Korinek, M., Danacikova, S., Horak, M., Chodounska, H., Kudova, E., & Vyklicky, L. (2018). Surface Expression, Function, and Pharmacology of Disease-Associated Mutations in the Membrane Domain of the Human GluN2B Subunit. *Frontiers in molecular neuroscience*, *11*, 110. https://doi.org/10.3389/fnmol.2018.00110